

New surfactants based on nanocellulose

Maria Mercedes Gonzalez Bernal

Thesis presented for the degree of PhD in Chemistry

Thesis Supervisor

Cristian Blanco Tirado

Chemist, Ph. D.

Thesis co-Supervisor

Marianny Yajaira Combariza

Chemist, Ph. D.

Universidad Industrial De Santander

Facultad De Ciencias

Escuela De Química

Doctorado en Química

Bucaramanga

2020

A mi familia

A mis perritas

A Ruca

Agradecimientos

Agradecimientos al personal a cargo de los laboratorios de RMN, DRX, microscopía y TGA del parque Industrial de Guatigurá de la Universidad Industrial de Santander.

A Ecopetrol en el marco del convenio 03-5211794 por su apoyo económico a este proyecto.

A Colciencias por el crédito condonable de la convocatoria 727 del 2016.

Un especial agradecimiento al personal del Departamento de Madera, Celulosa y Papel de la Universidad de Guadalajara por su apoyo durante la pasantía.

Table of Contents

Introduction.....	17
Chapter 1.....	17
1 Surfactants and emulsions in crude oil industry	17
1.1 Nanocellulose.....	20
1.2 Cellulose nanofibrils (CNF) isolation.....	22
1.3 Cellulose nanocrystals (CNC) isolation.....	23
1.4 NCN surface modification	26
1.5 Working Hypothesis	27
1.6 References.....	32
Chapter 2.....	41
2 Surface hydrophobization of cellulose nanocrystals via transesterification with triacylglycerols.....	41
2.1 Abstract.....	41
2.2 Introduction.....	42
2.3 Experimental.....	45
2.3.1 Materials.	45
2.3.2 Methods.....	45
2.3.2.1 CNC isolation.....	45
2.3.2.2 Sulfate Groups Quantitation in CNC.. ..	46

2.3.2.3	CNC Esterification.....	46
2.3.2.4	CNC Characterization.....	47
2.4	Results and discussion	49
2.4.1	Raw CNC Morphology.....	49
2.4.2	Spectroscopic characterization.....	50
2.4.3	Crystallinity.....	52
2.4.4	Thermal behavior.....	53
2.4.5	Solubility test.	54
2.5	Conclusions.....	55
2.6	References.....	55
Chapter 3.....		68
3	Nanocellulose as an inhibitor of water-in-crude oil emulsion formation	68
3.1	Abstract.....	68
3.2	Introduction.....	68
3.3	Experimental and Methods	74
3.3.1	Materials..	74
3.3.2	CNC isolation by hydrolysis.....	74
3.3.3	CNF isolation by TEMPO.	75
3.3.4	CNC and CNF characterization.	76
3.3.5	Preparation of model emulsions.....	77
3.3.6	Emulsion characterization.....	78

3.4	Results and discussion	79
3.4.1	Nanocellulose surface chemistry and structure.....	79
3.4.2	Inhibition of emulsion formation with CNC and CNF in w/o model systems.	83
3.4.3	Inhibition of emulsion formation with CNC in w/Crude Oil dispersions.....	89
3.4.3.1	Light crude oil.....	89
3.4.3.2	Heavy crude oil.....	93
3.5	Conclusions.....	94
3.6	References	96
Chapter 4.....		107
4	Surfactant behavior of surface modified cellulose nanocrystals	107
4.1	Abstract.....	107
4.2	Introduction.....	107
4.3	Material and methods.....	112
4.3.1	CNCOOH preparation.	112
4.3.2	CNC preparation.....	113
4.3.3	Amidation.	113
4.3.4	CNC esterification.....	114
4.3.5	Characterization.....	114
4.3.6	Bottle test.....	115
4.4	Hypotheses	116
4.5	Results.....	116

4.5.1	Characterization	116
4.5.2	Morphology.....	116
4.5.3	Spectral analysis.....	119
4.5.4	Crystallinity.....	122
4.5.5	Thermal stability	124
4.5.6	Emulsion breaking test.....	126
4.6	Conclusions.....	129
4.7	References.....	130
	Conclusions.....	142
	References.....	144

List of Figures

Figure 1. Demulsification process.	19
Figure 2. Cellobiose	21
Figure 3. Cellulose nanoparticles.....	22
Figure 4. Tempo oxidation.....	23
Figure 5. Mechanism of cellulose hydrolysis with sulfuric acid	25
Figure 6. Functionalization Nanocellulose	27
Figure 7. Schematic summary of our working hypothesis.	30
Figure 8. CNC and palm oil transesterification reaction	47
Figure 9. FESEM images of raw CNC, from a concentrated (A) and a diluted (B) solution. Dynamic light scattering (DLS) for a CNC solution (0,2 g/L).	49
Figure 10. (A) Full-range and (B) zoomed IR spectra of raw (black) and modified CNC (grey), (C) Full range solid NMR spectrum of raw CNC (black) and modified CNC (grey) and (D)zoom in the region between 150 to 200 ppm with elimination of rotational echoes.	51
Figure 11. XRD patterns, crystallinity index and crystallite size for raw (black) and modified CNC (grey).....	53
Figure 12. Thermal behavior of raw (black) and modified CNC (grey).....	54

Figure 13. Solubility test of Modified CNC in water and Toluene	55
Figure 14. CNF Charaterization, (A) FESEM, (B) TGA and derivative TGA, (C) DRX, (D) IRATR	80
Figure 15. CNC Characterization (A) FESEM, (B) DLS, (C) TGA and derivative TGA, (D) DRX, E: IRATR	80
Figure 16. Emulsion inhibition effects for CNC: visual tests (top left), optical micrographs of the control emulsion and the aqueous layer for the sample with 1000 ppm of CNC (bottom left); backscattering NIR measurements featuring the dynamics of the instability indexes for the overall mixture (top right) and the aqueous layer (bottom right).	84
Figure 17. Emulsion inhibition effects for CNF: visual tests (top left), optical micrographs of the control emulsion and the aqueous layer for the sample with 1500 ppm of CNF (bottom left); backscattering NIR measurements featuring the dynamics of the instability indexes for the overall mixture (top right) and the aqueous layer (bottom right).	87
Figure 18. Optical microscopy images of the organic aqueous and interfacial layers observed during an inhibition test with CNF, using Methylene Blue (cationic dye) as a label for cellulose.	88
Figure 19. Inhibition tests with suspensions of 1000 ppm of CNC in 1000 ppm NaCl brines.....	91
Figure 20. Inhibition tests with suspensions of 1000 ppm CNC in brines of 6000 ppm NaCl, pH 6 and 10.....	85
Figure 21. Inhibition tests with suspensions of 1000 ppm CNC in brines of 12,000 ppm NaCl, pH	

6 (black) and pH 10 (gray).....	93
Figure 22. Inhibition tests for a water-in-heavy oil emulsion with suspensions of 1000 ppm CNC in brines of 1000 ppm NaCl at pH 10.	94
Figure 23 (A) CNF, (B) CNC, (C) CNCONC12, (D)CNCONC18.....	117
Figure 24. SEM CNC (left) y CNC-Palm (right).....	118
Figure 25. Infrared spectrum.....	119
Figure 26 . (A) Full NMR C13-MAS spectrum for CNCOOH, CNCONC12 and CNCONC18 (B) Section NMR spectrum, (C) spectrum for CNC and CNC-Palm	121
Figure 27. DRX for CNCOOH and amidated (left), CNC and CNC-Palm.....	123
Figure 28. TGA and derivative	124
Figure 29. Bottle test using CNCONC18 (top) and CNCONC12 (bottom)	127
Figure 30. Bottle test with CNC-Palm.....	129

List of Tables

Table 1. CNC and CNF characterization	81
Table 2. Oxidation degree (OD) and substitution degree (SD)	117
Table 3. The stability of an emulsion Vs demulsifiers	129

Resumen

Título: Nuevos surfactantes basados en nanocelulosa*

Autor: Maria Mercedes González Bernal**

Palabras clave: nanocelulosa, inhibición, emulsiones W/O, materiales funcionales

Descripción

Durante los procesos de obtención de crudos, es común que se formen emulsiones de agua en aceite (W/O), las cuales traen inconvenientes en los sistemas de transporte, entre ellas: corrosión, depósito de sales en tuberías y viscosidades altas. Por ello en la industria petrolera es necesario disminuir la cantidad de agua presente en las emulsiones hasta un 0,5%, para lograrlo se utilizan surfactantes, generalmente sintéticos. En nuestro trabajo nos enfocamos en el diseño y creación de surfactantes ambientalmente amigables para aplicarlos en la solución del problema de las emulsiones W/O. Para ello realizamos dos enfoques diferentes, inicialmente, obtuvimos nanofibrillas y nanocristales de celulosa y usamos suspensiones acuosas de estas nanopartículas para inhibir la formación de las emulsiones. Encontramos que la aplicación de estas suspensiones acuosas de nanocelulosas puras permite disminuir la cantidad de agua emulsionada, inhibiendo la formación de emulsiones agua en aceite hasta en un 75%. Por otro lado, realizamos tres modificaciones superficiales a los nanocristales de celulosa con el fin de modular su hidrofobicidad y permitir su dispersión en solventes orgánicos, lo cual nos permitió realizar pruebas de estas nanopartículas como rompedores de emulsiones, obteniendo una recuperación del 70 % del agua presente. Se realizaron tres procesos de funcionalización: transesterificación en fase sólida, amidación con aminas de 12 y 18 carbonos y esterificación con fosfonato de palmitoilo. Las nanopartículas de celulosa fueron caracterizadas antes y después de la funcionalización, mediante FTIR, NMR, difracción de rayos X (XRD), microscopía electrónica de barrido (SEM) y análisis termogravimétrico (TGA).

*Trabajo de grado

**Facultad de Ciencias. Escuela de Química. Directores: Cristian Blanco Tirado y Marianny Yajaira Combariza

Abstract

TITLE: New surfactants based on nanocellulose*

AUTHOR: Maria Mercedes González Bernal**

KEYWORDS: nanocellulose, inhibition, W/O emulsion, functional materials

DESCRIPTION

During the processes of obtaining crude, it is common for water-in-oil (W / O) emulsions to be formed, which bring inconveniences in transport systems, including: corrosion, salt deposit in pipes and high viscosities. Therefore, in the oil industry it is necessary to reduce the amount of water present in emulsions up to 0.5%, to achieve this, surfactants, usually synthetic, are used. In our work we focus on the design and creation of environmentally friendly surfactants to apply them in solving the problem of W / O emulsions. To do this, we performed two different approaches, initially, we obtained nanofibrils and cellulose nanocrystals and used aqueous suspensions of these nanoparticles to inhibit the formation of emulsions. We found that the application of these aqueous suspensions of pure nanocelluloses allows to reduce the amount of emulsified water, inhibiting the formation of water-in-oil emulsions by up to 75%. On the other hand, we made three superficial modifications to the cellulose nanocrystals in order to modulate their hydrophobicity and allow their dispersion in organic solvents, which made us test these nanoparticles as emulsion breakers, obtaining a recovery of 70% of the water present. Three functionalization processes were performed: solid phase transesterification, amidation with 12 and 18 carbon amines and esterification with palmitoyl phosphonate. Cellulose nanoparticles were characterized before and after functionalization, by FTIR, NMR, X-ray diffraction (XRD), scanning electron microscopy (SEM) and thermogravimetric analysis (TGA).

*Bachelor Thesis

**Facultad de Ciencias. Escuela de Química. Director: Cristian Blanco Tirado -Marianny

Yajaira Combariza

Introduction

Chapter 1

1 Surfactants and emulsions in crude oil industry

Surfactants are chemical compounds with both polar and non-polar regions, also known as amphiphiles. In general, the polar group contains at least one heteroatom (O, N, S, P) while the hydrophobic region has a paraffinic or alkyl-aromatic group (Salager, 1992). These substances can alter the surface energy of interfaces by decreasing the surface tension of the phase they are in.

Normally, surfactants are classified in two large groups, ionic and non-ionic, according to their behavior in the aqueous phase. Ionic surfactants dissociate in water producing an amphiphilic ion and its corresponding counterion. There are no net charges on non-ionic surfactants; hence, they are less sensitive than the ionic ones to the presence of divalent cations (Fernandez, Salager & Scorzza, 2004). Non-ionic surfactants are also compatible with other surfactants which allows complex formulations. Surfactants are widely used in chemical, pharmaceutical, cosmetics, food, and oil industries, as well as in remediation processes such as crude oil spill control. Ethoxylated alkylphenols (Becerril, 2009) are the most commonly used non-ionic surfactants; however, their degradation products are pollutants and they are seeking to replace them with more environmentally friendly substances of natural origin that can be biodegradable. Among the polymers currently studied, we have proteins (McClements, 2004), lignin (Rojas *et al.*, 2007) and cellulose (Rein, Khalfin & Cohen, 2012).

Surfactants are adsorbed at the interfaces, forming monolayers with the polar region facing water, decreasing the interfacial tension and changing the stability of dispersed systems such as

emulsions. By subjecting a mixture containing water, oil and a surfactant to stirring, a dispersion occurs, where one of the liquid phases is in the form of small drops within the other phase; this is called an emulsion (Marfisi, 2005). Emulsions are classified according to the droplet size of the dispersed phase in: macroemulsions (1-100 μm) and microemulsions (less than 1 μm). Emulsions where the continuous phase is oil and the dispersed water are named as W/O emulsions, while in the opposite case, where the continuous phase is water and the dispersed oil is named as O/W emulsions.

In the oil production processes, at some point water begins to be extracted along with the oil, during pumping and transport shear forces occur, which have the effect of emulsifying the water present in the mixture, the presence of natural surfactants as asphaltenes, phenolic resins and naphthenic acids help in this process and generate stable and difficult to separate W / O emulsions, especially when it comes to heavy crudes such as those produced in Colombia. (Al-Sabagh, A. M., Nasser, N. M., & Abd El-Hamid, T. M. 2013, Kim, H., & Wasan, T. 1995, Kokal 2005)

To comply with requirements for transport and export of crude oil, this product must have less than 0.5% water, so several strategies relying in chemical, physical, and biological processes, are commonly used to break emulsions in the oil industry (Fan, Y., Simon, S., & Sjöblom, J. 2009). Thermal treatments are among the most widely used demulsification methods; however, there is a significant loss of volatile crude oil fractions associated with this strategy. There are also high-energy mechanical treatments that significantly increase operating costs (Schramm, 2001). However, the most effective method remains the application of surfactants, of synthetic, and lately biological origin, that can efficiently compete with the emulsifying agents present in the oil (asphaltenes, resins, naphthenic acids) reducing interfacial tension, destabilizing the emulsion and

allowing phase separation, as illustrated in Figure 1.

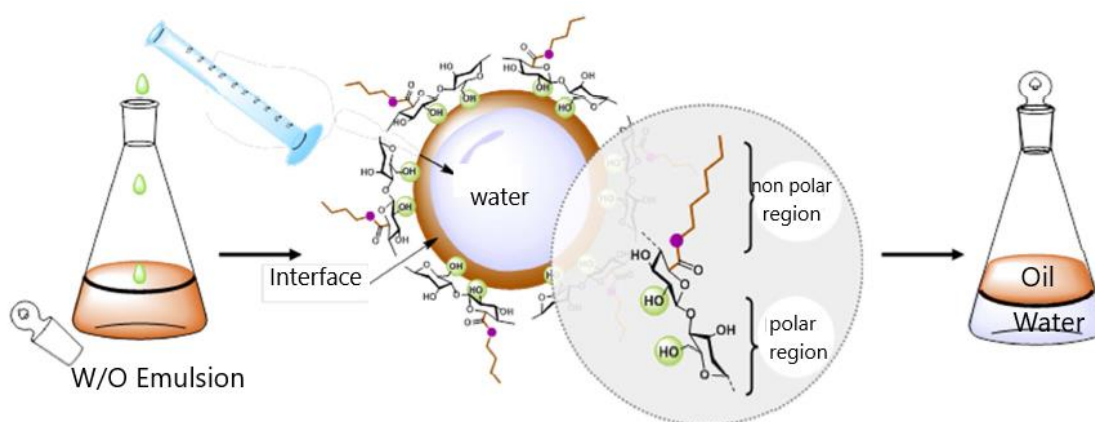


Figure 1. Demulsification process.

There is a lot of research dealing with demulsification processes in the oil industry. For instance, Djuve *et al.*, (2001) studied the process of destabilization of W/O emulsions stabilized by asphaltenes, and found that the molecular weight of emulsion breakers is a factor to be taken into account when selecting an appropriate compound. A compound with high molecular weight significantly improves emulsion breaking because it provides a large active surface. However, there are limits due to the need of mobility that the molecule must have to easily migrate to the interfacial region, where it competes with the natural surfactants in the crude, draining them from the interfacial layer, allowing the emulsion to destabilize and separate. They also carried out tests using the demulsifiers as inhibitors, by adding them directly to the oil before the formation of the emulsion, and found a strong interfacial competence and an improvement in the efficiency of the action of the surfactants used.

Emulsion breakers used in the oil industry are mixtures of surface-active agents. Typically,

compounds with high molecular weight compounds, most of synthetic origin, such as ethylene oxides and polypropylene oxides, nonylphenols and ethoxylated phenols, alcohols, ethoxylated amines, and sulphonic acid salts. (Al-Sabagh, Ahmed, Nassar & Gabr, 2003; Kokal, 2005; Bhardwaj & Hartland, 1993; Rondón, Bouriat, Lachaise & Salager, 2006). In some cases, acrylamide copolymers (AM), acrylic acid (AA), and N-allyloctadec-9-enamides are used. (Ye *et al.*, 2013).

1.1 Nanocellulose

Cellulose, a polymer widely distributed in nature (Khalil *et al.*, 2014), is the main component of secondary walls of plant cells, and it is also found in some marine animals (tunicates) as well as in microorganisms such as algae and bacteria. The structural unit of cellulose is the cellobiose disaccharide formed by two units of D-anhydroglucose linked by glycosidic β bonds as shown in Figure 2 (Du *et al.*, 2019; Habibi, Lucia & Rojas, 2010; Khalil *et al.*, 2014; Song, Winter, Bujanovic & Amidon, 2014). Cellulose degree of polymerization depends on its source, and can range from $n = 10,000$ to $30,000$. Each unit of D-anhydroglucose has three hydroxyl groups ($-OH$), located in positions C2, C3 (secondary alcohols) and C6 (primary alcohol). This structural characteristic of the polymer, combined with its three-dimensional arrangement, allows formation of hydrogen bonds between chains which provide rigidity to the structure and a high Young modulus (Habibi *et al.*, 2010).

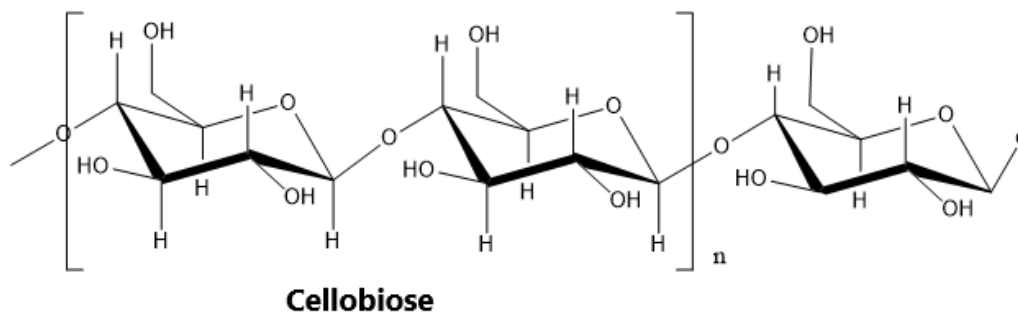


Figure 2. Cellobiose

Cellulose fibers contain sections that are highly organized or crystalline, and others relatively disorderly or amorphous (Habibi *et al.*, 2010). The crystalline regions are less accessible to the attack of acids and enzymes, and amorphous regions, on the other hand, are more susceptible to hydrolysis allowing removal of the smaller crystalline domains.

Nanocelluloses, derived from the bulk material, are known as nanofibrils (CNF) and nanocrystals (CNC). The former, containing both crystalline and amorphous cellulose, have widths of about 20 nm and lengths of a few microns. The latter, with a much higher degree of crystallinity, are smaller with more defined cylindrical shapes, exhibiting lengths between 100 and 400 nm and widths ranging from 5 to 20 nm (Du *et al.*, 2019). Figure 3 illustrates the two common types of cellulose nanoparticles.

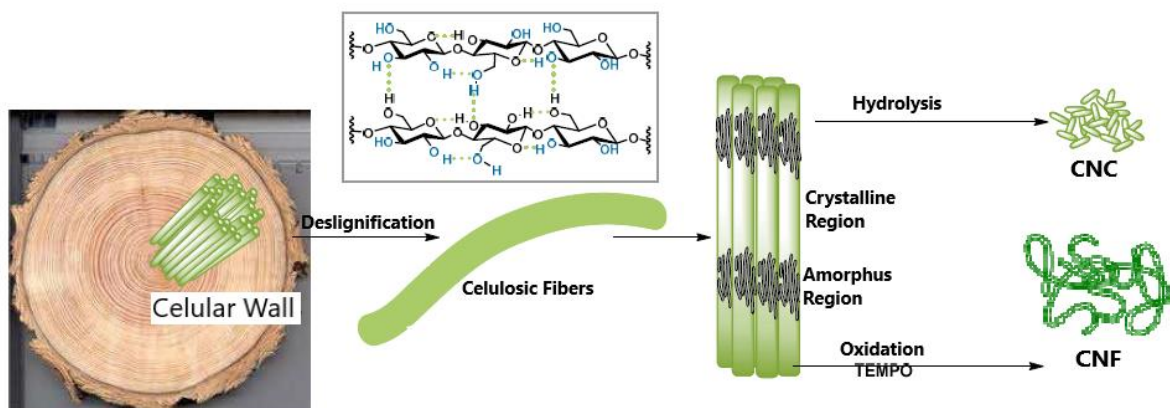


Figure 3. Cellulose nanoparticles

Nanocellulose isolation processes, using chemical, mechanical or enzymatic methods, is abundantly illustrated in scientific literature (Thomas *et al.*, 2018) Traditionally, nanocelluloses were extracted from wood and wood by-products; however, nowadays the materials are becoming more commonly isolated from agroindustrial residual biomass.

1.2 Cellulose nanofibrils (CNF) isolation

Mechanical methods, such as microfluidization, homogenization, grinding, cryocrushing, and ultrasonication, are used to obtain CNF from cellulosic fibers. (Khalil *et al.*, 2014). These methods require a high energy input; thus, alternative chemical and enzymatic treatments have been implemented to reduce costs. TEMPO oxidation stands out among the chemical methods for CNF isolation.

For TEMPO oxidation bleached cellulose is subjected to reaction with the 2,2,6,6-Tetramethylpiperidin-1-oxyl radical (TEMPO). TEMPO acts as an oxidation catalysts, particularly for the primary hydroxyl group in C6 of the AGU, to introduce carboxylic groups on the cellulose backbone which in turn induce repulsion between micro and nano fibrils allowing easy separation

to produce CNF (Fujisawa, Okita, Fukuzumi, Saito & Isogai, 2011; Song et al., 2014). This reaction is carried out with NaBr sodium bromide and NaClO sodium hypochlorite as precursors of the nitrosonium ion that is formed by the reaction of TEMPO with hypobromite ions (BrO^-) which are produced by the reaction between NaClO and NaBr. The nitrosonium ion, the true oxidizing agent of the reaction, promotes the oxidation of the OH group at C6 of AGU to aldehyde, which is then oxidized to the carboxylic acid by hypobromite as shown in Figure 4 (Fukuzumi, Saito & Isogai, 2013; Tanaka, Saito & Isogai, 2012). The final result is the introduction of uronic acid groups on the surface of the nanocellulose.

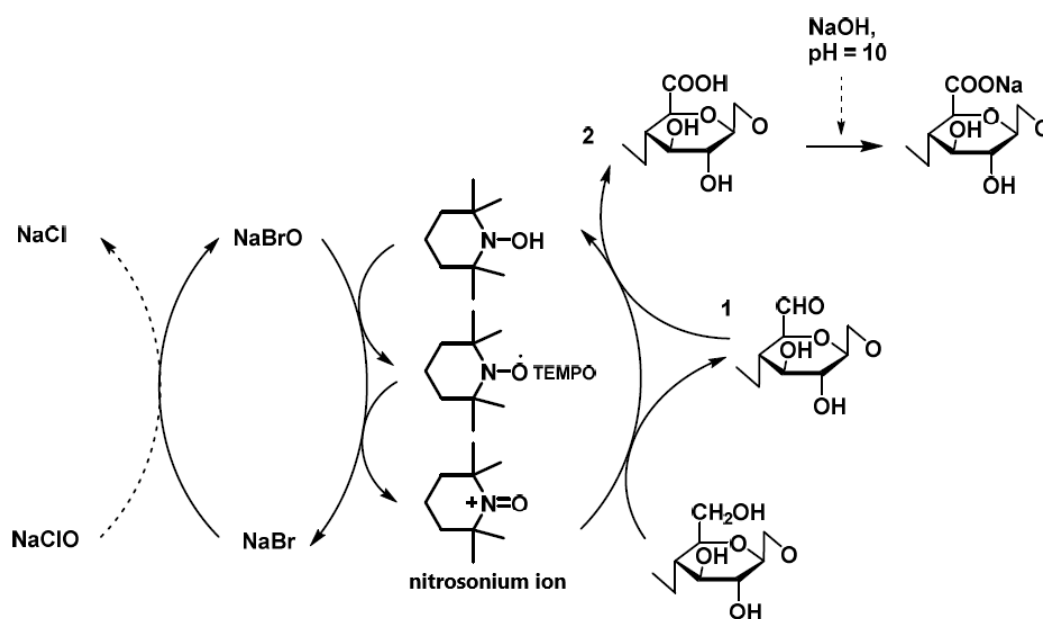


Figure 4. Tempo oxidation

1.3 Cellulose nanocrystals (CNC) isolation

CNC are smaller structures than CNF, with a greater degree of crystallinity arising from the removal of amorphous regions from native cellulose. CNC are normally obtained through acid

hydrolysis of bleached cellulose, with strong acids (liquid or solids), to break glycosidic bonds and to induce cellulose depolymerization. The process is followed by dispersion of the material using mechanical or ultrasound energy. During the reaction, the acid hydrolyzes preferably amorphous zones due to their random orientation and lower density, leaving the stable crystalline regions as rod-like structures (Habibi *et al.*, 2010). Various acids are used for the hydrolysis process such as hydrobromic acid (HBr) (Sadeghifar, Filpponen, Clarke, Brougham & Argyropoulos, 2011), hydrochloric (HCl) (George, 2012), nitric (HNO₃) (Revol, Bradford, Giasson, Marchessault & Gray, 1992), phosphoric (H₃PO₄) (Li *et al.*, 2013), maleic (Filson & Dawson, 2009) and phosphotungstic acid (HPW, H₃PW₁₂O₄₀) (Liu *et al.*, 2014). Finally, the most commonly used is sulfuric acid (H₂SO₄) (Martinez, López & Lagaron, 2011).

Hydrolysis with sulfuric acid involves protonation of the glycosidic oxygen atom and the breaking of the bond. Besides hydrolysis, reactions with sulfuric acid also result in partial esterification of the C6 in AGU with sulfate groups which can dissociate and provide negative charges (see Figure 5). This effect induces defibrillation and allows formation of stable suspensions of CNC in water driven by charge repulsion. However, some authors have reported decreased thermal stability by the presence of sulfate groups (Krishnamachari, Hashaiken, Chiesa & Gad, 2012).

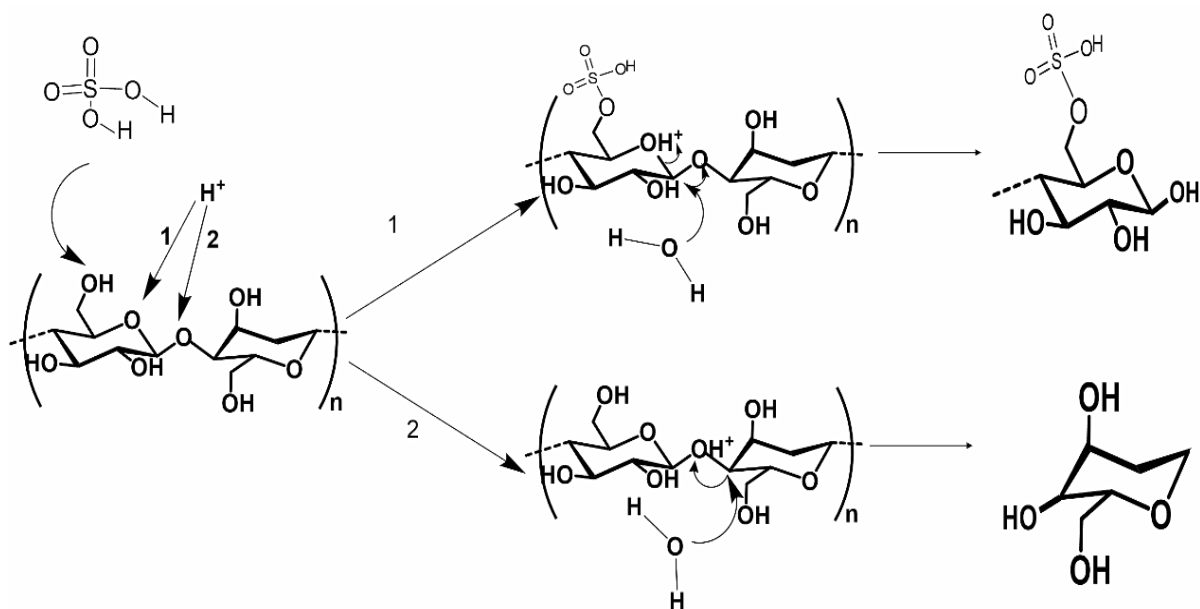


Figure 5. Mechanism of cellulose hydrolysis with sulfuric acid

The structure, properties and yields of CNC depend on the hydrolysis conditions. Commonly, stronger acids (H_2SO_4 , HCl) in high concentration, lengthy reactions, high temperature and mechanical assistance (ultrasound) produce CNC with high surface charge and uniform sizes; however, the yields, crystallinity and thermal stability of the material decrease under these conditions. For instance, Bondeson, Mathew & Oksman (2006) presented an experimental design for the optimization of hydrolysis with sulfuric acid. According to these studies, the best performance is achieved with a concentration of 63.5% sulfuric acid, 130 min of hydrolysis at 44 °C with 30 minutes of sonication and a concentration of 10.2 g of cellulose / 100 cm^3 , reporting the formation of crystals with lengths between 200 and 400 nm and thicknesses of less than 10 nm with a yield of 30% of the initial weight. As a last stage in the purification, it is necessary to carry out dialysis to completely eliminate the residual acid and the by-products of the hydrolysis.

1.4 NCN surface modification

Nanocellulose surface modification is fundamental to develop industrial applications for this material. CNF and CNC are polar in nature and easily dispersible in water and polar solvents. However, much of these materials uses are found as synthetic polymer reinforcements, and many synthetic polymers are non-polar in nature. Thus, to increase nanocellulose compatibility with non-polar matrices surface functionalization is performed.

Cellulose surface modification is a prolific topic in scientific literature. There are many different processes for the functionalization of the cellulosic surface that take advantage of the reactive hydroxyl units in its surface. For nanocellulose, in addition to hydroxyl groups, these modifications rely on the reactivity of carboxylic and sulfate moieties in CNF and CNC, respectively (see Figure 6). Nanocellulose surface functionalization can be performed through covalent and non-covalent modifications (Rol, Belgacem, Gandini & Bras, 2019). Most hydrophobic NCN originates from covalent bonding of alkyl chains via acylation, acetylation, esterification, silylation, and amidation reactions (Tang, Sisler, Grishkewich & Tam, 2017, Salajkova *et al.*, 2012, Berlioz, Molina, Nishiyama & Heux, 2009; Goussé, Chanzy, Excoffier, Soubeyrand & Fleury, 2002). The application of functionalized nanocellulose in emulsion stabilization is a new area of development (Bai, Huan, Xiang & Rojas; Chen *et al.*, 2018; Kalashnikova, Bizot, Cathala & Capron, 2012).

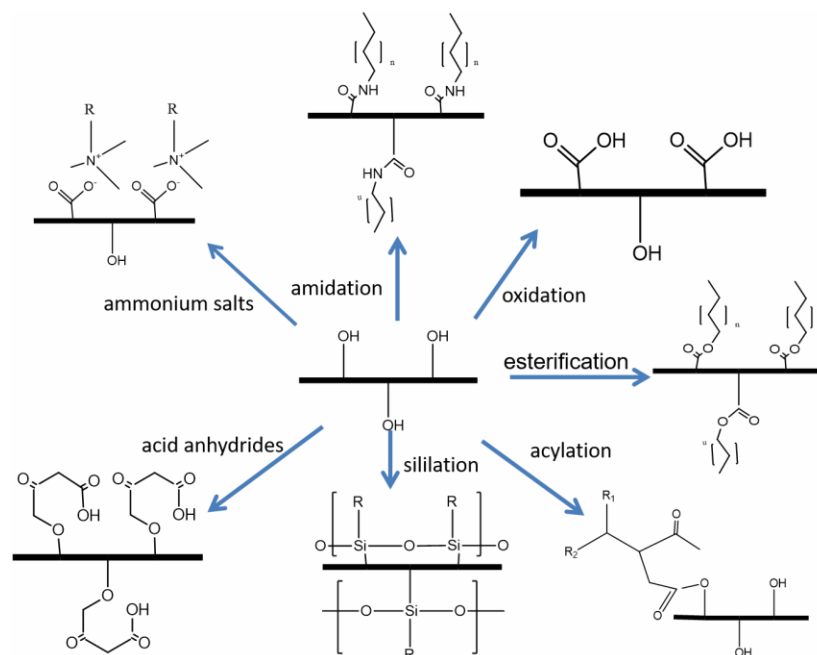


Figure 6. Functionalization Nanocellulose

1.5 Working Hypothesis

The wide range of cellulose surface modification strategies, aimed to modulate the material's interaction at interfaces prompted us to postulate the synthesis and characterization of a new generation of surfactants based on nanocellulose, and to test them as surface-active agents. Our working hypothesis is that nanocellulose can be used in improved oil recovery processes by either inhibiting emulsion formation or breaking them once they are formed. To test this hypothesis, we developed a two-pronged strategy. First, to synthesize and use hydrophilic nanocelluloses as additives, dissolved in water, to prevent or inhibit emulsion formation upon contact of the aqueous phase with the crude oil. Second, to synthesize and use hydrophobic celluloses (easily dispersible in organic solvents such as xylene) as emulsion breakers for both synthetic and natural W/crude

oil emulsions from the petroleum industry.

The chemical versatility of nanocelluloses, with abundant hydroxyl, carboxylic and sulfate groups in their surfaces (depending upon their form of isolation as explained above), facilitates modulation of their polarity by introduction of non-polar moieties via acylation, esterification, amidation, and many other reactions. Controlled introduction of hydrophobic groups on the nanocellulose surface gives the biopolymer a surfactant character, increasing its compatibility in non-polar media, such as crude oil, so that it that can be used as an emulsion breaker. Along the same lines, highly polar oxidized (or sulfated) raw nanocelluloses dispersed in aqueous phase, can be used as emulsion inhibitors to compete with surface-active compounds naturally found in crude oil responsible for emulsion formation and stabilization such as asphaltenes, naphthenic acids, and resins.

The use of nanocelluloses as a surfactant is a relatively new research field. Studies with cellulose microfibrils show that decreasing particle size and combining fractions of modified cellulose improves efficiency as a surfactant to stabilize water in toluene emulsions (Andresen & Stenius, 2007). Another example of this type of approach is the use of microfibrillated cellulose isolated from mangosteen rind pulp (*Garcinia mangostana*) to stabilize O/ W emulsions (Winuprasith & Suphantharika, 2013). The stabilization effect was linked to the material's homogeneity, with an increased emulsion stabilization as the number of stages involved in the process of purification of the fibrillated material increased. In 2010, Lif and collaborators (Lif, Stenstad, Syverud, Nydén & Holmberg, 2010) conducted a series of studies with modified cellulose microfibers (MCC) to stabilize diesel emulsions in water. In their tests, they used MCC with different degrees of hydrophobicity, finding that a combination of unmodified microcellulose

and hydrophobic microcellulose gave the best results.

There are also several reports on the effect of cellulose as a demulsifying agent. For instance, when ethyl cellulose was tested for the destabilization of W/bitumen emulsions, the compound was found to reduce the rigidity of the interfacial film (formed by natural surfactants present in the bitumen), promoting emulsion coalescence at a concentration of 300 ppm (Hou, Feng, Masliyah & Xu, 2012). Along the same lines, there is also research associated with use of functionalized nanocelluloses for emulsion stabilization in the cosmetic industry (Chen *et al.*, 2018; Tang *et al.*, 2017; Wang *et al.*, 2018). Zoppe *et al.*, (2012) found that nanocellulose grafted with polypickemers work efficiently in stabilizing pickering emulsions. However, in these studies extensive modifications are made to the nanocellulose, giving it a highly hydrophobic character, which limits its applications as a surfactant (Mikulcová, Bordes, Minařík & Kašpárková, 2018).

Nanocellulose has been studied extensively to stabilize Pickering emulsions (George & Sabapathi, 2015; Li *et al.*, 2018). Cellulose nanoparticles are efficient Pickering emulsions stabilizers in two ways. First, different CNC allotropes have different emulsifying capacities, and due to their crystalline structure, the nanocellulose has amphiphilic characteristics, since it contains hydrophobic and hydrophilic crystalline planes. (Capron, Roja & Bordes, 2017; Salas, Nypelö, Rodriguez-Abreu, Carrillo & Rojas, 2014). Second, nanocellulose is able to form a network-shaped interfacial film with large packaging, which prevents the coalescence of the drops and thus stabilizes the emulsion. (Wang *et al.*, 2018)

To the best of our knowledge there are no reports in the scientific literature, related to use of nanocelluloses to inhibit emulsion formation or to break stable emulsions. Bulk cellulose has been used to break emulsions; however, no tests have been carried out with cellulose nanoparticles since

most of the current work is aimed at using the nanocellulose as emulsion stabilizer and not as a destabilizer. Figure 7 shows an schematic representation of the rationale of our work.

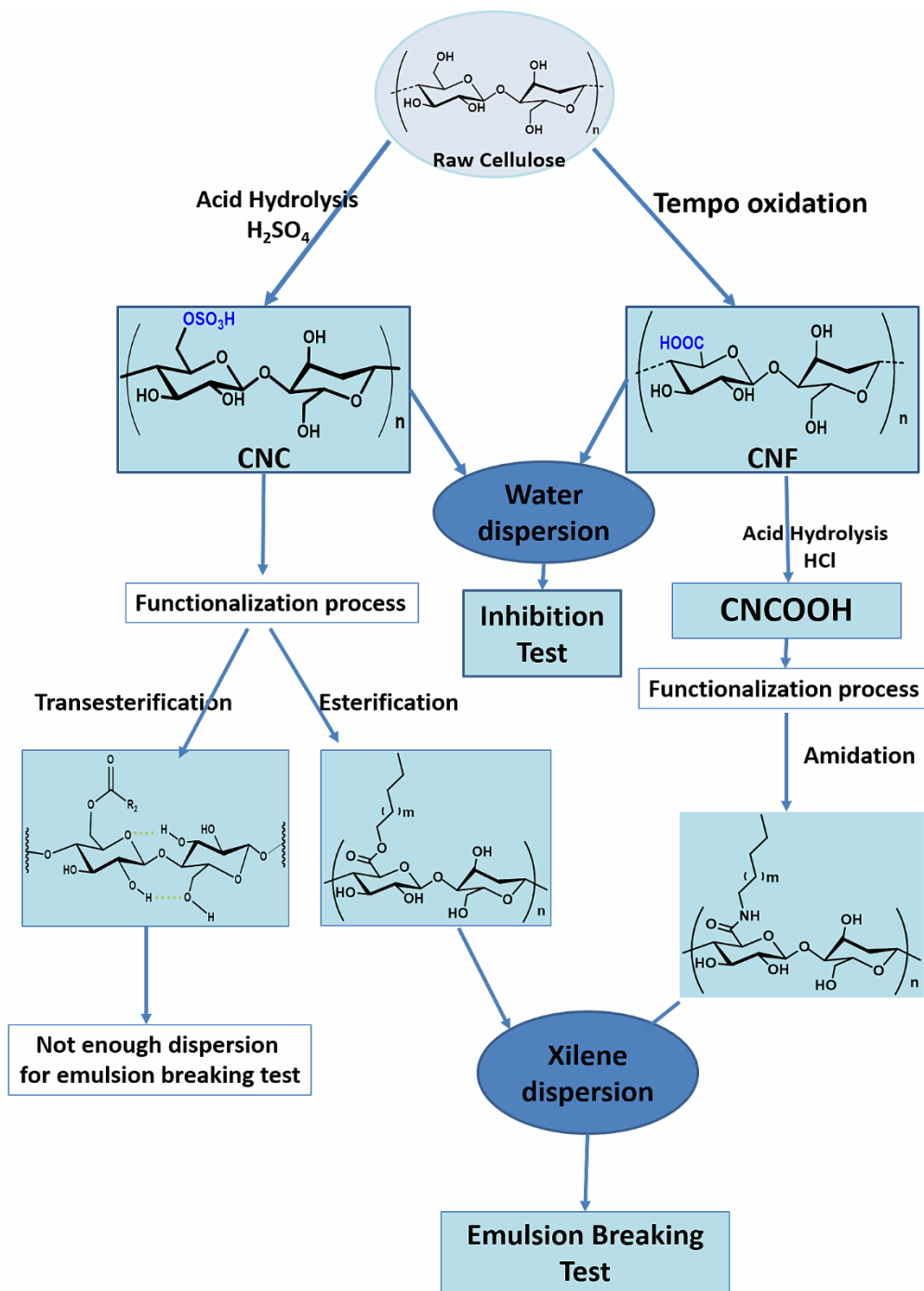


Figure 7. Schematic summary of our working hypothesis.

Each chapter in this manuscript describes the results associated with the structure shown in Figure 7. In chapter 2, we describe a process for cellulose nanocrystals (CNC) isolation via sulfuric acid hydrolysis, according to Bondenson *et al.*, (2006), followed by a CNC hydrophobization process by transesterification with palm oil using environmentally friendly reaction conditions. The raw and modified CNCs were characterized by spectroscopic, thermal, and microscopic methods. We observe formation of an ester functionality after the reaction, and improved thermal properties. However, when using this initial approach to obtain hydrophobic nanocelluloses, the raw CNC was dried in order to perform the reaction with the palm oil. Once modified, the hydrophobic material could not be redissolved in xylene at high enough concentrations as to perform demulsification tests. Thus, in this chapter we report the results of the materials characterization, but we were unable to test the material as an emulsion breaker as we initially intended. The results of this chapter were submitted as a Research Article to the Journal *Universitas Scientiarum*.

Chapter 3 focuses on the use of both CNF and CNC as w/o emulsion inhibitors. CNF with abundant COOH groups on the surface were isolated by oxidation with TEMPO while CNC, with sulfonic esters at the surface were produced by hydrolysis with acid sulfuric. We performed emulsion inhibition tests with the two types of nanocellulose in aqueous suspensions and found that they can compete efficiently with natural emulsifiers (such as asphaltenes), reducing the amount of emulsified water up to 75%. The results of this chapter were submitted as a Research Article to the Journal *Fuel*, and are also the basis of a patent currently under revision by the *Superintendencia de Industria y Comercio*.

In chapter 4, we describe the isolation and functionalization of CNC by two different methods.

Initially, we hydrolyze CNF with HCl to obtain CNC and then subjected this material to amidation to modulate its hydrophilicity. In the second approach, we obtained CNC directly acid hydrolysis with sulfuric acid, and then modified the material by reaction with palmitoyl phosphonates in the presence of NaH. The functionalization process was carried out with the aim of rendering the CNC hydrophobic, so that they could be dispersed in xylene and used as emulsion breakers. These materials were able to break a stable w/heavy oil emulsion and recover up to 77% of free water. We are currently working on a draft manuscript to submit the results of this chapter for publication.

Chapter 5 contains the conclusions of the research and recommendations for future developments in the subject.

1.6 References

- Al-Sabagh, A. M., Nasser, N. M., & Abd El-Hamid, T. M. (2013). Investigation of Kinetic and Rheological Properties for the Demulsification Process. *Egyptian Journal of Petroleum*, 22(1), 117–127. <https://doi.org/10.1016/j.ejpe.2012.11.013>
- Al-Sabagh, A., Ahmed, N. S., Nassar, A. M., & Gabr, M. (2003). Synthesis and evaluation of some polymeric surfactants for treating crude oil emulsions. *Colloids and Surfaces A: Physicochemical and Engineering Aspects*, 216(1–3), 9–19. [https://doi.org/10.1016/s0927-7757\(02\)00493-4](https://doi.org/10.1016/s0927-7757(02)00493-4)
- Andresen, M., & Stenius, P. (2007). Water-in-oil emulsions stabilized by hydrophobized microfibrillated cellulose. *Journal of Dispersion Science and Technology*, 28(6), 837–844. <https://doi.org/10.1080/01932690701341827>

- Bai, L., Huan, S., Xiang, W., & Rojas, O. J. (2018). Pickering emulsions by combining cellulose nanofibrils and nanocrystals: Phase behavior and depletion stabilization. *Green Chemistry*, *20*(7), 1571–1582. <https://doi.org/10.1039/c8gc00134k>
- Becerril, J. Contaminantes emergentes en el agua. *Revista Digital Universitaria Unam* [en línea], (2009), (10) 8. Disponible en Internet: <<http://www.revista.unam.mx/vol.10/num8/art54/int54.htm>>
- Berlitz, S., Molina-Boisseau, S., Nishiyama, Y., & Heux, L. (2009). Gas-phase surface esterification of cellulose microfibrils and whiskers. *Biomacromolecules*, *10*(8), 2144–2151. <https://doi.org/10.1021/bm900319k>
- Bhardwaj, A., & Hartland, S. (1993). Applications of Surfactants in Petroleum Industry. *Journal of Dispersion Science and Technology*, *14*(1), 87–116. <https://doi.org/10.1080/01932699308943389>
- Bondeson, D., Mathew, A., & Oksman, K. (2006). Optimization of the isolation of nanocrystals from microcrystalline cellulose by acid hydrolysis. *Cellulose*, *13*(2), 171–180. <https://doi.org/10.1007/s10570-006-9061-4>
- Capron, I., Rojas, O. J., & Bordes, R. (2017). Behavior of nanocelluloses at interfaces. *Current Opinion in Colloid and Interface Science*, *29*, 83–95. <https://doi.org/10.1016/j.cocis.2017.04.001>
- Chen, Q. H., Zheng, J., Xu, Y. T., Yin, S. W., Liu, F., & Tang, C. H. (2018). Surface modification improves fabrication of pickering high internal phase emulsions stabilized by cellulose

- nanocrystals. *Food Hydrocolloids*, 75, 125–130.
<https://doi.org/10.1016/j.foodhyd.2017.09.005>
- Du, H., Liu, W., Zhang, M., Si, C., Zhang, X., & Li, B. (2019). Cellulose nanocrystals and cellulose nanofibrils based hydrogels for biomedical applications. *Carbohydrate Polymers*, (209), 130–144. <https://doi.org/10.1016/j.carbpol.2019.01.020>
- Djuve, J., Yang, X., Fjellanger, I. J., Sjöblom, J., & Pelizzetti, E. (2001). Chemical destabilization of crude oil based emulsions and asphaltene stabilized emulsions. *Colloid and Polymer Science*, 279(3), 232–239. <https://doi.org/10.1007/s003960000413>
- Fan, Y., Simon, S., & Sjöblom, J. (2009). Chemical destabilization of crude oil emulsions: Effect of nonionic surfactants as emulsion inhibitors. *Energy and Fuels*, 23(9), 4575–4583. <https://doi.org/10.1021/ef900355d>
- Fernandez, A., Salager, J., & Scorzza, C. S. (2004). IV Surfactantes no Iónicos. *Universidad de los Andes, Mérida (Venezuela)*.
- Filson, P. B., & Dawson-andoh, B. E. (2009). Sono-chemical preparation of cellulose nanocrystals from lignocellulose derived materials. *Bioresource Technology*, 100(7), 2259–2264. <https://doi.org/10.1016/j.biortech.2008.09.062>
- Fujisawa, S., Okita, Y., Fukuzumi, H., Saito, T., & Isogai, A. (2011). Preparation and characterization of TEMPO-oxidized cellulose nanofibril films with free carboxyl groups. *Carbohydrate Polymers*, 84(1), 579–583. <https://doi.org/10.1016/j.carbpol.2010.12.029>
- Fukuzumi, H., Saito, T., & Isogai, A. (2013). Influence of TEMPO-oxidized cellulose nanofibril

- length on film properties. *Carbohydrate Polymers*, 93(1), 172–177.
<https://doi.org/10.1016/j.carbpol.2012.04.069>
- George, J. (2012). High performance edible nanocomposite films containing bacterial cellulose nanocrystals. *Carbohydrate Polymers*, 87(3), 2031–2037.
<https://doi.org/10.1016/j.carbpol.2011.10.019>
- George, J., & Sabapathi, S. N. (2015). Cellulose nanocrystals: Synthesis, functional properties, and applications. *Nanotechnology, Science and Applications*, 8, 45–54.
<https://doi.org/10.2147/NSA.S64386>
- Goussé, C., Chanzy, H., Excoffier, G., Soubeyrand, L., & Fleury, E. (2002). Stable suspensions of partially silylated cellulose whiskers dispersed in organic solvents. *Polymer*, 43(9), 2645–2651. [https://doi.org/10.1016/S0032-3861\(02\)00051-4](https://doi.org/10.1016/S0032-3861(02)00051-4)
- Habibi, Y., Lucia, L. A., & Rojas, O. J. (2010). Cellulose nanocrystals: Chemistry, self-assembly, and applications. *Chemical Reviews*, 110(6), 3479–3500.
<https://doi.org/10.1021/cr900339w>
- Hou, J., Feng, X., Masliyah, J., & Xu, Z. (2012). Understanding interfacial behavior of ethylcellulose at the water-diluted bitumen interface. *Energy and Fuels*, 26(3), 1740–1745.
<https://doi.org/10.1021/ef201722y>
- Kalashnikova, I., Bizot, H., Cathala, B., & Capron, I. (2012). Modulation of cellulose nanocrystals amphiphilic properties to stabilize oil/water interface. *Biomacromolecules*, 13(1), 267–275. <https://doi.org/10.1021/bm201599j>

- Khalil, H. A., Davoudpour, Y., Islam, M. N., Mustapha, A., Sudesh, K., Dungani, R., & Jawaid, M. (2014). Production and modification of nanofibrillated cellulose using various mechanical processes: a review. *Carbohydrate polymers*, *99*, 649-665.
- Kim, H., & Wasan, T. (1995). A study of dynamic interfacial mechanisms for demulsification of water-in-oil emulsions. *Colloids and Surface*, *95*, 235–247.
- Kokal, S. L. (2005). Crude Oil Emulsions: A State-Of-The-Art Review. *SPE Production & Facilities*, *20* (01), 5–13. <https://doi.org/10.2118/77497-PA>
- Krishnamachari, P., Hashaiken, M., Chiesa, M., Gad, K. R. (2012). Effects of acid hydrolysis time on cellulose nanocrystals properties: Nanoindentation and thermogravimetric studies. *Cellulose Chemistry and Technology*, *46*(1–2), 13–18. Retrieved from [http://www.cellulosechemtechnol.ro/pdf/CCT1-2\(2012\)/p.13-18.pdf](http://www.cellulosechemtechnol.ro/pdf/CCT1-2(2012)/p.13-18.pdf)
- Li, X., Li, J., Gong, J., Kuang, Y., Mo, L., & Song, T. (2018). Cellulose nanocrystals (CNCs) with different crystalline allomorph for oil in water Pickering emulsions. *Carbohydrate Polymers*, *183*(1), 303–310. <https://doi.org/10.1016/j.carbpol.2017.12.085>
- Li, S., Li, C., Li, C., Yan, M., Wu, Y., Cao, J., & He, S. (2013). Fabrication of nano-crystalline cellulose with phosphoric acid and its full application in a modified polyurethane foam. *Polymer Degradation and Stability*, *98*(9), 1940–1944. <https://doi.org/10.1016/j.polymdegradstab.2013.06.017>
- Lif, A., Stenstad, P., Syverud, K., Nydén, M., & Holmberg, K. (2010). Fischer–Tropsch diesel emulsions stabilised by microfibrillated cellulose and nonionic surfactants. *Journal of*

- colloid and interface science*, 352(2), 585-592. <https://doi.org/10.1016/j.jcis.2010.08.052>
- Liu, Y., Wang, H., Yu, G., Yu, Q., Li, B., & Mu, X. (2014). A novel approach for the preparation of nanocrystalline cellulose by using phosphotungstic acid. *Carbohydrate Polymers*, 110, 415–422. <https://doi.org/10.1016/j.carbpol.2014.04.040>
- Marfisi, S. (2005). “Estabilidad de emulsiones relacionada con el proceso de deshidratación de crudos.” Universidad de los Andes.
- Martínez-Sanz, M., Lopez-Rubio, A., & Lagaron, J. M. (2011). Optimization of the nanofabrication by acid hydrolysis of bacterial cellulose nanowhiskers. *Carbohydrate Polymers*, 85(1), 228–236. <https://doi.org/10.1016/j.carbpol.2011.02.021>
- McClements, D. J. (2004). Protein-stabilized emulsions. *Current Opinion in Colloid & Interface Science*, 9(5), 305–313. <https://doi.org/10.1016/j.cocis.2004.09.003>
- Mikulcová, V., Bordes, R., Minařík, A., & Kašpárková, V. (2018). Pickering oil-in-water emulsions stabilized by carboxylated cellulose nanocrystals – Effect of the pH. *Food Hydrocolloids*, 80, 60–67. <https://doi.org/10.1016/j.foodhyd.2018.01.034>
- Rein, D. M., Khalfin, R., & Cohen, Y. (2012). Cellulose as a novel amphiphilic coating for oil-in-water and water-in-oil dispersions. *Journal of Colloid and Interface Science*, 386(1), 456–463. <https://doi.org/10.1016/j.jcis.2012.07.053>
- Revol, J. F., Bradford, H., Giasson, J., Marchessault, R. H., & Gray, D. G. (1992). Helicoidal self-ordering of cellulose microfibrils in aqueous suspension. *International Journal of Biological Macromolecules*, 14(3), 170–172. <https://doi.org/10.1016/S0141->

8130(05)80008-X

- Rojas, O. J., Bullon, J., Ysambertt, F., Forgiarini, A., Salager, J.-L., & Argyropoulos, D. S. (2007). Lignins as emulsion stabilizers. *In ACS symposium series* (Vol. 954, pp. 182–199). Oxford University Press. Retrieved from <http://cat.inist.fr/?aModele=afficheN&cpsidt=18707830>
- Rol, F., Belgacem, M. N., Gandini, A., & Bras, J. (2019). Recent advances in surface-modified cellulose nanofibrils. *Progress in Polymer Science*, 88, 241–264. <https://doi.org/10.1016/j.progpolymsci.2018.09.002>
- Rondón, M., Bouriat, P., Lachaise, J., & Salager, J. L. (2006). Breaking of water-in-crude oil emulsions. 1. Physicochemical phenomenology of demulsifier action. *Energy and Fuels*, 20(4), 1600–1604. <https://doi.org/10.1021/ef060017o>
- Sadeghifar, H., Filpponen, I., Clarke, S. P., Brougham, D. F., & Argyropoulos, D. S. (2011). Production of cellulose nanocrystals using hydrobromic acid and click reactions on their surface. *Journal of Materials Science*, 46(22), 7344–7355. <https://doi.org/10.1007/s10853-011-5696-0>
- Salager, J. (1992). *El mundo de los surfactantes* (first, Vol. 01). Mérida-Venezuela: Universidad de los Andes.
- Salas, C., Nypelö, T., Rodríguez-Abreu, C., Carrillo, C., & Rojas, O. J. (2014). Nanocellulose properties and applications in colloids and interfaces. *Current Opinion in Colloid & Interface Science*, 19(5), 383–396. <https://doi.org/10.1016/j.cocis.2014.10.003>
- Salajkova, M., Berglund, L. a., Zhou, Q., Salajková, M., Berglund, L. a., & Zhou, Q. (2012).

- Hydrophobic cellulose nanocrystals modified with quaternary ammonium salts. *Journal of Materials Chemistry*, 22(37), 19798. <https://doi.org/10.1039/c2jm34355j>
- Schramm, L. L. (2001). *Surfactants: Fundamentals and Applications in the Petroleum Industry*. Cambridge University Press (First, Vol. 16). *Cambridge: press syndicate of the University of Cambridge*. <https://doi.org/10.2307/3515635>
- Song, Q., Winter, W., Bujanovic, B., & Amidon, T. (2014). Nanofibrillated Cellulose (NFC): A High-Value Co-Product that Improves the Economics of Cellulosic Ethanol Production. *Energies*, 7(2), 607–618. <https://doi.org/10.3390/en7020607>
- Tanaka, R., Saito, T., & Isogai, A. (2012). Cellulose nanofibrils prepared from softwood cellulose by TEMPO/NaClO/NaClO₂ systems in water at pH 4.8 or 6.8. *International Journal of Biological Macromolecules*, 51(3), 228–234. <https://doi.org/10.1016/j.ijbiomac.2012.05.016>
- Tang, J., Sisler, J., Grishkewich, N., & Tam, K. C. (2017). Functionalization of cellulose nanocrystals for advanced applications. *Journal of Colloid and Interface Science*, 494, 397–409. <https://doi.org/10.1016/j.jcis.2017.01.077>
- Thomas, B., Raj, M. C., Athira, K. B., Rubiyah, M. H., Joy, J., Moores, A., & Drisko, G. L. (2018). Nanocellulose, a Versatile Green Platform: From Biosources to Materials and Their Applications. *Chemical Reviews*, 118, 11575–11625. <https://doi.org/10.1021/acs.chemrev.7b00627>
- Wang, Y., Wang, W., Jia, H., Gao, G., Wang, X., Zhang, X., & Wang, Y. (2018). Using Cellulose

Nanofibers and Its Palm Oil Pickering Emulsion as Fat Substitutes in Emulsified Sausage.

Journal of Food Science, 0. <https://doi.org/10.1111/1750-3841.14164>

Winuprasith, T., & Suphantharika, M. (2013). Microfibrillated cellulose from mangosteen (*Garcinia mangostana* L.) rind: Preparation, characterization, and evaluation as an emulsion stabilizer. *Food Hydrocolloids*, 32(2), 383–394. <https://doi.org/10.1016/j.foodhyd.2013.01.023>

Ye, Z., Feng, M., Gou, S., Liu, M., Huang, Z., & Liu, T. (2013). Hydrophobically associating acrylamide-based copolymer for chemically enhanced oil recovery. *Journal of Applied Polymer Science*, 130(4), 2901–2911. <https://doi.org/10.1002/app.39424>

Zoppe, J. O., Venditti, R. A., & Rojas, O. J. (2012). Pickering emulsions stabilized by cellulose nanocrystals grafted with thermo-responsive polymer brushes. *Journal of Colloid and Interface Science*, 369(1), 202–209. <https://doi.org/10.1016/j.jcis.2011.12.011>

Chapter 2

2 Surface hydrophobization of cellulose nanocrystals via transesterification with triacylglycerols

2.1 Abstract

There is growing scientific interest in developing processes for cellulose nanocrystals (CNC) surface modification. Particularly, environmentally benign ways to modulate CNC polarity and to improve its compatibility with organic matrices for various applications. This contribution explores the use of a one-pot transesterification reaction between CNC and triacylglycerols from palm oil, to increase CNC hydrophobicity. Changes in CNC surface composition, chemical structure, crystallinity, morphology, and thermal stability were investigated by FTIR, NMR, X-ray diffraction (XRD), scanning electron microscopy (SEM), and thermogravimetric analysis (TGA), respectively. Molecular spectroscopy shows the presence of carboxylic moieties and alkyl groups on the CNC surface after the transesterification reaction. Modified CNC exhibits the same crystallographic pattern than raw CNC, indicating no alteration in the cellulose crystal structure after hydrolysis and surface modification. The presence of alkyl units on the surface of the cellulose hinders hydrogen bond formation, reducing aggregate formation and increasing the decomposition temperature of cellulose. The thermal stability of modified CNC increased up to 319 °C, in comparison with 290 °C for raw CNC.

2.2 Introduction

A growing world requires ever increased amounts of supplies and materials. Trends in sustainable development advocate for the use of renewable sources to replace synthetically derived products and to decrease negative environmental impacts. Biomaterials derived from lignocellulosic biomass — a by-product of intensive agro-industrial activity-, are currently transforming the field of material sciences. Cellulose-derived nanomaterials or nanocelluloses, in particular, are dynamic and innovative structures with a wide range of applications (Durán, Lemes & Seabra, 2012; Habibi, Lucia & Rojas, 2010; Islam, Alam & Zoccola, 2013; Jonoobi *et al.* 2015; Mariano, El Kissi, & Dufresne, 2014). While these materials preserve the structural identity of the cellulosic biopolymer, they have improved mechanical, thermal, rheological, and surface-active properties (Liu *et al.*, 2011) when compared with the bulk material.

Cellulose is invariably biosynthesized in nature by plants, animals, and microorganisms (Krishnamachari, P., Hashaikeh, R., & Tiner, 2011; Park, Baker, Himmel, Parilla & Johnson, 2010; Ummartyotin & Manuspiya, 2015; Zhu *et al.*, 2016), as a complex polymeric structure with crystalline and amorphous sections. Deconstruction of native cellulosic macrofibers, via chemical, mechanical or enzymatic treatments, produces two kinds of nanomaterials: nanofibers (CNF) and nanocrystals (CNC). The former exhibit widths of about 20 nm and lengths of a few microns and contains both crystalline and amorphous cellulose; while the latter is smaller, with widths between 3 nm to 50 nm and lengths of 100–500 nm (Peng, Dhar, Liu & Tam, 2011; George & Sabapathi 2015), displaying cylindrical shapes and a much higher degree of crystallinity (Habibi *et al.*, 2010). There are numerous ways of producing CNC, with the sulfuric acid hydrolysis as the most common method at the laboratory and commercial scales (Lu & Hsieh 2010, Lu & Hsieh, 2012; Mandal &

Chakrabarty 2011). From a chemical reactivity point of view, the crystalline regions of cellulose are inaccessible to attack by acids and enzymes; while the amorphous parts are susceptible to hydrolysis due to increased chain spacing and diminished density (Krishnamachari, Hashaiken, Chiesa & Gad, 2011; Rosa *et al.*, 2010). Hydrochloric (HCl) (Araki & Mishima, 2015; Lin, Chang & Hsu, 2009), sulfuric (H₂SO₄) (Araki, Wada, Kuga & Okano, 1998), hydrobromic (HBr) (Qiao, Chen, Zhang & Yao, 2016; Habibi *et al.*, 2006), nitric (HNO₃) (Liu, Zhong, Chang, Li & Wu, 2010), phosphoric (H₃PO₄) (Wei, Kumar & Banker, 1996; Li *et al.*, 2013), maleic (Filson & Dawsonandoh, 2009) and, recently, phosphotungstic (HPW, H₃PW₁₂O₄₀) (Liu *et al.*, 2014) are the acids reportedly used in the cellulose hydrolysis process. The substitution of mineral acids for acid solids such as HPW has been investigated for environmental and sustainability reasons.

In 2006 Bodenson and his colleagues reported one of the most used procedures for CNC extraction involving the hydrolysis of cellulose (130 min/45°C) with sulfuric acid (63,5%) using a loading of 10,2 g cellulose/100 mL acid (Bondeson, Mathew & Oksman, 2006). This reaction was followed by 30 min of mechanical disintegration by sonication. The procedure afforded a 30% yield of CNC, with lengths between 200 and 400 nm and widths around 10 nm. We followed this procedure for CNC extraction in this contribution.

Cellulose hydrolysis with sulfuric acid involves protonation of the glycosidic oxygen atom followed by bond cleavage, particularly in the amorphous regions of cellulose. Also, this process introduces negative charges on the resultant CNC, in the form of sulfate groups at carbon C6 in the anhydroglucose unit, due to esterification reactions between primary -OH (C6) and sulfuric acid (Beck-Candanedo, Roman & Gray, 2005; Roman & Winter, 2004). Thus, CNC from acid hydrolysis form stable suspensions in water as charge repulsion prevents agglomeration; however,

the thermal stability of CNC is affected negatively by the presence of sulfate groups (Roman & Winter, 2004; Rosa *et al.*, 2010). In general, raw CNC from acid hydrolysis have polar surfaces, readily dispersible in polar/hydrophilic matrices.

Surface modification is at the heart of CNC research since it is fundamental for tailoring properties related to compatibility with hydrophilic and hydrophobic media. A recent review by Thomas *et al.* (2018) summarizes the main surface modifications of nanocellulose to date. Among the most common processes to produce ionic surfaces are phosphorylation, carboxymethylation, oxidation, and sulfonation. On the other hand, hydrophobization typically involves non-specific self-assembly processes, *e.g.*, non-covalent adsorption of molecules through electrostatic interactions (Lam, Chong, Leung & Luong, 2012; Salajkova *et al.*, 2012), or covalent bonding of non-polar compounds/functional groups (Yuan, Nishiyama & Kuga, 2006; Zaman, Xiao, Chibante & Ni, 2012). The latter include acetylation, etherification, esterification, silylation, urethanization, and amidation (Peng *et al.*, 2011; Eyley & Thielemans, 2014). Increasing CNC hydrophobicity is fundamental to improve affinity with nonpolar solvents for applications such as synthetic polymer reinforcements (Yu, Qin & Zhou, 2011; Liu *et al.*, 2010, Oksman *et al.*, 2016), rheology modifiers, or fabrication of hydrophobic surfaces and films.

However, most hydrophobization methods are costly, elaborated, and time-consuming. In 2007 Dankovich & Hsieh, reported a straightforward process for bulk cellulose esterification where a wide variety of substrates (microcrystalline cellulose, Whatman filter paper, and cotton fabrics) were treated with plant-derived triacylglycerols to yield hydrophobic materials. Based on Dankovich report, we investigate the hydrophobization of CNC using triacylglycerols in Palm oil. Also, we report the spectroscopic, thermal, and morphologic features of raw and hydrophobic

CNC.

2.3 Experimental

2.3.1 Materials. Sulfuric acid (H₂SO₄) sodium hydroxide (NaOH) and acetone (CH₃COCH₃) were purchased from Merck (Darmstadt, Germany). Whatman qualitative filter paper (grade 1) was acquired from Sigma Aldrich (St. Louis, MO, USA). A cellulose dialysis membrane (12-14 kDa) was purchased from Spectrum Labs (Irving, TX, USA). Aqueous solutions were prepared using deionized water (18.2 MΩ). Commercial palm oil was used as triacylglycerol source with an average composition of unsaturated fatty acids: oleic (36-44%) and linoleic (9-12%); and saturated: palmitic (39.3-47.5%) and stearic (3.5-6%) (Rincón & Martínez, 2009). All reagents were used without further purification.

2.3.2 Methods

2.3.2.1 CNC isolation. Whatman paper (5 g) was mixed with a concentrated sulfuric acid solution (60 mL, 62%), the mixture was heated at 45 °C for two hours after which a ten-fold excess of deionized water was added to stop the hydrolysis reaction. The resulting suspension was then centrifuged (4700 rpm), the supernatant was discarded, and the solid was sequentially washed with water until pH 1 and dialyzed for ten days (batch 1). Similarly, a second batch of CNC was prepared, but instead of the final dialysis step, a NaOH solution (0.1 N) was added to the suspension until pH 7 (batch 2).

Finally, to achieve a stable colloidal suspension, both CNC batches were sonicated for 20 min using an Ultrasonic processor (Sonic Vibra cell VC750, 20 kHz, 750 Watt). The vessel with the CNC suspensions was placed in an ice bath to prevent heating during sonication. The amount of

CNC in the suspension was determined via gravimetric analysis. The second batch was subjected to rotary evaporation and dispersion in acetone. The first batch was used in characterization processes and the second in functionalization.

2.3.2.2 Sulfate Groups Quantitation in CNC. Conductometric titrations were performed using a HANNA HI 8733 conductivity meter (Carrollton, TX, USA), before CNC modification, to determine the number of sulfate groups on the CNC surface. Titrations were performed on mixtures of CNC suspensions (100 mL, 2 g/L) with NaCl (2 mL, 0.05 M) solutions, adding 10 μ L aliquots of NaOH (0.0197 N) dropwise under continuous stirring, according to a procedure previously reported (Abitbol, Kloser & Gray, 2013; Beck, Méthot & Bouchard, 2015; Roman & Winter, 2004) The modified CNC does not disperse in water so that the number of sulfate groups remaining after the functionalization process could not be measured.

2.3.2.3 CNC Esterification. We followed a transesterification procedure, slightly modified from the one reported by Dankovich and Hsieh (2007), using Palm oil as the triacylglyceride source. In short, a solution of the vegetable oil in acetone (1% p/v, 50 mL) was mixed with a CNC suspension in acetone from the second batch (2.5 g/L, 100 mL) under continuous stirring. The mixture was allowed to dry at room temperature, under a fume hood.

The resulting solid was heated at 120°C for 60 min in an oven. The reaction occurs according to the following mechanism (Figure 8.), where labile sulfate groups in CNC are replaced by fatty acids (Habibi *et al.*, 2006; Zaman *et al.* 2012; Capron, Guellec, Perrin, Cherhal & Saidane, 2016). Sulfate moieties are better-leaving groups than the C6-OH primary alcohol in the anhydroglucose unit.

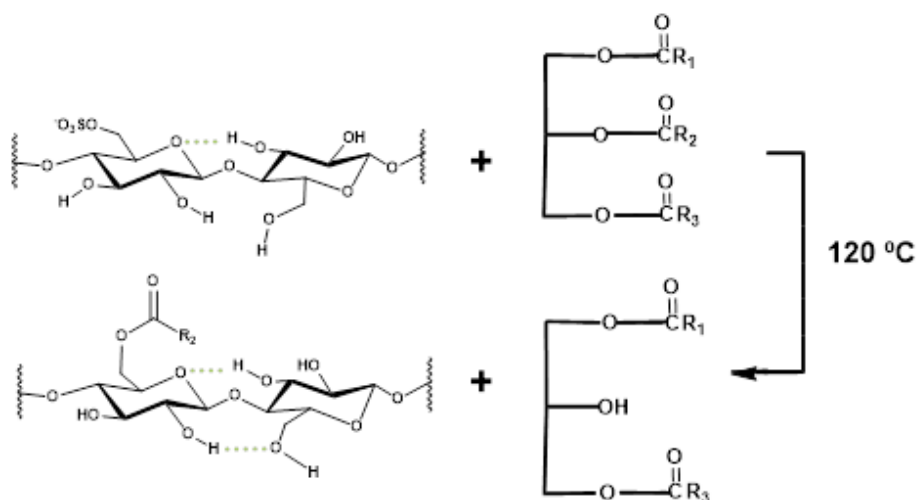


Figure 8. CNC and palm oil transesterification reaction

After reaction completion, reaction by-products were removed by a 12h Soxhlet cleaning step using acetone as solvent. The final product was lyophilized and stored under vacuum for characterization. Sodium sulfate and other sub-products, soluble in acetone, are eliminated in the filtrate.

2.3.2.4 CNC Characterization. FESEM images were acquired at 10 kV on a FEI QUANTA FEG 650 instrument (Oregon, USA) equipped with a Large Field Detector; samples were coated with a thin layer of gold before imaging. X-Ray diffraction analysis was performed on a Bruker D8 DISCOVER X-ray diffractometer (Billerica, MA) with DaVinci geometry, with a CuK α 1 radiation source (40 kV and 30 mA), an area detector VANTEC-500, and a poly (methyl methacrylate) sample holder. CNC crystallinity indices were determined using Segal's Method (Segal, Creely, Martin & Conrad, 1959) according to Equation 1:

$$CI = ((I_{002} - I_{AM})/I_{002}) \times 100$$

Equation 1

Where I_{002} correspond to the intensity at $2\theta = 24.2^\circ$ and I_{AM} the intensity in the amorphous region at $2\theta = 20^\circ$. Also, we used the Scherrer equation (Equation 2) to determine the size of the crystallite.

$$D = \frac{\lambda}{\beta \cos\theta}$$

Equation 2

Where λ is the X-rays wavelength, θ the diffraction angle for the (002) plane, and β the FWHM (full width at half maximum) of that same peak (French & Cintrón, 2013).

Attenuated Total Reflectance Fourier Transform Infrared spectroscopy (ATR-FTIR) measurements were performed using a Bruker Tensor 27 FTIR instrument equipped with a Platinum Diamond ATR unit A225/Q (Billerica, MA). A resolution of 2 cm^{-1} , 32 scans were accumulated for each spectrum. Solid-state ^{13}C -NMR experiments were performed with a Bruker Avance DSX 450 MHz spectrometer (Billerica, MA), using proton decoupling and magic angle spinning (CP/MAS) methods. Experimental parameters for ^{13}C CP-MAS NMR experiments include 7000 scans, spinning rate of 11.3 kHz, acquisition time of 0.02 s, and temperature of 278 K. Thermal analysis of raw and modified CNC was performed on a TA Discovery TGA (Newcastle, England), instrument fitted with an infrared heating oven, a temperature controlled thermobalance, a gas supply module, and an autosampler system. Nitrogen was used as an inert gas at a flow of 50 mL/min and a heating rate of $10^\circ\text{C}/\text{min}$ starting from room temperature to 600

°C (Roman and Winter 2004b).

2.4 Results and discussion

2.4.1 Raw CNC Morphology. We observed CNC yields of 60% for the hydrolysis process using Whatman paper as cellulose source and sulfate contents of 110 mmol SO_3^-/kg on their surface. In Figure 9. FESEM micrographs of CNC show a porous aerogel structure, for a concentrated CNC solution; and elongated structures with diameters up to 30 nm and lengths between 100 to 300 nm for a diluted CNC solution. These values coincide with DLS measurements, where a single peak at 170 nm is observed. The sizes and shapes from FESEM analysis are consistent with data reported in the literature (Brinchi, Cotana, Fortunati & Kenny, 2013). Because CNC shapes and sizes are source-dependent, the material extracted from Whatman paper is similar to CNC isolated from cotton linter.

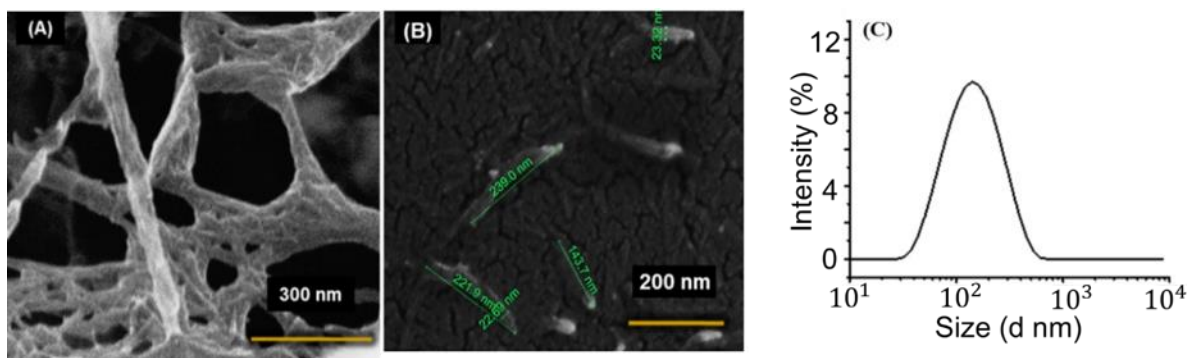


Figure 9. FESEM images of raw CNC, from a concentrated (A) and a diluted (B) solution.

Dynamic light scattering (DLS) for a CNC solution (0,2 g/L).

2.4.2 Spectroscopic characterization. Figure 10.A shows the full-range IR spectra of raw and modified CNC. We observed typical cellulose signals in both samples, which are consistent with those reported by several authors (Abraham *et al.*, 2011; Jiang & Hsieh 2013; Sheltami, Abdullah, Ahmad, Dufresne & Kargarzadeh, 2012; Yuan & Kuga 2005). For instance, a broad band between 3650 and 3000 cm^{-1} corresponds to stretching vibrations of the OH bond while the signal at 2896 cm^{-1} is due to C-H stretch. The C6-H2 flexion was observed at 1424, and 1315 cm^{-1} and the characteristic C-O-C and C-O stretching vibrations of cellulose were detected at 1160 cm^{-1} and 1055, 1032 cm^{-1} , respectively (Jiang & Hsieh, 2013). The anomeric carbon (C1-H) vibration lies at 900 cm^{-1} (Braun and Dorgan 2009). Figure 10.A also shows a zoom of the region between 1900 and 1500 cm^{-1} where a new peak at 1743 cm^{-1} was observed only for the modified CNC. This particular signal, attributed to the presence of carboxylic moieties of esters in cellulose, has been previously reported by several authors (Boujemaoui, Mongkhontreerat, Malmström & Carlmark, 2015; Braun & Dorgan, 2009; Lee *et al.*, 2011; Lee & Bismarck 2012; Sèbe, Ham-Pichavant & Pecastaings, 2013).

Figure 10. B presents the full solid-state ^{13}C NMR spectra of raw and modified CNC showing signals characteristic of crystalline cellulose I at 105, 89, 74-72 and 65 ppm corresponding to C1, C4, C2, C3, C5, and C6 of the anhydroglucose unit, respectively, as reported by several authors (Gårdebjer *et al.*, 2015; Hu, Berry, Pelton & Cranston, 2017; Sèbe, Ham-Pichavant, Ibarboue, Koffi & Tingaut, 2012). A peak at 30 ppm in the NMR-MAS spectrum of the modified CNC indicates the presence of CH_2 units corresponding to alkyl chains on the CNC surface as reported previously by other authors (Spinella *et al.*, 2016). We also observed some signals around 170 ppm in the full -range NMR spectrum of the modified sample. A zoom of the region (Figure 10. B) shows, in fact, a weak signal at 176 ppm corresponding to carbonyl ester moieties in the sample,

also reported by previous studies on nanocellulose esterification (Berlioz, Molina-Boisseau, Nishiyama & Heux, 2009; Ramírez, Suriano, Cerrutti & Foresti, 2014; Vuoti, Talja, Johansson, Heikkinen & Tammelin, 2013)

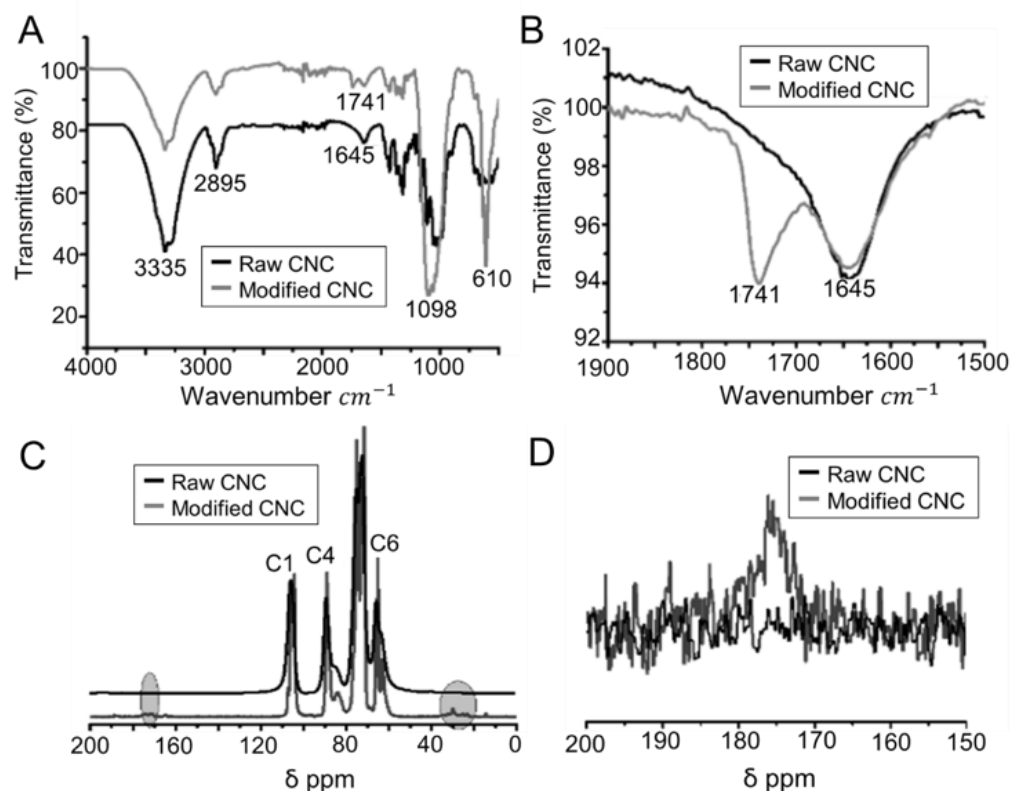
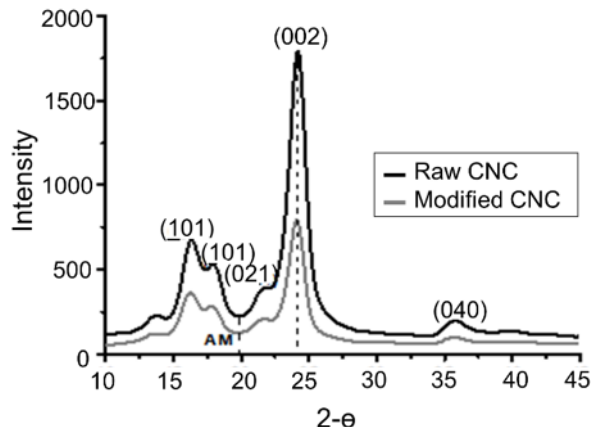


Figure 10. (A) Full-range and (B) zoomed IR spectra of raw (black) and modified CNC (grey), (C) Full range solid NMR spectrum of raw CNC (black) and modified CNC (grey) and (D) zoom in the region between 150 to 200 ppm with elimination of rotational echoes.

The presence of signals characteristic of carbonyl groups in both IR and solid NMR spectra demonstrate the occurrence of a transesterification reaction between raw CNC and the acyl glycerides in Palm oil. Thus, we believe that it is possible to modify CNC using the hydrophobization process developed initially by Dankovich & Hsieh (2007) for bulk cellulose.

2.4.3 Crystallinity. Interactions between native cellulose and strong acids/bases can potentially alter the crystal structure of the biopolymer. We used XRD measurements to determine the impact of the H₂SO₄ hydrolysis and the transesterification reaction on the crystallinity of the resultant CNC. In Figure 11. the X-ray diffractogram of CNC shows five signals at $2\theta = 16.3^\circ, 18^\circ, 21.8^\circ, 24^\circ$ and 35.8° corresponding to (-101), (101), (021), (002), (040) planes characteristic of cellulose type I (French, 2014). The XRD data indicates no change in crystal structure during the hydrolysis reaction used to obtain the raw CNC. Besides, on Figure 11. also shows (overlapped) the XRD pattern for the modified CNC after transesterification with Palm oil. The hydrophobic CNC exhibits the same crystallographic pattern than the raw CNC, with only slight variations in the intensities, indicating that the functionalization process does not interfere with the internal structure of CNC and the reactions occur only on the surface of the material. The crystallinity indexes (CI) for raw and modified CNC, using Segal's method are 88 and 84 %, respectively. The small decrease in CI, after modification, is perhaps a consequence of alkyl chains addition to the cellulose surface during transesterification. The CI values of Figure 11. agree with those reported in the literature for CNC from other sources (Boujemaoui *et al.*, 2015). Interestingly, we also observed a slight increase in crystallite size, from 6,23 to 6.63 nm, after the functionalization process.



Sample	%CI	Crystallite size (nm)
Raw CNC	88.3	6.23
Modified CNC	84.0	6.63

Figure 11. XRD patterns, crystallinity index and crystallite size for raw (black) and modified CNC (grey).

2.4.4 Thermal behavior. The thermal stability of raw and modified CNC was investigated by thermogravimetric analysis (TGA) as seen in Figure 12.. TGA shows an initial loss of mass in the region of 30-200 °C related to moisture present in the sample. For CNC this loss corresponds to 3.35% of the initial mass, while for modified CNC corresponds to 2.1%, which is consistent with decreased hydrophilicity of the sample. The second part of the graph shows a sudden mass loss related to cellulose degradation processes. According to Peng *et al.*, (2013) between 200 and 350 °C dehydration, depolymerization and pyrolysis reactions occur involving loss of low molecular weight volatiles, levoglucosan formation, and production of flammable gases. In this region, we observed a weight loss of 62.1% for CNC and 73.2% for the modified CNC. For the raw CNC the maximum mass loss was observed at 290 °C, while for the modified CNC this loss is shifted to a higher temperature (319 °C).

The 29 °C difference in the mass loss maxima between raw and modified CNC may be due to a decrease of the sulfate groups on the surface of the modified CNC (Roman & Winter, 2004;

Wang, Ding & Cheng, 2007) and the presence of fatty acids on its surface. It is well known that the presence of alkyl units on the cellulose surface shields the material from thermal damage, delaying its degradation (Ashori, Babae, Jonoobi & Hamzeh, 2014; Lin, Chang, Yu, Huang & Feng, 2010; Ramírez *et al.*, 2014). At the end of the process, the mass loss slows leaving a residue of 14.3% for the raw CNC and 1.7% for the modified CNC. It has been reported that the presence of alkyl units on the surface of the cellulose also hinders aggregate formation by blocking hydrogen bonds between cellulose fibrils thus promoting complete degradation of the material and lowering the carbonaceous residue at high temperatures. (Peng *et al.*, 2013).

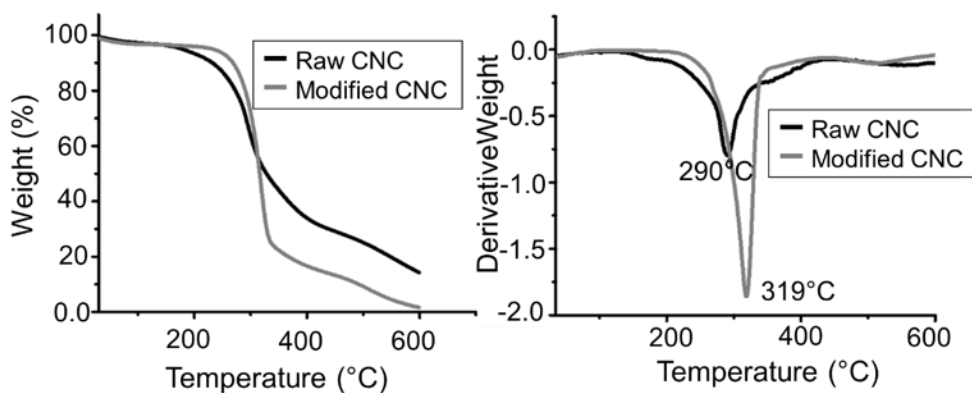


Figure 12. Thermal behavior of raw (black) and modified CNC (grey).

2.4.5 Solubility test. Finally, we tested the change in CNC surface polarity after esterification using a solubility test. We found that modified nanocellulose CNC (0,1 g/mL) completely disperses toluene and not in water as shown in Figure 13.

This behavior demonstrates an increased hydrophobic character for the modified CC, when compared with the raw CNC which completely disperse in aqueous phases.

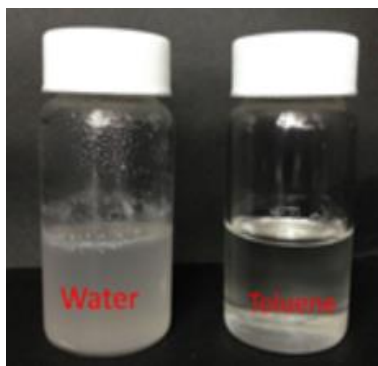


Figure 13. Solubility test of Modified CNC in water and Toluene

2.5 Conclusions

We use a one-pot transesterification reaction between CNC and triacylglycerols from palm oil, to increase CNC hydrophobicity. After transesterification with palm oil we observe characteristic signals for carbonyl groups and alkyl units in modified CNC by FTIR-ATR and solid NMR measurements. Thus, we corroborate the possibility of modifying CNC using the hydrophobization process initially developed by Dankovich & Hsieh (2007) for bulk cellulose. The crystallographic pattern for modified CNC is similar to the one for raw CNC, indicating no alteration in the cellulose crystal structure after hydrolysis and surface modification. The degradation temperature (T_d) for modified CNC increases 29 °C, in comparison with raw CNC, supporting the idea that the presence of fatty acids on the CNC surface hinders the material from thermal decomposition to a certain extent.

2.6 References

Abitbol, T., Kloser, E., & Gray, D. G. (2013). Estimation of the surface sulfur content of cellulose nanocrystals prepared by sulfuric acid hydrolysis. *Cellulose*, 20(2), 785–794.

<https://doi.org/10.1007/s10570-013-9871-0>

Abraham, E., Deepa, B., Pothan, L. a., Jacob, M., Thomas, S., Cvelbar, U., & Anandjiwala, R. (2011). Extraction of nanocellulose fibrils from lignocellulosic fibres: A novel approach. *Carbohydrate Polymers*, 86(4), 1468–1475. <https://doi.org/10.1016/j.carbpol.2011.06.034>

Araki, J., & Mishima, S. (2015). Steric stabilization of “charge-free” cellulose nanowhiskers by grafting of poly(ethylene glycol). *Molecules*, 20(1), 169–184. <https://doi.org/10.3390/molecules20010169>

Araki, J., Wada, M., Kuga, S., & Okano, T. (1998). Flow properties of microcrystalline cellulose suspension prepared by acid treatment of native cellulose. *Colloids and Surfaces A: Physicochemical and Engineering Aspects*, 142(1), 75–82. [https://doi.org/10.1016/S0927-7757\(98\)00404-X](https://doi.org/10.1016/S0927-7757(98)00404-X)

Ashori, A., Babae, M., Jonoobi, M., & Hamzeh, Y. (2014). Solvent-free acetylation of cellulose nanofibers for improving compatibility and dispersion. *Carbohydrate Polymers*, 102(1), 369–375. <https://doi.org/10.1016/j.carbpol.2013.11.067>

Beck, S., Méthot, M., & Bouchard, J. (2015). General procedure for determining cellulose nanocrystal sulfate half-ester content by conductometric titration. *Cellulose*, 22(1), 101–116. <https://doi.org/10.1007/s10570-014-0513-y>

Beck-Candanedo, S., Roman, M., & Gray, D. G. (2005). Effect of reaction conditions on the properties and behavior of wood cellulose nanocrystal suspensions. *Biomacromolecules*, 6(2), 1048–1054. <https://doi.org/10.1021/bm049300p>

- Benkaddour, A., Journoux-Lapp, C., Jradi, K., Robert, S., & Daneault, C. (2014). Study of the hydrophobization of TEMPO-oxidized cellulose gel through two routes: Amidation and esterification process. *Journal of Materials Science*, *49*(7), 2832–2843. <https://doi.org/10.1007/s10853-013-7989-y>
- Berlitz, S., Molina-Boisseau, S., Nishiyama, Y., & Heux, L. (2009). Gas-phase surface esterification of cellulose microfibrils and whiskers. *Biomacromolecules*, *10*(8), 2144–2151. <https://doi.org/10.1021/bm900319k>
- Bondeson, D., Mathew, A., & Oksman, K. (2006). Optimization of the isolation of nanocrystals from microcrystalline cellulose by acid hydrolysis. *Cellulose*, *13*(2), 171–180. <https://doi.org/10.1007/s10570-006-9061-4>
- Boujemaoui, A., Mongkhontreerat, S., Malmström, E., & Carlmark, A. (2015). Preparation and characterization of functionalized cellulose nanocrystals. *Carbohydrate Polymers*, *115*, 457–464. <https://doi.org/10.1016/j.carbpol.2014.08.110>
- Braun, B., & Dorgan, J. R. (2009). Single-step method for the isolation and surface functionalization of cellulosic nanowhiskers. *Biomacromolecules*, *10*(2), 334–341. <https://doi.org/10.1021/bm8011117>
- Brinchi, L., Cotana, F., Fortunati, E., & Kenny, J. M. (2013). Production of nanocrystalline cellulose from lignocellulosic biomass: technology and applications. *Carbohydrate Polymers*, *94*(1), 154–169. <https://doi.org/10.1016/j.carbpol.2013.01.033>
- Capron, I., Guellec, F., Perrin, E., Cherhal, F., & Saidane, D. (2016). Some modification of

- cellulose nanocrystals for functional Pickering emulsions. *Philosophical Transactions of the Royal Society A: Mathematical, Physical and Engineering Sciences*, 374(2072), 20150139. <https://doi.org/10.1098/rsta.2015.0139>
- Chen, J., Liu, W., Liu, C. M., Li, T., Liang, R. H., & Luo, S. J. (2015). Pectin Modifications: A Review. *Critical Reviews in Food Science and Nutrition*, 55(12), 1684–1698. <https://doi.org/10.1080/10408398.2012.718722>
- Cunha, A. G., & Gandini, A. (2010). Turing polysaccharides into hydrophobization materiales a crítica, review. Part 1. Cellulose. *Cellulose*, 17, 875–889. <https://doi.org/10.1007/s10570-010-9434-6>
- Cunha, A. G., & Gandini, A. (2010). Turning polysaccharides into hydrophobic materials: A critical review. Part 2. Hemicelluloses, chitin/chitosan, starch, pectin and alginates. *Cellulose*, 17(6), 1045–1065. <https://doi.org/10.1007/s10570-010-9435-5>
- Dankovich, T. A., & Hsieh, Y. Lo. (2007). Surface modification of cellulose with plant triglycerides for hydrophobicity. *Cellulose*, 14(5), 469–480. <https://doi.org/10.1007/s10570-007-9132-1>
- Durán, N., Lemes, A. P., & Seabra, A. B. (2012). Review of cellulose nanocrystals patents: preparation, composites and general applications. *Recent Patents on Nanotechnology*, 6(1), 16–28. Retrieved from <http://www.ncbi.nlm.nih.gov/pubmed/21875405>
- Eyley, S., & Thielemans, W. (2014). Surface modification of cellulose nanocrystals. *Nanoscale*, 6(14), 7764–7779. <https://doi.org/10.1039/c4nr01756k>

- Filson, P. B., & Dawson-andoh, B. E. (2009). Sono-chemical preparation of cellulose nanocrystals from lignocellulose derived materials. *Bioresource Technology*, *100*(7), 2259–2264. <https://doi.org/10.1016/j.biortech.2008.09.062>
- French, A. D. (2014). Idealized powder diffraction patterns for cellulose polymorphs. *Cellulose*, *21*(2), 885–896. <https://doi.org/10.1007/s10570-013-0030-4>
- French, A. D., & Santiago Cintrón, M. (2013). Cellulose polymorphy, crystallite size, and the Segal Crystallinity Index. *Cellulose*, *20*(1), 583–588. <https://doi.org/10.1007/s10570-012-9833-y>
- Gårdebjer, S., Bergstrand, A., Idström, A., Börstell, C., Naana, S., Nordstierna, L., & Larsson, A. (2015). Solid-state NMR to quantify surface coverage and chain length of lactic acid modified cellulose nanocrystals, used as fillers in biodegradable composites. *Composites Science and Technology*, *107*, 1–9. <https://doi.org/10.1016/j.compscitech.2014.11.014>
- George, J., & Sabapathi, S. N. (2015). Cellulose nanocrystals: Synthesis, functional properties, and applications. *Nanotechnology, Science and Applications*, *8*, 45–54. <https://doi.org/10.2147/NSA.S64386>
- Habibi, Y., Chanzy, H., & Vignon, M. R. (2006). TEMPO-mediated surface oxidation of cellulose whiskers. *Cellulose*, *13*(6), 679–687. <https://doi.org/10.1007/s10570-006-9075-y>
- Habibi, Y., Foulon, L., Aguié-Béghin, V., Molinari, M., & Douillard, R. (2007). Langmuir-Blodgett films of cellulose nanocrystals: preparation and characterization. *Journal of Colloid and Interface Science*, *316*(2), 388–397. <https://doi.org/10.1016/j.jcis.2007.08.041>

- Habibi, Y., Lucia, L. A., & Rojas, O. J. (2010). Cellulose nanocrystals: Chemistry, self-assembly, and applications. *Chemical Reviews*, *110*(6), 3479–3500.
<https://doi.org/10.1021/cr900339w>
- Hu, Z., Berry, R. M., Pelton, R., & Cranston, E. D. (2017). One-Pot Water-Based Hydrophobic Surface Modification of Cellulose Nanocrystals Using Plant Polyphenols. *ACS Sustainable Chemistry and Engineering*, *5*(6), 5018–5026.
<https://doi.org/10.1021/acssuschemeng.7b00415>
- Islam, M. T., Alam, M. M., & Zoccola, M. (2013). Review on modification of nanocelulose for application in composites. *International Journal of Innovative Research in Science, Engineeriong and Technology*, *2*(10), 5444–5451.
- Jiang, F., & Hsieh, Y. Lo. (2013). Chemically and mechanically isolated nanocellulose and their self-assembled structures. *Carbohydrate Polymers*, *95*(1), 32–40.
<https://doi.org/10.1016/j.carbpol.2013.02.022>
- Jonoobi, M., Oladi, R., Davoudpour, Y., Oksman, K., Dufresne, A., Hamzeh, Y., & Davoodi, R. (2015). Different preparation methods and properties of nanostructured cellulose from various natural resources and residues: a review. *Cellulose*.
<https://doi.org/10.1007/s10570-015-0551-0>
- Krishnamachari, P., Hashaikeh, R., & Tiner, M. (2011). Modified cellulose morphologies and its composites; SEM and TEM analysis. *Micron*, *42*(8), 751–761.
<https://doi.org/10.1016/j.micron.2011.05.001>

- Krishnamachari, P., Hashaiken, M., Chiesa, M., Gad, K. R. (2012). Effects of acid hydrolysis time on cellulose nanocrystals properties: Nanoindentation and thermogravimetric studies. *Cellulose Chemistry and Technology*, 46(1–2), 13–18. Retrieved from [http://www.cellulosechemtechnol.ro/pdf/CCT1-2\(2012\)/p.13-18.pdf](http://www.cellulosechemtechnol.ro/pdf/CCT1-2(2012)/p.13-18.pdf)
- Lam, E., Male, K. B., Chong, J. H., Leung, A. C. W., & Luong, J. H. T. (2012). Applications of functionalized and nanoparticle-modified nanocrystalline cellulose. *Trends in Biotechnology*, 30(5), 283–290. <https://doi.org/10.1016/j.tibtech.2012.02.001>
- Lee, K. Y., & Bismarck, A. (2012). Susceptibility of never-dried and freeze-dried bacterial cellulose towards esterification with organic acid. *Cellulose*, 19(3), 891–900. <https://doi.org/10.1007/s10570-012-9680-x>
- Lee, K. Y., Quero, F., Blaker, J. J., Hill, C. A. S., Eichhorn, S. J., & Bismarck, A. (2011). Surface only modification of bacterial cellulose nanofibres with organic acids. *Cellulose*, 18(3), 595–605. <https://doi.org/10.1007/s10570-011-9525-z>
- Li, S., Li, C., Li, C., Yan, M., Wu, Y., Cao, J., & He, S. (2013). Fabrication of nano-crystalline cellulose with phosphoric acid and its full application in a modified polyurethane foam. *Polymer Degradation and Stability*, 98(9), 1940–1944. <https://doi.org/10.1016/j.polymdegradstab.2013.06.017>
- Lin, J. H., Chang, Y. H., & Hsu, Y. H. (2009). Degradation of cotton cellulose treated with hydrochloric acid either in water or in ethanol. *Food Hydrocolloids*, 23(6), 1548–1553. <https://doi.org/10.1016/j.foodhyd.2008.10.005>

- Lin, N., Chang, P. R., Yu, J., Huang, J., & Feng, J. (2010). Surface acetylation of cellulose nanocrystal and its reinforcing function in poly(lactic acid). *Carbohydrate Polymers*, 83(4), 1834–1842. <https://doi.org/10.1016/j.carbpol.2010.10.047>
- Liu, D., Chen, X., Yue, Y., Chen, M., & Wu, Q. (2011). Structure and rheology of nanocrystalline cellulose. *Carbohydrate Polymers*, 84(1), 316–322. <https://doi.org/10.1016/j.carbpol.2010.11.039>
- Liu, D., Zhong, T., Chang, P. R., Li, K., & Wu, Q. (2010). Starch composites reinforced by bamboo cellulosic crystals. *Bioresource Technology*, 101(7), 2529–2536. <https://doi.org/10.1016/j.biortech.2009.11.058>
- Liu, H., Liu, D., Yao, F., & Wu, Q. (2010). Fabrication and properties of transparent polymethylmethacrylate/cellulose nanocrystals composites. *Bioresource Technology*, 101(14), 5685–5692. <https://doi.org/10.1016/j.biortech.2010.02.045>
- Liu, Y., Wang, H., Yu, G., Yu, Q., Li, B., & Mu, X. (2014). A novel approach for the preparation of nanocrystalline cellulose by using phosphotungstic acid. *Carbohydrate Polymers*, 110, 415–422. <https://doi.org/10.1016/j.carbpol.2014.04.040>
- Lu, P., & Hsieh, Y.-L. (2010). Preparation and properties of cellulose nanocrystals: Rods, spheres, and network. *Carbohydrate Polymers*, 82(2), 329–336. <https://doi.org/10.1016/j.carbpol.2010.04.073>
- Lu, P., & Hsieh, Y.-L. (2012). Preparation and characterization of cellulose nanocrystals from rice straw. *Carbohydrate Polymers*, 87(1), 564–573.

<https://doi.org/10.1016/j.carbpol.2011.08.022>

Mandal, A., & Chakrabarty, D. (2011). Isolation of nanocellulose from waste sugarcane bagasse (SCB) and its characterization. *Carbohydrate Polymers*, 86(3), 1291–1299. <https://doi.org/10.1016/j.carbpol.2011.06.030>

Mariano, M., El Kissi, N., & Dufresne, A. (2014). Cellulose nanocrystals and related nanocomposites: Review of some properties and challenges. *Journal of Polymer Science, Part B: Polymer Physics*, 52(12), 791–806. <https://doi.org/10.1002/polb.23490>

Oksman, K., Aitomäki, Y., Mathew, A. P., Siqueira, G., Zhou, Q., Butylina, S., ... & Hooshmand, S. (2016). Review of the recent developments in cellulose nanocomposite processing. *Composites Part A: Applied Science and Manufacturing*, 83, 2–18. <https://doi.org/10.1016/j.compositesa.2015.10.041>

Park, S., Baker, J. O., Himmel, M. E., Parilla, P. a, & Johnson, D. K. (2010). Cellulose crystallinity index: measurement techniques and their impact on interpreting cellulase performance. *Biotechnology for Biofuels*, 3, 10. <https://doi.org/10.1186/1754-6834-3-10>

Peng, B. L., Dhar, N., Liu, H. L., & Tam, K. C. (2011). Chemistry and applications of nanocrystalline cellulose and its derivatives: A nanotechnology perspective. *Canadian Journal of Chemical Engineering*. <https://doi.org/10.1002/cjce.20554>

Peng, Y., Gardner, D. J., Han, Y., Kiziltas, A., Cai, Z., & Tshabalala, M. A. (2013). Influence of drying method on the material properties of nanocellulose I: Thermostability and crystallinity. *Cellulose*, 20(5), 2379–2392. <https://doi.org/10.1007/s10570-013-0019-z>

- Qiao, C., Chen, G., Zhang, J., & Yao, J. (2016). Structure and rheological properties of cellulose nanocrystals suspension. *Food Hydrocolloids*, 55, 19–25. <https://doi.org/10.1016/j.foodhyd.2015.11.005>
- Ramírez, J. A., Suriano, C. J., Cerrutti, P., & Foresti, M. L. (2014). Surface esterification of cellulose nanofibers by a simple organocatalytic methodology. *Carbohydrate Polymers*, 114, 416–423. <https://doi.org/10.1016/j.carbpol.2014.08.020>
- Rincón, M., & Martínez, D. (2009). Análisis de las propiedades del aceite de palma en el desarrollo de su industria. *Revista Palmas*, 30(2), 11–24. Retrieved from <http://publicaciones.fedepalma.org/index.php/palmas/article/view/1432>
- Roman, M., & Winter, W. T. (2004). Effect of sulfate groups from sulfuric acid hydrolysis on the thermal degradation behavior of bacterial cellulose. *Biomacromolecules*, 5(5), 1671–1677. <https://doi.org/10.1021/bm034519+>
- Rosa, M. F., Medeiros, E. S., Malmonge, J. a., Gregorski, K. S., Wood, D. F., Mattoso, L. H. C., ... & Imam, S. H. (2010). Cellulose nanowhiskers from coconut husk fibers: Effect of preparation conditions on their thermal and morphological behavior. *Carbohydrate Polymers*, 81(1), 83–92. <https://doi.org/10.1016/j.carbpol.2010.01.059>
- Salajkova, M., Berglund, L. a., Zhou, Q., Salajková, M., Berglund, L. a., & Zhou, Q. (2012). Hydrophobic cellulose nanocrystals modified with quaternary ammonium salts. *Journal of Materials Chemistry*, 22(37), 19798. <https://doi.org/10.1039/c2jm34355j>
- Sèbe, G., Ham-Pichavant, F., & Pecastaings, G. (2013). Dispersibility and emulsion-stabilizing

- effect of cellulose nanowhiskers esterified by vinyl acetate and vinyl cinnamate. *Biomacromolecules*, 14(8), 2937-2944.
- Sèbe, G., Ham-Pichavant, F., Ibarboure, E., Koffi, A. L. C., & Tingaut, P. (2012). Supramolecular structure characterization of cellulose II nanowhiskers produced by acid hydrolysis of cellulose I substrates. *Biomacromolecules*, 13(2), 570-578. <https://doi.org/bm201777j>
- Segal, L., Creely, J. J., Martin, A. E., & Conrad, C. M. (1959). An Empirical Method for Estimating the Degree of Crystallinity of Native Cellulose Using the X-Ray Diffractometer. *Textile Research Journal*, 29(10), 786–794. <https://doi.org/10.1177/004051755902901003>
- Sheltami, R. M., Abdullah, I., Ahmad, I., Dufresne, A., & Kargarzadeh, H. (2012). Extraction of cellulose nanocrystals from mengkuang leaves (*Pandanus tectorius*). *Carbohydrate Polymers*, 88(2), 772–779. <https://doi.org/10.1016/j.carbpol.2012.01.062>
- Spinella, S., Maiorana, A., Qian, Q., Dawson, N. J., Hepworth, V., Mccallum, S. A., ... Gross, R. A. (2016). Concurrent Cellulose Hydrolysis and Esterification to Prepare a Surface-Modified Cellulose Nanocrystal Decorated with Carboxylic Acid Moieties. *ACS Sustainable Chemistry and Engineering*, 4, 1538–1550. <https://doi.org/10.1021/acssuschemeng.5b01489>
- Thomas, B., Raj, M. C., Athira, K. B., Rubiyah, M. H., Joy, J., Moores, A., & Drisko, G. L. (2018). Nanocellulose, a Versatile Green Platform: From Biosources to Materials and Their Applications. *Chemical Reviews*, 118, 11575–11625. <https://doi.org/10.1021/acs.chemrev.7b00627>

- Ummartyotin, S., & Manuspiya, H. (2015). A critical review on cellulose : From fundamental to an approach on sensor technology. *Renewable and Sustainable Energy Reviews*, *41*, 402–412. <https://doi.org/10.1016/j.rser.2014.08.050>
- Vuoti, S., Talja, R., Johansson, L. S., Heikkinen, H., & Tammelin, T. (2013). Solvent impact on esterification and film formation ability of nanofibrillated cellulose. *Cellulose*, *20*(5), 2359–2370. <https://doi.org/10.1007/s10570-013-9983-6>
- Wang, N., Ding, E., & Cheng, R. (2007). Thermal degradation behaviors of spherical cellulose nanocrystals with sulfate groups. *Polymer*, *48*(48), 3486–3493. <https://doi.org/10.1016/j.polymer.2007.03.062>
- Wei, S., Kumar, V., & Banker, G. S. (1996). Phosphoric acid mediated depolymerization and decrystallization of cellulose: Preparation of low crystallinity cellulose - A new pharmaceutical excipient. *International Journal of Pharmaceutics*, *142*(2), 175–181. [https://doi.org/10.1016/0378-5173\(96\)04673-X](https://doi.org/10.1016/0378-5173(96)04673-X)
- Yu, H., Qin, Z., & Zhou, Z. (2011). Cellulose nanocrystals as green fillers to improve crystallization and hydrophilic property of poly(3-hydroxybutyrate-co-3-hydroxyvalerate). *Progress in Natural Science: Materials International*, *21*(6), 478–484. [https://doi.org/10.1016/S1002-0071\(12\)60086-0](https://doi.org/10.1016/S1002-0071(12)60086-0)
- Yuan, H., Nishiyama, Y., & Kuga, S. (2005). Surface Esterification of Cellulose by Vapor-Phase Treatment With Trifluoroacetic Anhydride. *Cellulose*, *12*(5), 543–549. <https://doi.org/10.1007/s10570-005-7136-2>

- Yuan, H., Nishiyama, Y., Wada, M., & Kuga, S. (2006). Surface acylation of cellulose whiskers by drying aqueous emulsion. *Biomacromolecules*, 7(3), 696–700. <https://doi.org/10.1021/bm050828j>
- Zaman, M., Xiao, H., Chibante, F., & Ni, Y. (2012). Synthesis and characterization of cationically modified nanocrystalline cellulose. *Carbohydrate Polymers*, 89(1), 163–170. <https://doi.org/10.1016/j.carbpol.2012.02.066>
- Zhu, H., Luo, W., Ciesielski, P. N., Fang, Z., Zhu, J. Y., Henriksson, G., ... Hu, L. (2016). Wood-Derived Materials for Green Electronics, Biological Devices, and Energy Applications. *Chemical Reviews*, 116(16), 9305–9374. <https://doi.org/10.1021/acs.chemrev.6b00225>
- Zouambia, Y., Moulai-Mostefa, N., & Krea, M. (2009). Structural characterization and surface activity of hydrophobically functionalized extracted pectins. *Carbohydrate Polymers*, 78(4), 841–846. <https://doi.org/10.1016/j.carbpol.2009.07.007>

Chapter 3

3 Nanocellulose as an inhibitor of water-in-crude oil emulsion formation

3.1 Abstract

Formation of water/oil emulsions is a frequent and challenging problem to deal with during crude oil extraction and processing. Crude oil must have water contents (BS&W) below 0,5% to meet transport and export requirements. Lowering BS&W values in crude oils involve physical and chemical processes or their combinations. Chemical demulsifiers, particularly, are structurally diverse and predominantly petrochemically-derived; however, alternative surface-active compounds such as biosurfactants are nowadays the topic of active research. In this contribution, we report the use of aqueous suspensions of cellulose nanoparticles, both nanocrystals (CNC) and nanofibrils (CNF), to inhibit the formation of w/o emulsions. HLB values of 13.0 for CNF and 10.7 for CNC indicate that these materials are hydrophilic o/w emulsifying agents, and as such can also act as destabilizers for w/o emulsions. We observe, by recovered water and Near-Infrared (NIR) scattering measurements, that CNC and CNF can effectively function as inhibitors of w/o synthetic and w/crude oil emulsions. Aqueous suspensions of CNC and CNF decrease the amount of emulsified water, inhibiting the formation of w/o emulsions up to 75% in some cases.

Keywords: Nanocellulose; w/o emulsion; inhibition; crude oil

3.2 Introduction

Stable water-in-oil emulsions form between hydrocarbons and formation water due to high-energy mixing conditions during crude oil extraction and pumping. Also, the presence of naphthenic acids

and other surface-active compounds found in asphaltenes and resins increase the stability of these emulsions (Kokal, 2006). Similarly, in the case of non-conventional fossil fuel sources, the use of enhanced recovery (EOR) techniques where mixtures of surfactants and polymers are used to extract the oil, aggravate the issue of emulsion formation.

Before transport and processing, water is removed from the crude oil by demulsification to avoid issues such as increased viscosity, corrosion, and salt deposits formation in pipelines and catalyst poisoning in refining schemes. Demulsification of crude oils is typically carried out through physical, biological, and chemical methods or their combinations (Lemarchand, Couvreur, Vauthier, Costantini & Gref, 2003; Salam, Alade, Arinkoola & Opawale, 2013; Wen *et al.*, 2010). The use of chemical methods is widespread due to the low cost and convenience of application of surfactants and demulsifiers. These substances (petrochemically-derived in most cases) are known as emulsion inhibitors or emulsion breakers if applied before or after emulsion formation, respectively. In general, commercially available additives for inhibiting or breaking emulsions are mixtures of synthetic surfactants with known negative environmental impact.

Back in 1995, Dalmazzone et al developed a methodology to study the action of emulsion inhibitors and breakers, in this study an inhibitor is defined as a surfactant added before the oil water mixture is performed, and the percentage of recovered water is reported as a percentage of inhibition, whereas the added agent after the emulsion is considered a demulsifier.(Dalmazzone, Bocard & Ballerini 1995). The inhibition or separation of the aqueous and oily phases of an emulsion is achieved by changing the hydro-lipophilic balance (HLB) of the surfactant added to the system. The effect of inhibitors and demulsifiers is achieved because they compete for the interface against surfactants naturally present in samples, in the case of water-in-oil emulsions,

natural surfactants are mainly asphaltenes and resins (Hjartnes, Sørland, Simon & Sjöblom 2019, Cheng, Ye, Chang, Zhang 2017). More recently, Hjartnes et al. discuss how in oil processing chemical treatment of emulsions involves the use of non-emulsifiers and demulsifiers. Non-emulsifiers (or inhibitors) are added almost exclusively to the oil to avoid emulsion formation during production, transport and process; hence, these materials have hydrophobic properties represented by low HLB values. Demulsifiers, on the other hand, are used to break already formed w/o or o/w emulsions (Hjartnes *et al* 2019)

Nowadays trends in sustainable development promote the use of renewable sources of materials, in place of synthetic raw sources for new products, to change the current Linear Economy model. Within this framework, lignocellulosic biomass, derived from intensive agro-industrial activity, emerges as an attractive raw material because of its availability and low cost. Production and usage of advanced nanocellulose materials (nanocrystals or nanofibrils – CNC, CNF) from biomass is currently an active research and innovation topic (Abraham *et al.*, 2011; Beck-Candanedo, Roman & Gray, 2005; Isogai, Saito & Fukuzumi, 2011; Khalil, 2014). Sulfuric acid hydrolysis and TEMPO-oxidation are the main processes for CNC and CNF production and many researchers reported the optimized conditions for these methods such as Bondeson, Mathew & Oksman (2006) and Saito, Kimura, Nishiyama & Isogai (2007).

CNC has many applications in medicine (biomedical implants, pharmaceuticals) and material sciences (Pickering emulsions, antimicrobial films, reinforcing fillers for polymers, flexible displays, oil absorbents, fabric and textiles) (Habibi, Lucia, & Rojas, 2010; Hubbe, Rojas, Lucia & Sain, 2008; Korhonen, Kettunen, Ras & Ikkala, 2011; Qiu & Hu, 2013). Several studies concerning the use of cellulose as surface-active agent are reported in the scientific literature. For

instance, Andresen & Stenius (2007) examining the ability of microfibrillated cellulose for stabilizing oil in water emulsions found that increasing the hydrophobicity of the biopolymer resulted in an increased surfactant activity. Lif, Stenstad, Syverud, Nydén & Holmberg (2010) also reported the use of microfibrillated cellulose with different degrees of hydrophobicity to stabilize water-diesel emulsions, and determined that using a mixture of hydrophobic and hydrophilic microfibrillated cellulose provided efficient stabilization of the emulsion.

Furthermore, Hou, Feng, Masliyah & Xu (2012), showed that ethyl-cellulose can be used to destabilize water/bitumen emulsions. Also, some reports indicate the use of hydrophobic nanocellulose for stabilizing Pickering emulsions in food, cosmetic formulations and pharmaceuticals, (Cunha, Mougél, Cathala, Berglund & Capron, 2014; Fujisawa, Togawa & Kuroda, 2017; Kalashnikova, Bizot, Cathala & Capron, 2012; Li *et al.*, 2018; Zoppe, Venditti & Rojas, 2012). Usually, for Pickering emulsions concentrations of nanocellulose range from 0.1 to 1.5 %. TEMPO nanofibrils (TOCN) produce more stable emulsions than CNC, probably due to network formation as a result of longer fibril length and increased ionic charge, in comparison with nanocrystals. (Niu *et al.*, 2018). On the other hand, studies of emulsion stabilization using hydrolyzed cellulose showed that increasing hydrolysis times results in smaller cellulosic particles, which in turn produce stable o/w emulsions by decreasing drop size (Gestranius, Stenius, Kontturi, Sjöblom & Tammelin, 2017; Li, Wang, Ma, & Wang, 2018).

The use of nanocellulose in fluids for EOR processes has also been reported. For instance, surface modified cellulose nanofibrils containing hydrophobic alkyl units were used as emulsifiers to increase the amount of extractable crude (Li *et al.*, 2017) in experimental micromodels. On another application, Wei et al used CNF solutions (0.2 and 0.5%) to change source rocks

wettability, to water-wet, and allow crude oil extraction by inducing formation of w/o emulsions (Aoudia, Al-shibli, Al-kasimi, Al-maamari & Al-bemani, 2006; Wei, Li, Jin, Li & Wang, 2016).

Also Li, Wei, Xue, Wen & Li (2016) found that hydrophobization of CNC increases thermal stability, hinders aggregation in the presence of electrolytes, and reduces viscoelasticity of the materials. All of these properties are of fundamental importance in EOR processes (Li, Wei, Xue, Wen & Li, 2016). Nanocellulose-based additives can also be used as foam stabilizers in foam-flooding EOR strategies, by reducing oil/water interfacial tension and promoting oil displacement in the source rock (Aoudia *et al.*, 2006; Gestranus *et al.*, 2017; Li *et al.*, 2016; Li *et al.*, 2017; Li *et al.*, 2018; Molnes, Mamonov, Paso, Strand & Syverud, 2018; Wei *et al.*, 2016; Wei *et al.*, 2017; Wei *et al.*, 2018). Also, CNC can cross sandstone nuclei and alter mineral surfaces properties to allow crude migration and efficient extraction (Molnes *et al.*, 2018; Molnes, Torrijos, Strand, Paso & Syverud, 2016). Besides, the stability of CNC suspensions is not affected by pH changes or high temperatures (90 ° C), which is of fundamental importance for crude oil recovery applications (Molnes, Paso, Strand & Syverud, 2017).

In this contribution our rationale involves a simple assumption: If a hydrophilic (water-soluble) surfactant with high HLB is able to stabilize o/w emulsions, then the same type of material could hinder the formation of w/o emulsions. In fact, Roodbari, Badiei, Soleimani, & Khaniani demonstrated how a group of non-ionic polymers (Tweens analogues), typically used to stabilize o/w emulsions, exhibit destabilizing properties in w/crude oil mixtures. The authors reported that the demulsification effect increases as the HLB of the surfactant increases, and also as the number of electronegative atoms (oxygen) increase in the molecules. These surfactants were able to recover up to 80% water from the w/crude oil emulsion. However, the authors used the Tweens as

demulsifiers by adding them once the w/o emulsion was formed (Roodbari, Badiei, Soleimani, Khaniani, 2016). Currently, high-molecular-weight (HMW) surfactants are attracting a lot of attention as demulsifiers in w/o emulsions. For instance, Wang et al using polyethoxylated dendrimers as demulsifiers and found that the amount of recovered water increases as the numbers of propylene oxide and ethylene oxide units increase. These HMW are believed to alter interfacial water/oil film rheology promoting coalescence and sedimentation (Wang, Hu, Li, Li, Yang, 2010). We hypothesize that highly hydrophilic nanocelluloses, with abundant oxygen atoms, high-molecular-weight, and high HLB values, can efficiently inhibit w/o emulsion formation.

Thus, here we investigate the role of cellulose nanoparticles -nanocrystals (CNC) and nanofibrils (CNF) obtained by acid hydrolysis and TEMPO, respectively- as surface active agents for water in oil emulsion formation. An aqueous carrier phase containing CNC and CNF with different amounts of active surface groups (SO_3^- and COOH^- , respectively) was mixed with the non-polar phase employing a high shear mixer. We observed a dramatic decrease in the amount of emulsified water when the aqueous carrier contained above 1000 ppm of nanocellulose. In this way, the use of activated CNC suspensions can decrease the amount of emulsified water in w/o systems. Besides, the use of biodegradable polymers can reduce the environmental impacts associated with synthetic additives commonly used to break w/o emulsions in the petroleum industry.

3.3 Experimental and Methods

3.3.1 Materials. Sulfuric acid (H_2SO_4), sodium hydroxide (NaOH), sodium bromide (NaBr), hydrochloric acid (HCl , 37% weight), sodium hypochlorite (NaClO , 5-9% chlorine) and ethanol (95%) were purchased from Merck (Darmstadt, Germany). TEMPO (2,2,6,6-tetramethylpiperidin-1-oxyl, 98 %) and Grade 1 Whatman cellulose filters were acquired from Sigma Aldrich (St. Louis, MO, USA). Microcrystalline cellulose was purchased from Alfa Aesar (Ward Hill, Massachusetts, United States). All chemical reagents were used as supplied. Commercial-grade diesel and gasoline were also used as received aqueous solutions and suspensions were prepared with ultrapure water ($12 \text{ M}\Omega\cdot\text{cm}$ @ $25 \text{ }^\circ\text{C}$).

3.3.2 CNC isolation by hydrolysis. Typically, cellulose nanocrystals (CNC) extraction involves removal of amorphous cellulose from bleached fibers via acid hydrolysis. CNCs were prepared via acid hydrolysis, according to Bodenson *et al.*, (2006), using Whatman filters as cellulose source (5 g) and H_2SO_4 (60 mL, 62.5%).

The reaction was performed at $45 \text{ }^\circ\text{C}$ and two different reaction times were used (130 and 180 min) to obtain CNCs with various degrees of surface charge.

After the reaction was stopped, by adding cold water, the mixture was centrifuged and washed until pH 1. Dialysis using a Spectra Dialysis membrane (12-14 kDa) was conducted for 6 days to remove cellulosic reaction residues. The dialysate was subjected to ultrasonic radiation using a Sonics Vibra Cell VC (20 kHz, 750 W) for 20 min in an ice water bath. Finally, the CNC suspension was lyophilized and stored for further characterization and use in emulsion inhibition tests.

3.3.3 CNF isolation by TEMPO. Carboxylated Cellulose nanofibrils (CNF) were prepared according to the procedure described by Isogai *et al* (2011). In short, microcrystalline cellulose (1 g) was dispersed in deionized water (100 mL) and catalytic amounts of TEMPO (16 mg) and NaBr (100 mg) were added to the suspension under stirring at room temperature. The reaction mixture was placed on an ultrasonic bath (Bransonic, 40 kHz, 130 Watt) and a solution of NaClO, used as primary oxidant (2 mmol), was added dropwise while the pH of the mixture was kept between 10 and 11, by adding NaOH (0,1 M) when required. When there was no pH change the reaction was quenched by ethanol addition.

The reaction mixture was then centrifuged and washed with water repeatedly, until pH 7. Aqueous suspensions (1% w) of CNF were sonicated by ten-minute cycles (Sonics vibra-cell VC750, 20 kHz, 750 Watt) to achieve uniform dispersion of the material. The suspensions were centrifuged at 4700 rpm (4643*g) for 20 min to remove unreacted cellulose. Finally, the dispersed CNF (1 %), in the form of sodium carboxylate, were transformed into the free acid form by adding HCl (0,1 M) until pH~2. The mixture was left to react 30 min, under constant stirring, according to Fujisawa, Okita, Fukuzumi, Saito & Isogai (2011). Free carboxylate CNF appeared as a translucent gel.

3.3.4 CNC and CNF characterization. TEM images were collected on a FEI Tecnai T12 Spirit TEM (FEI, Hillsboro, OR) with an acceleration voltage of 120 keV. Samples for TEM imaging were drop casted onto carbon coated copper grids and left to dry at ambient conditions. X-Ray diffraction patterns were measured on a Bruker D8 DISCOVER X-ray diffractometer (Billerica, MA) with a DaVinci geometry, equipped with a $\text{CuK}\alpha 1$ radiation source (40 kV and 30 mA), an area detector VANTEC-500, and a poly (methyl methacrylate) sample holder.

Attenuated total reflectance (ATR-IR) measurements were performed on a Bruker Tensor 27 (Billerica, MA) FTIR instrument equipped with a Platinum Diamond ATR unit A225/Q (Billerica, MA) with resolution of 2 cm^{-1} and scan accumulation of 32 per spectrum. CNC and CNF thermal stability was tested on a TA Discovery TGA (Newcastle, England) instrument equipped with an infrared heating oven, a temperature controlled thermobalance, a gas supply module and an autosampler system. TGA analysis were carried out with Nitrogen as inert gas (50 mL/min) and a heating rate of $10\text{ }^\circ\text{C/min}$ from 30 to $600\text{ }^\circ\text{C}$. Finally, the colloidal stability of CNC and CNF aqueous suspensions (1% wt) was assessed according to their zeta potential value (ζ) determined with a Malvern Zetasizer Nano ZS90 instrument (Worcestershire, UK), equipped with a capillary cell 1070. Conductometric titrations were performed using a HANNA HI 8733 conductometer, to assess the amount of sulfate groups on the CNC surface and the carboxylic groups on nanofibrils surface. The titrations were performed using a CNC suspension (100 mL, 2g/L), initially subjected to sonication for 15 min, to which a solution of NaCl (2 mL, 0,05M) was added. Titration was carried out by adding 10 μl aliquots of NaOH 0,0197N under continuous stirring, according to the procedure previously reported by Abitbol, Kloser, & Gray (2013). To determine the degree of oxidation of the nanofibrils, the method described by Habibi et al (Habibi, Chanzy & Vignon,

2006) was used. The size of the nanocrystals was determined by Dynamic Light Scattering using a Zetasizer Nano Series S90 Malvern.

Also, for theoretical HLB values we used the Davie's method (Davies, 1957) as shown in equation 3:

$$\text{HLB} = 7 + \sum \text{HLB}_{\text{Hydrophilic groups}} - \sum \text{HLB}_{\text{Hydrophobic groups}}$$

Equation 3

3.3.5 Preparation of model emulsions. Synthetic stable w/o emulsions were prepared by mixing a solution of commercial gasoline plus asphaltenes (non-polar phase + surfactant) and brine (pH 6) with a composition similar to that of the average formation water (0,3088 mg/L KCl, 9,93 mg/L NaCl, and 2,52 mg/L CaCl₂·2H₂O) (Maaref & Ayatollahi, 2018). The brine was spiked with CNC or CNF to achieve concentrations from 500 up to 1500 ppm. A 10000 ppm asphaltene stock solution in toluene was used as surface-active material for w/o emulsions formation; the asphaltenes were mixed with gasoline to reach concentrations of 1000 ppm with respect to the total volume of the mixture. The asphaltenes were isolated from a South American crude oil API 31,7° according to the ASTM D6560-12 procedure.

For emulsions preparation, 20 mL of the aqueous phase (with and without CNC and CNF) was added dropwise to 20 mL of the organic phase (Ultraturrax T-25 at 13000 rpm) to reach 50 % of water content. The type of emulsion was confirmed by wettability tests in pure water and toluene. Since all the emulsions prepared easily dissolved in toluene they were catalogued as w/o. Micrographs were taken to confirm the formation of w/o emulsions. All w/o emulsions prepared were stable for up to 12 months.

The previous procedure was also applied to preparation of w/o emulsions with crude oil. In these emulsions the gasoline/asphaltene mixture was replaced by a crude oil (API: 31,7° and 14.7°). Brines were prepared with concentrations of 1000, 6000 and 12000 ppm of NaCl. The pH values were adjusted by the addition of 0.01 M HCl and 0.01 M NaOH to the brine as required, to obtain values of 6 and 10. All tests were carried out at room temperature.

3.3.6 Emulsion characterization. The stability of the emulsions was determined by visual inspection (measuring recovered water volume) and Near-Infrared (NIR) scattering via Turbiscan Lab instrument (Formulaction, L'Union, and France). The Turbiscan Lab instrument follows variations in backscattered or transmitted radiation (NIR, λ 850 nm) vs. sample height as a function of time to yield dispersion stability data. The backscattering mode is commonly used to study opaque dispersions such as crude oil emulsions. Equation 4 shows the Instability Index, a statistical parameter calculated from variations in backscattering intensity of the sample, relative to the original, over time. This index is a convenient way to observe the dynamics of aggregation processes and emulsion stability (Giraldo-Dávila *et al.*, 2018).

$$Instability\ Index = \frac{\sum_0^n |BS_i - BS_{i-1}|}{n}$$

Equation 4

Where BS_i and $BS_{(i-1)}$ are the dimensionless backscattering value for each scan and n is the number of scans. High values of Instability Index indicate a high probability of phase separation, which translates into low emulsion stability in the case of w/o emulsions (Kang *et al.*, 2011).

3.4 Results and discussion

3.4.1 Nanocellulose surface chemistry and structure. CNC and CNF behavior at interfaces (self-assembly, adsorption, solvent interactions, among others) depends on two key parameters: surface chemistry and particle structure. In CNC and CNF, the isolation methods (e.g., polar/charged surfaces if isolated via H₂SO₄ acid hydrolysis or TEMPO) or specific surface modifications (e.g., hydrophobization reactions) determine their surface properties. Regarding particle structure, nanocelluloses are considered as one-dimensional particles due to the biopolymer's unidirectional **biosynthetic** pathway. (Aveyard, Binks & Clint, 2013; Johnson, Zink-Sharp & Glasser, 2011; Leal-Calderon & Schmitt, 2008).

We obtained CNC, via acid hydrolysis from Whatman filter paper, with lengths between 100 and 300 nm and widths up to 30 nm, exhibiting crystallinity of 88.3% and thermal stability up to 170 °C. On the other hand, CNF obtained by TEMPO oxidation from microcrystalline cellulose showed micrometric lengths and widths between 30 and 50 nm, with lower degrees of crystallinity than the CNC (66%) and higher thermal stability up to 225 °C. Table 1 shows the characteristics of the isolated materials, Figure 14. and Figure 15. shows FESEM, DLS, TGA, DRX and FTIR-ATR data for CNF and CNC respectively.

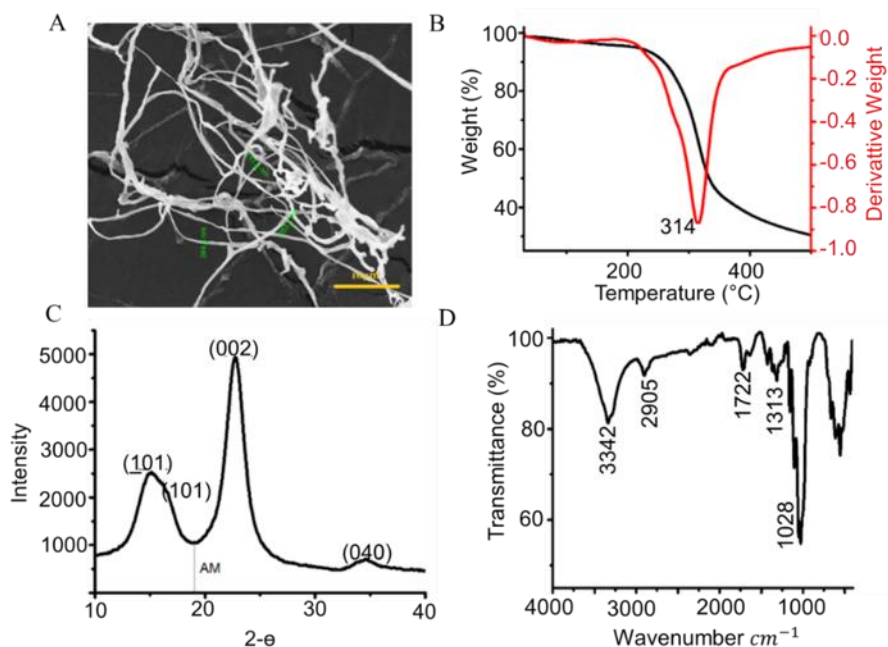


Figure 14. CNF Characterization, (A) FESEM, (B) TGA and derivative TGA, (C) DRX, (D)

IRATR

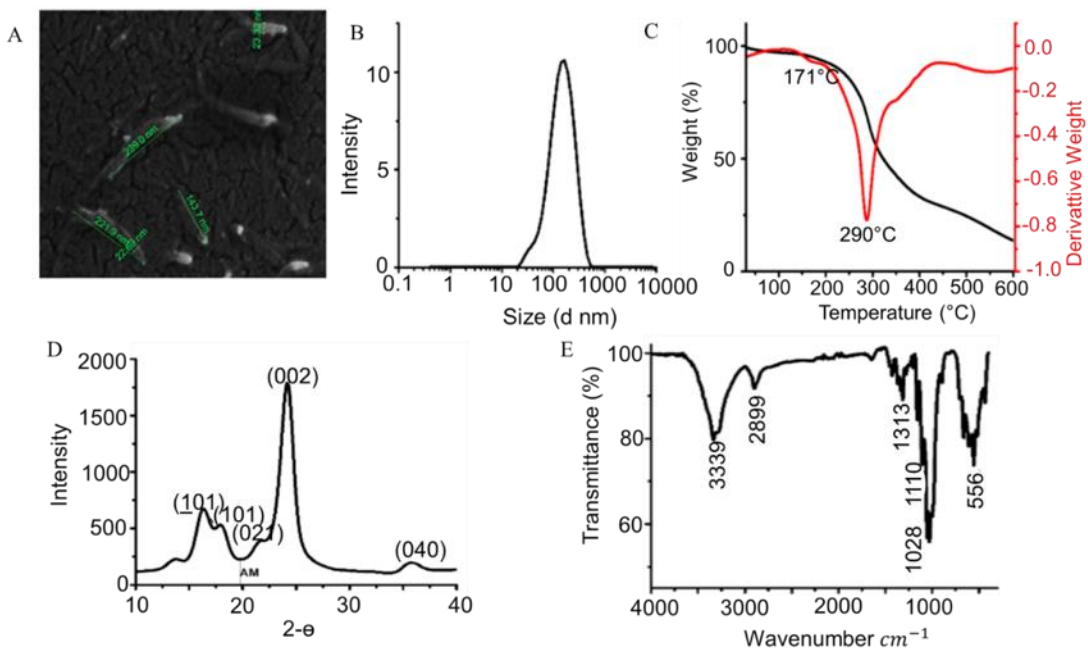


Figure 15. CNC Characterization (A) FESEM, (B) DLS, (C) TGA and derivative TGA, (D)

DRX, E: IRATR

Table 1.
CNC and CNF characterization

Parameter (Method)	CNC	CNF
Length (DLS)	100-250 nm	1-30 μm
Width (TEM)	20-30 nm	30-50 nm
Surface charge (ζ -potential)	-39 mV	-59 mV
Surface groups (Conductimetry)	117 mmol SO_3^-/kg	1200 mmol COOH/kg
Thermal stability (TGA)	170 $^\circ\text{C}$	225 $^\circ\text{C}$
Crystallinity Index (XRD)	88.3 %	62.0 %
Wettability (visual)	Water	Water
Theoretical HLB	10.7	13.0

The size, charge, crystallinity and thermal stability of CNC and CNF (as listed in Table 1) lie within the ranges reported in the literature for similar materials (Jonoobi et al., 2015; Li, Wang,

Ma & Wang, 2018; Lu & Hsieh, 2010; Roman & Winter, 2004). As expected, CNCs have smaller sizes than CNFs while exhibiting higher crystallinity and a reduced amount of surface charges. The high amount of carboxylate units on NFC is reflected in a ζ -potential value of -59 mV for this material, in contrast with -39 mV for the CNC. The presence of surface charges ($-\text{SO}_3^-$ or $-\text{COO}^-$) prevents agglomeration – by Coulombic repulsions- allowing formation of stable aqueous dispersions of CNC and CNF.

The surface chemistry of nanocelluloses, and their use as interfacial-active compounds, depends on the type and number of polar groups at the surface. In our case CNC has 117 mmol / kg of highly ionizable sulfate groups ($\text{pK}_a \sim 3.0$) that can be completely ionized at $\text{pH} > 3$. These groups are highly polar, however, due to their low concentration on the surface of the CNC they don't affect the theoretical HLB value dramatically (10.3) (Aveyard *et al.*, 2003; Davies, 1957; Giraldo-Dávila *et al.*, 2018; Guo, Rong & Ying, 2006; Johnson *et al.*, 2011; Jonoobi *et al.*, 2015; Kang *et al.*, 2011; Leal- Calderon & Schmitt, 2008; Li *et al.*, 2018; Ly & Hsieh, 2010; Maaref & Ayatollahi, 2018; Roman & Winter, 2004). On the other hand, CNF contains more ionizable groups (1200 mmol of COOH/kg) than CNC. In CNF, COOH units ($\text{pK}_a \sim 4.0$) are completely ionized (to the $-\text{COO}^-$ form) at the pH used in the tests ($\text{pH} 6$). Using hydrophilicity values for polar groups in CNC and CNF we calculated the theoretical HLB using Equation 4. The results were HLB values of 13 for CNF and 10.3 for CNC, these values correspond to hydrophilic (water soluble) o/w emulsifying agents. Interestingly, it is well known that surface active agents used for stabilizing o/w emulsions can also act as destabilizers for w/o emulsions; thus we hypothesize that CNC and NFC can effectively be used as inhibitors of water-crude oil emulsions as demonstrated below (Oliveira, Santos, Vieira, Fraga & Mansur, 2017; Xia, Lu & Cao, 2004).

3.4.2 Inhibition of emulsion formation with CNC and CNF in w/o model systems.

Several authors agree that the process of formation of water-in-oil emulsions, in petroleum processing, involves formation of a fairly rigid interfacial layer due to the presence of surface-active agents in the crude (polar species in asphaltenes, naphthenic acids). Therefore, avoiding w/o emulsion formation requires inhibiting agents that efficiently compete against naturally-present emulsifiers, preventing formation of the interfacial layer and allowing water separation (Abdurahman & Mahmood, 2012; Ortiz, Baydak & Yarranton, 2010). The properties of nanocellulose particles (both nanocrystals and nanofibers) as surface active materials to stabilize emulsions, particularly of the oil-in-water kind, are abundantly illustrated in literature (Brinchi, Cotana, Fortunati & Kenny, 2013; Buffiere *et al.*, 2017; Capron, Rojas & Bordes, 2017; Laitinen, Ojala, Sirviö & Liimatainen, 2017; Mikulcová, Bordes & Kašpárková, 2016; Ojala, Sirviö & Liimatainen, 2016). However, to the best of our knowledge there are no reports regarding the use of nanocelluloses to destabilize water-in-crude oil emulsions, with current applications of these materials focused mostly on EOR processes as described in the introductory remarks.

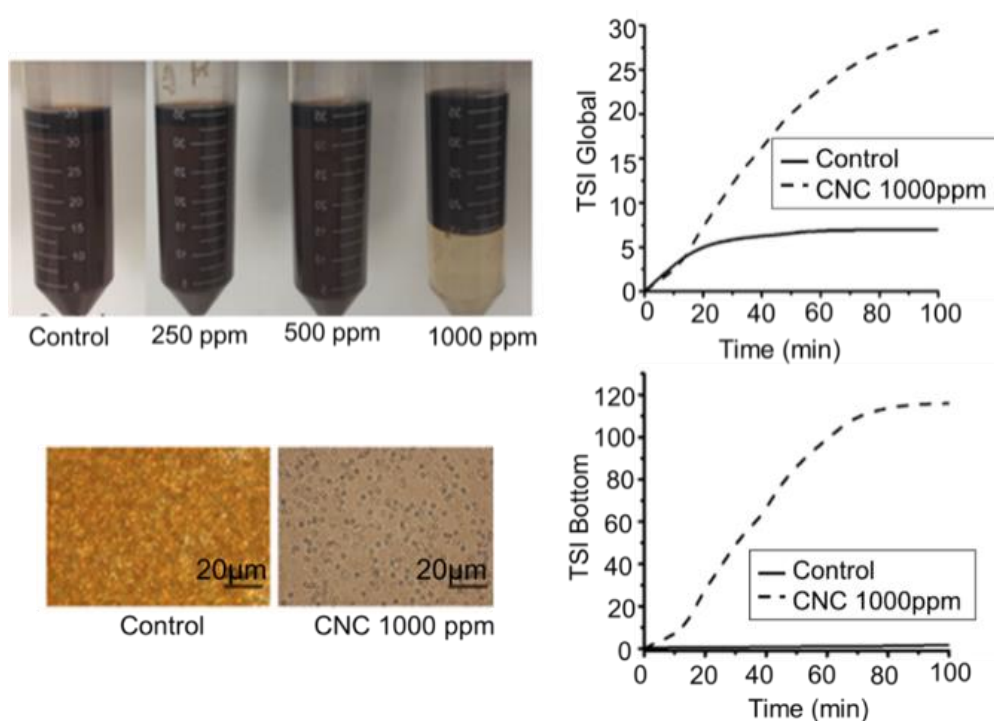


Figure 16. Emulsion inhibition effects for CNC: visual tests (top left), optical micrographs of the control emulsion and the aqueous layer for the sample with 1000 ppm of CNC (bottom left); backscattering NIR measurements featuring the dynamics of the instability indexes for the overall mixture (top right) and the aqueous layer (bottom right).

We performed preliminary inhibition tests using a synthetic w/o emulsion made of commercial gasoline plus asphaltenes and a brine (pH 6) with composition similar to that of the average formation water, as described in the Experimental section. When CNC was added to the brine before emulsion preparation, for final concentrations of 1000 to 5000 ppm, we were able to inhibit emulsion formation in all tests. Without CNC we obtained stable (up to six months) w/o emulsions. We lowered the amount of CNC for the inhibition test and found that no inhibition was observed for concentrations below 1000 ppm. Figure 16. clearly illustrates the emulsion formation inhibiting effect of adding CNC (1000 ppm) to the brine. In visual tests, we obtain a normalized

water recovery of 80% assuming a total volume of the sample in the tube of 37.5 mL as seen in Figure 16. Likewise, optical micrographs (bottom left) show a decrease in the amount of dispersed water in the organic phase of the sample with added CNC (1000 ppm) in contrast with the control sample. Interestingly, we observe no significant change in water drop sizes upon CNC addition to the w/o emulsion, there is only change in their amount in the emulsion as seen in Figure 16. (bottom left). Also, the remaining water in the organic phase is in the form of a water-in-oil dispersion ruling out a possible phase inversion when using CNC.

Emulsion formation and stability are complex processes at the molecular level; however, from a macroscopic perspective, these processes can be studied by following variations in optical characteristics of opaque dispersions. To assess emulsion stability, we followed changes over time in the Instability Index (TSI), a statistical parameter calculated from variations in the backscattering intensity of NIR radiation interacting with the sample, relative to the original. High values of TSI indicate phase separation, which translate into low emulsion stability in the case of w/o emulsions. Figure 16. (top right) shows the global TSI vs time plot for the control emulsion and the emulsions prepared with CNC. The TSI plateaus at 5 after 20 minutes for the control sample, indicating a highly stable emulsion.

In contrast, the sample with CNC (1000 ppm) exhibits a maximum TSI value of 30 after 100 minutes, indicating complete phase separation in agreement with the visual tests. Interestingly, when following only backscattering changes in the lower part of the sample vial (where the aqueous phase collects in case of phase separation) we observe dramatic changes in the TSI values for the sample with CNC (1000 ppm). A maximum TSI value of 120, plateauing after 70 minutes, for the aqueous phase indicates a fast destabilization kinetics and rapid phase separation, in other

words low emulsion stability.

As reported by Djuve, Yang, Fjellanger, Sjöblom & Pelizzetti (2001), an emulsion inhibitor must compete with natural surfactants, draining them from the interfacial layer and decreasing the surface tension gradient so that breaking or inhibiting emulsion formation occurs. In the model emulsions we prepared, the asphaltenes act as surface-active compounds forming an interfacial film and stabilizing the emulsion for several months. Such was the case of the control emulsion, which remained stable for more than six months. When the CNC were added to the aqueous medium, in concentrations above 1000 ppm, emulsion formation was hindered as a consequence of efficient competition between the CNC and the surface-active compounds in asphaltenes.

Using the same w/o model emulsion system described above, we performed inhibition tests using CNF. As with CNC, when CNF was added to the brine before emulsion preparation, for final concentrations of 1500 to 5000 ppm, we were able to inhibit emulsion formation in all tests. Without CNF we obtained stable (up to six months) w/o emulsions. We lowered the amount of CNF and found that the inhibition concentration threshold was 1500 ppm, below which w/o emulsions were readily formed. In Figure 17.7 the visual tests (top left) we obtain a normalized water recovery of 77.8%.

Optical micrographs (bottom left) indicate decrease amount of water in the final dispersion after CNF addition; however, there is a significant increase in water droplet size with CNF when compared to the same experiment with CNC. Figure 17. (top right) shows the global TSI vs time plot for the control emulsion and the emulsion prepared with 1500 ppm of CNF. The TSI slowly rises up to 4.2 after 100 minutes for the control sample, indicating a stable emulsion. In contrast, the sample with CNF (1500 ppm) becomes steadily unstable after 100 minutes, indicating phase

separation.

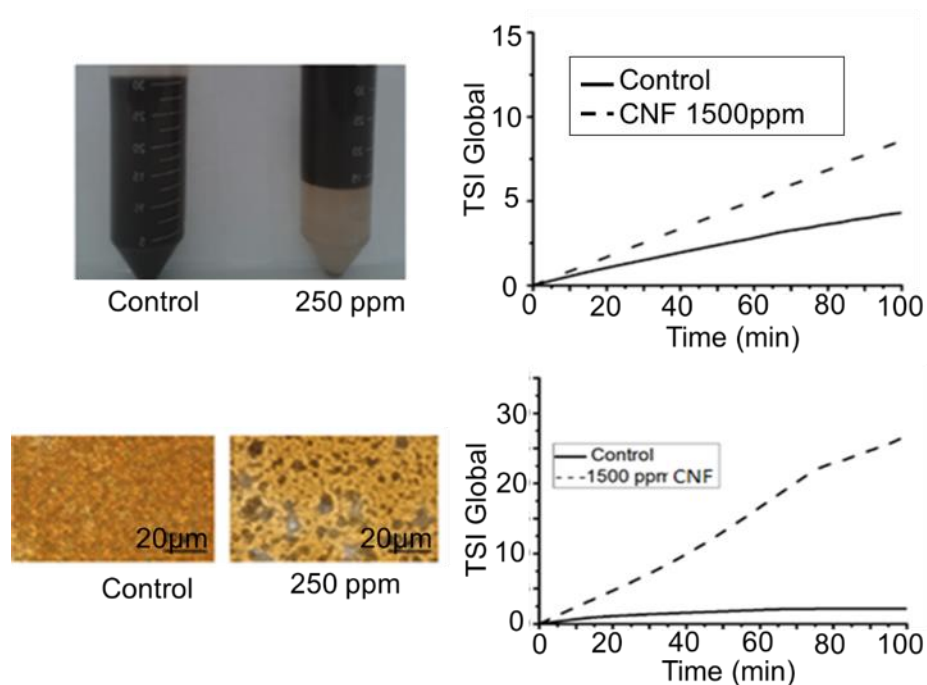


Figure 17. Emulsion inhibition effects for CNF: visual tests (top left), optical micrographs of the control emulsion and the aqueous layer for the sample with 1500 ppm of CNF (bottom left); backscattering NIR measurements featuring the dynamics of the instability indexes for the overall mixture (top right) and the aqueous layer (bottom right).

The backscattering dynamics in the lower part of the sample vial (where the aqueous phase collects in case of phase separation) show a clearer picture than the TSI global. A maximum TSI value for the aqueous phase of 25, plateauing after 70 minutes, indicates a fast destabilization and rapid phase separation with CNF, in other words low emulsion stability.

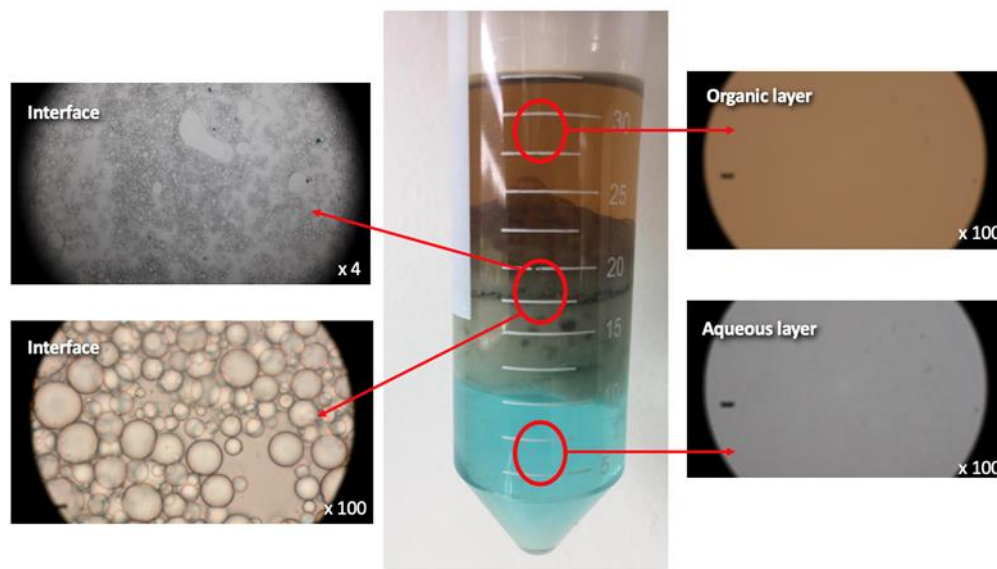


Figure 18. Optical microscopy images of the organic aqueous and interfacial layers observed during an inhibition test with CNF, using Methylene Blue (cationic dye) as a label for cellulose.

To establish the distribution of CNF we studied the phases formed during the inhibition test using optical microscopy. The CNF tested in our work have negatively charged surfaces, due to the presence of carboxylate groups, thus we selected Methylene Blue (a cationic dye) as label to observe the distribution of the cellulosic material in the mixture. Figure 18 shows optical images of the aqueous, organic, and interfacial layers five minutes after mixing the phases with the high shear mixer, note that the amount of asphaltenes in this particular experiment was reduced to facilitate light transmission. The characteristic blue color of MB was observed in the aqueous and interfacial layers. When zooming at the interfacial layer, we noticed that the boundary of the water/oil interface was tinted blue. This observation indicates that CNF is preferably located at the interfacial water/oil film. Interestingly, several investigations dealing with the use of high molecular weight surfactants with abundant oxygen-containing moieties agree in that these materials can alter the interfacial water/oil film rheology promoting coalescence and sedimentation

(Wang *et al.* 2010). We believe that, along the same lines, highly hydrophilic nanocelluloses, with abundant oxygen atoms, high-molecular-weight, and high HLB values, can also efficiently inhibit w/o emulsion formation by migrating to the w/o interface as seen in Figure 18.

On the other hand, as mentioned above, the type of emulsion and its stability are closely related to the surfactant's hydrophilic/hydrophobic nature (Fan, Simon & Sjöblom, 2009), with mildly polar surfactants such as asphaltenes tending to stabilize w/o emulsions, while CNC or CNF of a strongly hydrophilic nature tend to either stabilize o/w emulsions or even act as solubilizing agents. Therefore, adding CNC or CNF to the water before emulsion formation can efficiently hinder stabilization of water droplets in the oil phase by competing with natural surfactants. According to reports by Rondón (Rondón *et al.*, 2008; Rondón, Bouriat, Lachaise & Salager, 2006) an efficient w/o demulsifier must have opposite properties to those of the surfactants that stabilize the w/o emulsion. An efficient w/o emulsifier must be then highly hydrophilic (such as CNC and CNF with HLB of 10.7 and 13, respectively), since the surfactants stabilizing the emulsion (asphaltenes) have low hydrophilicity when compared with CNC.

3.4.3 Inhibition of emulsion formation with CNC in w/Crude Oil dispersions.

3.4.3.1 Light crude oil. We hypothesize that CNC, smaller and less hydrophilic than CNF, can migrate easily to the w-o interface hindering emulsion formation. According to their HLB values, CNC (10.7) and CNF (13.0) qualify as o/w emulsion stabilizers and also as w/o emulsions destabilizers. However, CNC are slightly less hydrophilic than CNF, due to a lower amount of sulfate groups. In addition, CNC have greater mobility than CNF due to their size.

Thus, we selected CNC for further testing as emulsion inhibitors in w/o dispersions prepared using

a light crude oil (API: 31,7°).

In real-world situations the success of a formulation to inhibit emulsion formation does not only depend on the nature of the surfactant but also on factors such as pH, temperature, and water salinity (Rondón *et al.*, 2008). Therefore, we varied experimental conditions in order to test the effect of pH and salinity on emulsion inhibition by CNC. To determine pH influence on emulsion inhibition we carried out tests mixing a light crude oil with CNC suspensions (1000 ppm) in various brines (1000, 6000, and 12000 ppm NaCl) at pH 6 and 10. Starting with 1000 ppm NaCl brines, the optical images in Figure 19 clearly show more water recovery at pH 10 (70%) than at pH 6 (25%). No water was recovered from the control experiments (where CNC was not added to the brine). Both, global and bottom TSI graphs show the same backscattering behavior for the control mixtures, supporting the visual assessment of no phase separation occurring in these samples.

On the other hand, the global TSI profiles for the samples with CNC show increased destabilization with time. However, the effect is clearer if we examine the TSI bottom corresponding to the lower part of the vial where the free water is observed. Increasing the CNC carrier fluid pH has a significant effect on emulsion destabilization (higher TSI values), while a low pH does not promote significant water recovery (lower TSI values). pH plays an important role in the emulsion inhibition process by modulating surface charge density on CNC. The higher the pH the more superficial charges available for interaction with water and to promote coalescence and separation of the aqueous phase. Interestingly, the water recovery in these closer-to-real systems is slightly lower than the observed recoveries in model systems (see above) implying that CNC can not only compete with the asphaltenes but also with other natural surfactants present in

the crude, promoting coalescence of water droplets and inducing phase separation.

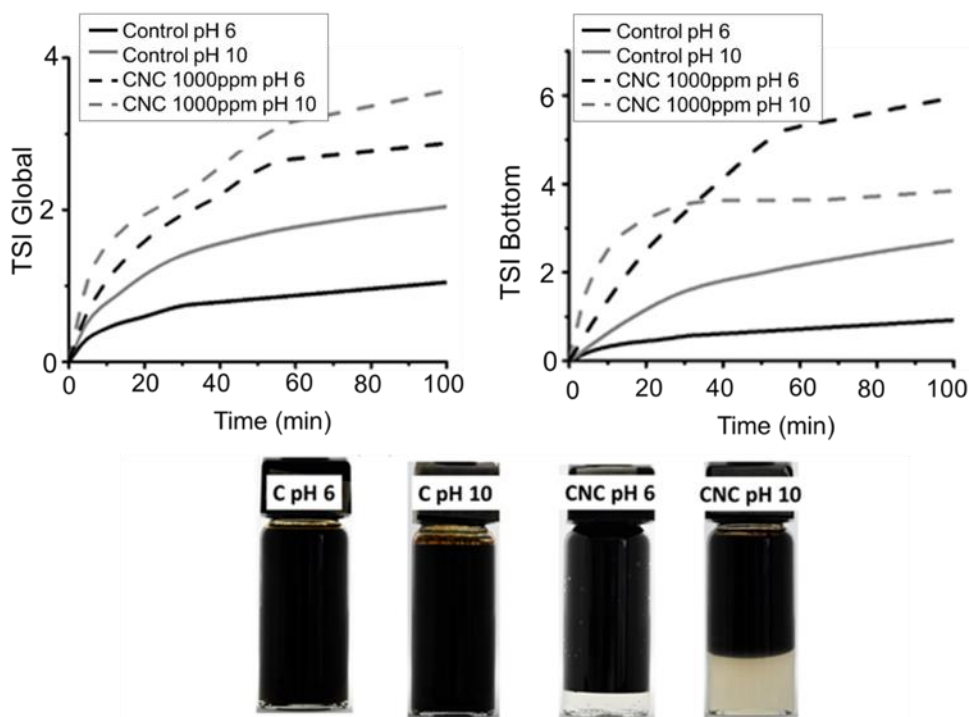


Figure 19. Inhibition tests with suspensions of 1000 ppm of CNC in 1000 ppm NaCl brines.

For brines with 6000 ppm of NaCl, optical images in Figure 20 show very little water recovery at pH 10 (10%) and pH 6 (25%). No water was recovered from the control experiments (where CNC was not added to the brine). Both, global and bottom TSI graphs show the same backscattering behavior for the control mixtures, supporting the visual assessment of no phase separation occurring in these samples. Increasing dissolved ions in the water dramatically affects the performance of CNC as emulsion inhibitor. Also, increasing salt concentration up to 12000 ppm results in similar behavior than with 6000 ppm (See Figure 21.)

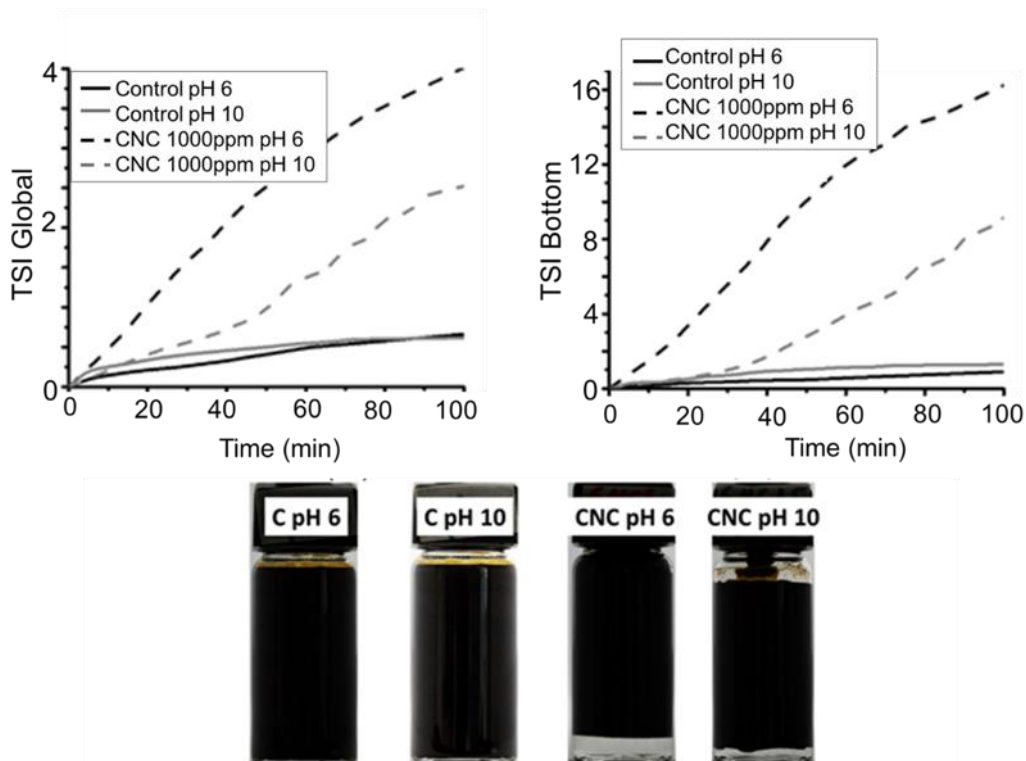
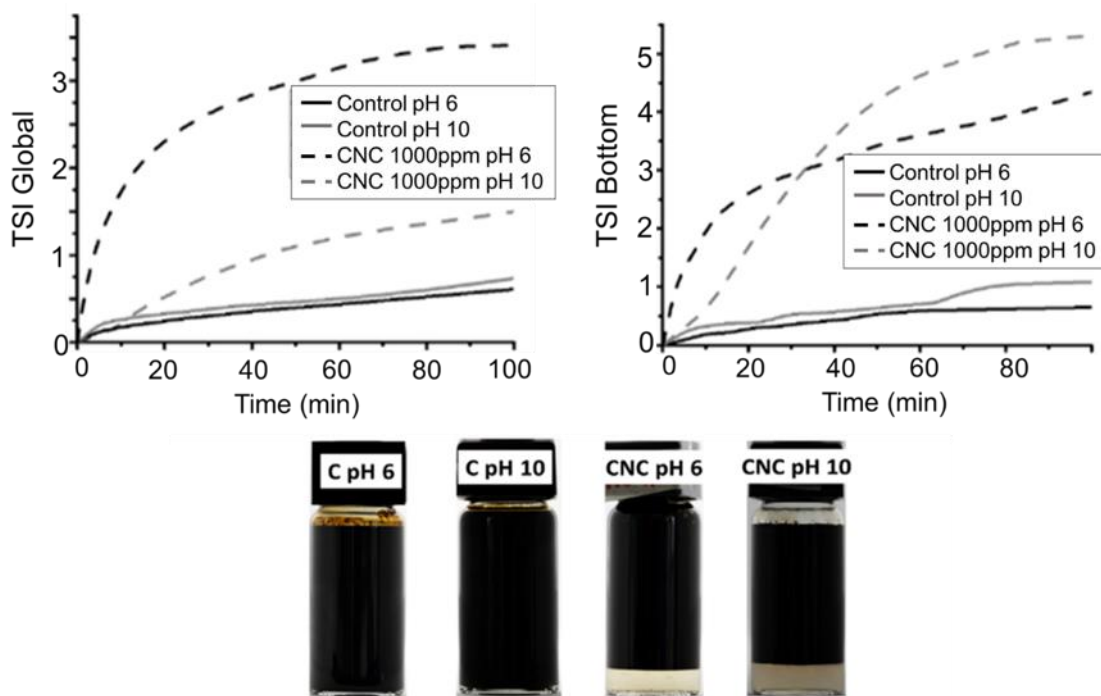


Figure 20. Inhibition tests with suspensions of 1000 ppm CNC in brines of 6000 ppm NaCl, pH 6



and 10.

Figure 21. Inhibition tests with suspensions of 1000 ppm CNC in brines of 12,000 ppm NaCl, pH 6 (black) and pH 10 (gray)

Up to this point, when using CNC as emulsion inhibitor we observed the highest efficiency at pH 10 and 1000 ppm of NaCl in the aqueous phase. CNC has a high surface charge as a result of sulfate groups; at pH 10 these groups are completely ionized making CNC highly active towards the aqueous interface where it can displace or counteract natural emulsifiers naturally present in the crude oil.

3.4.3.2 Heavy crude oil. Selecting an appropriate emulsion breaker/inhibitor is not an easy task, and there is currently no “one size fits all” solution. Literature reports indicate the choice depends on many variables such as crude oil composition, properties and formation water composition, among others. Thus, we wanted to determine whether or not CNC could be used as inhibitor in both water-in-oil emulsions of light and heavy oils.

Figure 22. shows the instability index for a water-in-heavy crude oil (API 14.7) emulsion prepared with a NaCl brine (1000 ppm); the dispersion is stable for several months. Addition of CNC (1000 ppm) to the water before emulsion formation results in dramatic instability. In fact, up to 60% of water release is observed during the first 20 minutes of the stability test as seen in Figure 22.

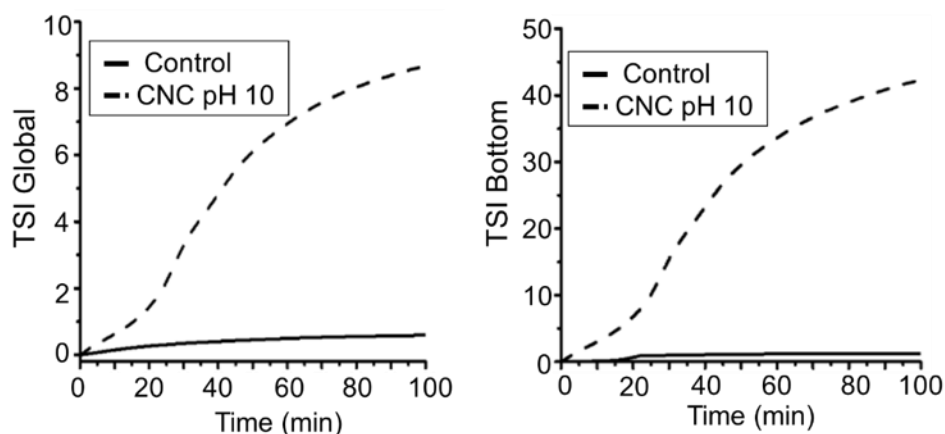


Figure 22. Inhibition tests for a water-in-heavy oil emulsion with suspensions of 1000 ppm CNC in brines of 1000 ppm NaCl at pH 10.

In the graphs for global destabilization we observed an increase of the TSI, up to 10 for the emulsion prepared with the CNC, this behavior indicates a destabilization process induced by the nanocrystals, while in the control emulsion of this crude there is no significant change in the TSI, indicating high stability. TSI values in the lower part of the test vial are much higher, 40 for the emulsion prepared with CNC; this is consistent with the amount of water recovered in this experiment (60%). The tests, using real crudes oil, show that the CNC can compete efficiently with the different surfactants present in the sample, as expected the degree of inhibition depends on the type of crude oil and the characteristics of the brine.

3.5 Conclusions

CNC and CNF behavior at interfaces depends on two key parameters: surface chemistry and particle structure. The ionic groups present in the surface of nanocelluloses (SO_3^- in CNC and COOH^- in CNF) give these materials affinity for polar phases, while their shape allows them to diffuse efficiently in solution. We observe significant emulsion inhibition behavior with both CNC

and CNF, however CNC can be used at lower concentrations. An efficient emulsion inhibitor must compete with natural surfactants, draining them from the interfacial layer and decreasing the surface tension gradient so that breaking or inhibiting emulsion formation occurs. CNC can efficiently disrupt or inhibit formation of a stable interfacial layer upon water interaction with surface active compounds present in light and heavy crude oils.

From an economic perspective, the nanocelluloses (NCCs) market is fast growing due to their many applications. NCCs are biodegradable, biocompatible, non-toxic, and carbon neutral materials with outstanding mechanical, thermal, and physicochemical properties. Currently, NCCs are used by the paints and coatings, oil and gas, cosmetics and pharma, and food and beverage industries. The fastest growing market for NCCs is Asia, and many well established companies such as CelluForce, American Process Inc., Melodea Ltd, Chuetsu Pulp and Paper, Nippon Paper Industries Co. Ltd, and Borregaard, among others, are able to produce NCCs in industrial quantities.

However, the market for NCCs does not have enough traction and the production prices are still very high, when compared with materials with similar characteristics from petrochemical sources. Lowering NCCs prices depend on finding widespread applications for the materials. The oil industry, with the highest CO₂ footprint in the planet, is a suitable candidate for NCCs applications. With current fossil fuel reserves switching to heavy oils, demulsifiers and non-emulsifiers consumption will increase at an accelerated pace. According to a recent study, the demulsifier market will be worth 2.53 Billion USD by 2022. With this forecast in mind, there is space, from our point of view, for alternative carbon-neutral materials (such as NCCs) in this particular market.

3.6 References

- Abdurahman, N. H., & Mahmood, W. K. (2012). Stability of water-in-crude oil emulsions: Effect of cocamide diethanolamine (DEA) and Span83. *International Journal of Physical Sciences*, 7(41), 5585–5597. <https://doi.org/10.5897/IJPS12.405>
- Abitbol, T., Kloser, E., & Gray, D. G. (2013). Estimation of the surface sulfur content of cellulose nanocrystals prepared by sulfuric acid hydrolysis. *Cellulose*, 20(2), 785–794. <https://doi.org/10.1007/s10570-013-9871-0>
- Abraham, E., Deepa, B., Pothan, L. a., Jacob, M., Thomas, S., Cvelbar, U., & Anandjiwala, R. (2011). Extraction of nanocellulose fibrils from lignocellulosic fibres: A novel approach. *Carbohydrate Polymers*, 86(4), 1468–1475. <https://doi.org/10.1016/j.carbpol.2011.06.034>
- Andresen, M., & Stenius, P. (2007). Water-in-oil emulsions stabilized by hydrophobized microfibrillated cellulose. *Journal of Dispersion Science and Technology*, 28(6), 844–851. Retrieved from <http://cat.inist.fr/?aModele=afficheN&cpsidt=19120733>
- Aoudia, M., Al-shibli, M. N., Al-kasimi, L. H., Al-maamari, R., & Al-bemani, A. (2006). Novel Surfactants for Ultralow Interfacial Tension in a Wide Range of Surfactant Concentration and Temperature, 9, 287–293.
- Aveyard, R., Binks, B. P., & Clint, J. H. (2003). Emulsions stabilised solely by colloidal particles. *Advances in Colloid and Interface Science*, 100–102(SUPPL.), 503–546. [https://doi.org/10.1016/S0001-8686\(02\)00069-6](https://doi.org/10.1016/S0001-8686(02)00069-6)

- Beck-Candanedo, S.; Roman, M.; Gray, D. (2005). Effect of conditions on the properties behavior of wood cellulose nanocrystals suspensions. *Biomacromolecules*, 6, 1048–1054. <http://doi.org/10.1021/bm049300p>
- Bondeson, D., Mathew, A., & Oksman, K. (2006). Optimization of the isolation of nanocrystals from microcrystalline cellulose by acid hydrolysis. *Cellulose*, 13(2), 171–180. <https://doi.org/10.1007/s10570-006-9061-4>
- Brinchi, L., Cotana, F., Fortunati, E., & Kenny, J. M. (2013). Production of nanocrystalline cellulose from lignocellulosic biomass: technology and applications. *Carbohydrate Polymers*, 94(1), 154–169. <https://doi.org/10.1016/j.carbpol.2013.01.033>
- Buffiere, J., Balogh-Michels, Z., Borrega, M., Geiger, T., Zimmermann, T., & Sixta, H. (2017). The chemical-free production of nanocelluloses from microcrystalline cellulose and their use as Pickering emulsion stabilizer. *Carbohydrate Polymers*, 178(September), 48–56. <https://doi.org/10.1016/j.carbpol.2017.09.028>
- Capron, I., Rojas, O. J., & Bordes, R. (2017). Behavior of nanocelluloses at interfaces. *Current Opinion in Colloid and Interface Science*, 29, 83–95. <https://doi.org/10.1016/j.cocis.2017.04.001>
- Cheng Q, Ye D, Chang C, Zhang L. (2017). Facile fabrication of superhydrophilic membranes consisted of fibrous tunicate cellulose nanocrystals for highly efficient oil/water separation. *J Memb Sci*, 525, 1–8. doi:10.1016/j.memsci.2016.11.084.
- Cunha, A. G., Mougel, J. B., Cathala, B., Berglund, L. A., & Capron, I. (2014). Preparation of

- double pickering emulsions stabilized by chemically tailored nanocelluloses. *Langmuir*, 30(31). <https://doi.org/10.1021/la5017577>
- Dalmazzone C, Bocard C, Ballerini D. (1995). IFP methodology for developing water-in-crude oil emulsion inhibitors. *Spill Sci Technol Bull*, 2, 143–50. doi:10.1016/S1353-2561(96)00013-8.
- Davies, J. T. (1957). Emulsion Type. I. Physical Chemistry of. *Gas/Liquid and Liquid/Liquid Interfaces*, 426–438.
- Djuve, J., Yang, X., Fjellanger, I. J., Sjöblom, J., & Pelizzetti, E. (2001). Chemical destabilization of crude oil based emulsions and asphaltene stabilized emulsions. *Colloid and Polymer Science*, 279(3), 232–239. <https://doi.org/10.1007/s003960000413>
- Fan, Y., Simon, S., & Sjöblom, J. (2009). Chemical destabilization of crude oil emulsions: Effect of nonionic surfactants as emulsion inhibitors. *Energy and Fuels*, 23(9), 4575–4583. <https://doi.org/10.1021/ef900355d>
- Fujisawa, S., Okita, Y., Fukuzumi, H., Saito, T., & Isogai, A. (2011). Preparation and characterization of TEMPO-oxidized cellulose nanofibril films with free carboxyl groups. *Carbohydrate Polymers*, 84(1), 579–583. <https://doi.org/10.1016/j.carbpol.2010.12.029>
- Fujisawa, S., Togawa, E., & Kuroda, K. (2017). Nanocellulose-stabilized Pickering emulsions and their applications. *Science and Technology of Advanced Materials*, 18(1), 959–971. <https://doi.org/10.1080/14686996.2017.1401423>

- Gestranius, M., Stenius, P., Kontturi, E., Sjöblom, J., & Tammelin, T. (2017). Phase behavior and droplet size of oil-in-water Pickering emulsions stabilised with plant-derived nanocellulosic materials. *Colloids and Surfaces A: Physicochemical and Engineering Aspects*, 519, 60–70. <https://doi.org/10.1016/j.colsurfa.2016.04.025>
- Giraldo-Dávila, D., Chacón-Patiño, M. L., McKenna, A. M., Blanco-Tirado, C., & Combariza, M. Y. (2018). Correlations between Molecular Composition and Adsorption, Aggregation, and Emulsifying Behaviors of PetroPhase 2017 Asphaltenes and Their Thin-Layer Chromatography Fractions. *Energy & Fuels*, *acs.energyfuels.7b02859*. <https://doi.org/10.1021/acs.energyfuels.7b02859>
- Guo, X., Rong, Z., & Ying, X. (2006). Calculation of hydrophile-lipophile balance for polyethoxylated surfactants by group contribution method. *Journal of Colloid and Interface Science*, 298(1), 441–450. <https://doi.org/10.1016/j.jcis.2005.12.009>
- Habibi, Y., Chanzy, H., & Vignon, M. R. (2006). TEMPO-mediated surface oxidation of cellulose whiskers. *Cellulose*, 13(6), 679–687. <https://doi.org/10.1007/s10570-006-9075-y>
- Habibi, Y., Lucia, L. A., & Rojas, O. J. (2010). Cellulose nanocrystals: Chemistry, self-assembly, and applications. *Chemical Reviews*, 110(6), 3479–3500. <https://doi.org/10.1021/cr900339w>
- Hjartnes TN, Sørland GH, Simon S, Sjöblom J. (2019). Demulsification of Crude Oil Emulsions Tracked by Pulsed Field Gradient (PFG) Nuclear Magnetic Resonance (NMR). Part I: Chemical Demulsification. *Ind Eng Chem Res*, 58, 2310–23. doi:10.1021/acs.iecr.8b05165

- Hou, J., Feng, X., Masliyah, J., & Xu, Z. (2012). Understanding Interfacial Behavior of Ethylcellulose at the Water – Diluted Bitumen Interface.
- Hubbe, M. a., Rojas, O. J., Lucia, L. a., & Sain, M. (2008). Cellulosic Nanocomposites: a Review. *BioResources*, 3(3), 929–980. <https://doi.org/10.15376/biores.3.3.929-980>
- Isogai, A., Saito, T., & Fukuzumi, H. (2011). TEMPO-oxidized cellulose nanofibers. *Nanoscale*, 3(1), 71–85. <https://doi.org/10.1039/c0nr00583e>
- Johnson, R. K., Zink-Sharp, A., & Glasser, W. G. (2011). Preparation and characterization of hydrophobic derivatives of TEMPO-oxidized nanocelluloses. *Cellulose*, 18(6), 1599–1609. <https://doi.org/10.1007/s10570-011-9579-y>
- Jonoobi, M., Oladi, R., Davoudpour, Y., Oksman, K., Dufresne, A., Hamzeh, Y., & Davoodi, R. (2015). Different preparation methods and properties of nanostructured cellulose from various natural resources and residues: a review. *Cellulose*. <https://doi.org/10.1007/s10570-015-0551-0>
- Kalashnikova, I., Bizot, H., Cathala, B., & Capron, I. (2012). Modulation of cellulose nanocrystals amphiphilic properties to stabilize oil/water interface. *Biomacromolecules*, 13(1), 267–275. <https://doi.org/10.1021/bm201599j>
- Kang, W., Xu, B., Wang, Y., Li, Y., Shan, X., An, F., & Liu, J. (2011). Stability mechanism of W/O crude oil emulsion stabilized by polymer and surfactant. *Colloids and Surfaces A: Physicochemical and Engineering Aspects*, 384(1–3), 555–560. <https://doi.org/10.1016/j.colsurfa.2011.05.017>

- Khalil, A. (2014). Production and modification of nanofibrillated cellulose using various mechanical process: a review. *Carbohydrate Polymers*, 99, 649–665. <http://doi.org/10.1016/j.carbpol.2013.08.069>
- Kokal, S. L. (2006). Crude Oil Emulsions: A State-Of-The-Art Review. *SPE Production & Facilities*, 20(01), 5–13. <https://doi.org/10.2118/77497-pa>
- Korhonen, J. T., Kettunen, M., Ras, R. H. a, & Ikkala, O. (2011). Hydrophobic nanocellulose aerogels as floating, sustainable, reusable, and recyclable oil absorbents. *ACS Applied Materials & Interfaces*, 3(6), 1813–1816. <https://doi.org/10.1021/am200475b>
- Laitinen, O., Ojala, J., Sirviö, J. A., & Liimatainen, H. (2017). Sustainable stabilization of oil in water emulsions by cellulose nanocrystals synthesized from deep eutectic solvents. *Cellulose*, 24(4), 1679–1689. <https://doi.org/10.1007/s10570-017-1226-9>
- Leal-Calderon, F., & Schmitt, V. (2008). Solid-stabilized emulsions. *Current Opinion in Colloid and Interface Science*, 13(4), 217–227. <https://doi.org/10.1016/j.cocis.2007.09.005>
- Lemarchand, C., Couvreur, P., Vauthier, C., Costantini, D., & Gref, R. (2003). Study of emulsion stabilization by graft copolymers using the optical analyzer Turbiscan. *International Journal of Pharmaceutics*, 254(1), 77–82. [https://doi.org/10.1016/S0378-5173\(02\)00687-7](https://doi.org/10.1016/S0378-5173(02)00687-7)
- Li, Q., Wei, B., Lu, L., Li, Y., Wen, Y., Pu, W., ... Wang, C. (2017). Investigation of physical properties and displacement mechanisms of surface-grafted nano-cellulose fluids for enhanced oil recovery. *Fuel*, 207, 352–364. <https://doi.org/10.1016/j.fuel.2017.06.103>

- Li, Q., Wei, B., Xue, Y., Wen, Y., & Li, J. (2016). Improving the physical properties of nano - cellulose through chemical grafting for potential use in enhancing oil recovery. *Journal of Bioresources and Bioproducts*, 1(4), 186–191.
- Li, X., Li, J., Gong, J., Kuang, Y., Mo, L., & Song, T. (2018). Cellulose nanocrystals (CNCs) with different crystalline allomorph for oil in water Pickering emulsions. *Carbohydrate Polymers*, 183(January), 303–310. <https://doi.org/10.1016/j.carbpol.2017.12.085>
- Li, Y., Wang, B., Ma, M., & Wang, B. (2018). Review of Recent Development on Preparation, Properties, and Applications of Cellulose-Based Functional Materials. *International Journal of Polymer Science*, 2018. <https://doi.org/10.1155/2018/8973643>
- Li, Y., Wang, B., Ma, M., & Wang, B. (2018). Review of Recent Development on Preparation, Properties, and Applications of Cellulose-Based Functional Materials. *International Journal of Polymer Science*, 2018. <https://doi.org/10.1155/2018/8973643>
- Lif, A., Stenstad, P., Syverud, K., Nydén, M., & Holmberg, K. (2010). Fischer-Tropsch diesel emulsions stabilised by microfibrillated cellulose and nonionic surfactants. *Journal of Colloid and Interface Science*, 352(2), 585–92. <http://doi.org/10.1016/j.jcis.2010.08.052>
- Lu, P., & Hsieh, Y.-L. (2010). Preparation and properties of cellulose nanocrystals: Rods, spheres, and network. *Carbohydrate Polymers*, 82(2), 329–336. <https://doi.org/10.1016/j.carbpol.2010.04.073>
- Maaref, S., & Ayatollahi, S. (2018). The effect of brine salinity on water-in-oil emulsion stability through droplet size distribution analysis: A case study. *Journal of Dispersion Science and*

Technology, 39(5), 721–733. <https://doi.org/10.1080/01932691.2017.1386569>

Mikulcová, V., Bordes, R., & Kašpárková, V. (2016). On the preparation and antibacterial activity of emulsions stabilized with nanocellulose particles. *Food Hydrocolloids*, 61, 780–792. <https://doi.org/10.1016/j.foodhyd.2016.06.031>

Molnes, S. N., Mamonov, A., Paso, K. G., Strand, S., & Syverud, K. (2018). Investigation of a new application for cellulose nanocrystals: a study of the enhanced oil recovery potential by use of a green additive. *Cellulose*, 25(4), 2289–2301. <https://doi.org/10.1007/s10570-018-1715-5>

Molnes, S. N., Paso, K. G., Strand, S., & Syverud, K. (2017). The effects of pH, time and temperature on the stability and viscosity of cellulose nanocrystal (CNC) dispersions: implications for use in enhanced oil recovery. *Cellulose*, 24(10), 4479–4491. <https://doi.org/10.1007/s10570-017-1437-0>

Molnes, S. N., Torrijos, I. P., Strand, S., Paso, K. G., & Syverud, K. (2016). Sandstone injectivity and salt stability of cellulose nanocrystals (CNC) dispersions—Premises for use of CNC in enhanced oil recovery. *Industrial Crops and Products*, 93, 152–160. <https://doi.org/10.1016/j.indcrop.2016.03.019>

Niu, F., Han, B., Fan, J., Kou, M., Zhang, B., Feng, Z.-J., ... Zhou, W. (2018). Characterization of structure and stability of emulsions stabilized with cellulose macro/nano particles. *Carbohydrate Polymers*, 199(April), 314–319. <https://doi.org/10.1016/j.carbpol.2018.07.025>

- Ojala, J., Sirviö, J. A., & Liimatainen, H. (2016). Nanoparticle emulsifiers based on bifunctionalized cellulose nanocrystals as marine diesel oil-water emulsion stabilizers. *Chemical Engineering Journal*, 288, 312–320. <https://doi.org/10.1016/j.cej.2015.10.113>
- Oliveira, P. F., Santos, I. C. V. M., Vieira, H. V. P., Fraga, A. K., & Mansur, C. R. E. (2017). Interfacial rheology of asphaltene emulsions in the presence of nanoemulsions based on a polyoxide surfactant and asphaltene dispersant. *Fuel*, 193, 220–229. <https://doi.org/10.1016/j.fuel.2016.12.051>
- Ortiz, D. P., Baydak, E. N., & Yarranton, H. W. (2010). Effect of surfactants on interfacial films and stability of water-in-oil emulsions stabilized by asphaltenes. *Journal of Colloid and Interface Science*, 351(2), 542–555. <https://doi.org/10.1016/j.jcis.2010.08.032>
- Qiu, X., & Hu, S. (2013). “Smart” materials based on cellulose: A review of the preparations, properties, and applications. *Materials*. <https://doi.org/10.3390/ma6030738>
- Roman, M., & Winter, W. T. (2004). Effect of sulfate groups from sulfuric acid hydrolysis on the thermal degradation behavior of bacterial cellulose. *Biomacromolecules*, 5(5), 1671–1677. <https://doi.org/10.1021/bm034519+>
- Rondón, M., Bouriati, P., Lachaise, J., & Salager, J. L. (2006). Breaking of water-in-crude oil emulsions. 1. Physicochemical phenomenology of demulsifier action. *Energy and Fuels*, 20(4), 1600–1604. <https://doi.org/10.1021/ef060017o>
- Rondón, M., Pereira, J. C., Bouriati, P., Graciaa, A., Lachaise, J., & Salager, J. L. (2008). Breaking of water-in-crude-oil emulsions. 2. Influence of asphaltene concentration and diluent

- nature on demulsifier action. *Energy and Fuels*, 22(2), 702–707.
<https://doi.org/10.1021/ef7003877>
- Roodbari NH, Badiei A, Soleimani E, Khaniani Y. (2016). Tweens demulsification effects on heavy crude oil/water emulsion. *Arab J Chem*, 9, S806–11.
doi:10.1016/j.arabjc.2011.08.009.
- Saito, T., Kimura, S., Nishiyama, Y., & Isogai, A. (2007). Cellulose nanofibers prepared by TEMPO-mediated oxidation of native cellulose. *Biomacromolecules*, 8(8), 2485–2491.
<https://doi.org/10.1021/bm0703970>
- Salam, K. K., Alade, a. O., Arinkoola, a. O., & Opawale, a. (2013). Improving the Demulsification Process of Heavy Crude Oil Emulsion through Blending with Diluent. *Journal of Petroleum Engineering*, 2013, 1–6. <https://doi.org/10.1155/2013/793101>
- Wang, J., Hu, F-L., Li, C-Q., Li, J., Yang, Y., (2010) Synthesis of dendritic polyether surfactants for demulsification, *Separation and Purification Technology*, 73(3), pp.349-354.
- Wei, B., Li, H., Li, Q., Wen, Y., Sun, L., Wei, P., ... Li, Y. (2017). Stabilization of Foam Lamella Using Novel Surface-Grafted Nanocellulose-Based Nanofluids. *Langmuir*, 33(21), 5127–5139. <https://doi.org/10.1021/acs.langmuir.7b00387>
- Wei, B., Li, Q., Jin, F., Li, H., & Wang, C. (2016). The Potential of a Novel Nanofluid in Enhancing Oil Recovery. *Energy and Fuels*, 30(4), 2882–2891.
<https://doi.org/10.1021/acs.energyfuels.6b00244>
- Wei, B., Wang, Y., Wen, Y., Xu, X., Wood, C., & Sun, L. (2018). Bubble breakup dynamics and

- flow behaviors of a surface-functionalized nanocellulose based nanofluid stabilized foam in constricted microfluidic devices. *Journal of Industrial and Engineering Chemistry*, 68, 24–32. <https://doi.org/10.1016/j.jiec.2018.07.025>
- Wen, Y., Cheng, H., Lu, L. J., Liu, J., Feng, Y., Guan, W., ... Huang, X. F. (2010). Analysis of biological demulsification process of water-in-oil emulsion by *Alcaligenes* sp. S-XJ-1. *Bioresource Technology*, 101(21), 8315–8322. <https://doi.org/10.1016/j.biortech.2010.05.088>
- Xia, L., Lu, S., & Cao, G. (2004). Stability and demulsification of emulsions stabilized by asphaltenes or resins. *Journal of Colloid and Interface Science*, 271(2), 504–506. <https://doi.org/10.1016/j.jcis.2003.11.027>
- Zoppe, J. O., Venditti, R. A., & Rojas, O. J. (2012). Pickering emulsions stabilized by cellulose nanocrystals grafted with thermo-responsive polymer brushes. *Journal of Colloid and Interface Science*, 369(1), 202–209. <https://doi.org/10.1016/j.jcis.2011.12.011>

Chapter 4

4 Surfactant behavior of surface modified cellulose nanocrystals

4.1 Abstract

We modified cellulose nanocrystals surfaces to reduce their hydrophilicity and modulate their Hydrophilic Lipophilic Balance to explore their use as surfactants. We performed an amidation of oxidized cellulose nanocrystals surface in a reaction involving free carboxylic acids and primary amines. Cellulose nanocrystals were prepared using the oxidation process described by Saito et al., where the radical TEMPO is used as a catalyst and NaOCl and NaBr as an oxidant and co-oxidant respectively, followed by a hydrolysis procedure with HCl. We also prepared cellulose nanocrystals by acid hydrolysis with H₂SO₄; these were subjected to an esterification process with palmitoyl phosphonate using NaH as base. The structural characterization by SEM indicated a decrease in the size of the particles after of the hydrolysis process. We use IR-ATR, and NMR to confirm the efficiency of the functionalization process, as TGA to determine thermal stability and RXD to calculate its crystallinity. The degree of oxidation was determined by conductometric titration. It is interesting that during the hydrolysis process, not only the size but also the degree of oxidation thereof, compared to the nanofibrils, which it suggests that the amorphous region removed during the hydrolysis contains more groups than those of the crystalline region. These two types of modified nanocellulose were tested as emulsion breakers.

4.2 Introduction

Recently, the conversion of fuel derives for biobased materials has shown interest due to environmental concern. (Phanthong *et al.*, 2018, Hubbe, 2019). Some of these studies are based

on cellulose; the most abundant polymer in nature. Nanocellulose in the form of nanofibrils (CNF) or nanocrystals (CNC) is of special interest. Several sources of cellulose are used to obtain CNC and CNF. For instance, regular paper pulp produces different types of nanocrystals depending on the source and the oxidation protocol. More recently, bacterial cellulose (BC) was used to obtain nanoparticles that differ mainly in their dimensions and preparation methods (Blanco *et al.*, 2018).

Cellulose nanofibrils (CNF) are obtained using several mechanical methods, among them: microfluidizers, "steam explosion," and Masuko mills, in addition to ultrasound (Kalil, 2014). These methods are energy-consuming, requiring pretreatment to reduce costs production costs. Among these treatments we have: maleic acid, enzymes, TEMPO oxidation, carboxymethylation, and acetylation.

Reaction of cellulose microfibrils with 2,2,6,6-tetramethylpiperidine-N-Oxyl (TEMPO) is a conventional method for obtaining nanofibrils, TEMPO is a strong oxidant that reacts preferably with C6 OH groups of cellulose, producing carboxylic groups, permanent charges that results in repulsions among fibrils (Lu & Hsieh, 2010; Saito, Okita, Nge, Sugiyama & Isogai, 2006). To obtain smaller structures with higher crystallinity it is necessary to remove amorphous areas from cellulose. The mechanism of this reaction involves acid hydrolysis and comprises protonation of glycosidic oxygen atoms, breakdown of glycosidic bonds, and restoration of chemical structures formed by water molecules of the matrix (Lu & Hsieh, 2010). In general, acid induces rapid depolymerization of cellulose via dissociation of amorphous regions, whose random orientation translate in lower density and makes them more susceptible to hydrolysis. Crystalline regions, given their compact and impenetrable structure, are preserved intact during processing (Habibi, Lucia & Rojas, 2010).

Because of its molecular structure, cellulose is a surface reactive material, particularly because of the presence of three -OH groups per unit of D-anhydroglucose. These functional groups are responsible for the chemical reactions which can be carried out on the cellulose surface. In general, it is possible to control the polymer reactivity by modeling its surface chemistry. It is possible, for example, to introduce electrostatic charges (1), or (2) synthesize hydrophobic surfaces to achieve better coupling of the biopolymer with different matrices (Gómez, Combariza & Blanco, 2017; Thomas *et al.*, 2018, Zhen, 2017)

Surface modification of nanocellulose is a topic of great interest in recent years. This trend is correlated with the increasing amount of recent studies published where changing hydrophilicity of nanocellulose is the key feature. Probably, the most studied reactions are those related to cellulose acetylation (Ashori, Babaei, Jonoobi & Hamzeh, 2014; Lin, Chang, Yu, Huang & Feng, 2010), esterification with fatty acids (Ávila, Fortunati, Kenny, Torre & Foresti, 2017; Wang, Wang, Xie & Zhang, 2018), carbamation, silylation, amination, amidations, oxidations, and non-covalent modification processes such as the adsorption of quaternary ammonium salts and metallic nanoparticles have been studied. (Batmaz, Berry, Loh & Chiu, 2015; Eyley & Thielemans, 2014; Qiu & Hu, 2013; Mariano, El Kissi, & Dufresne, 2014; Thomas *et al.*, 2018)

Particular physical and morphological characteristics of nanocellulose (Ma, Wang, Shen, Huang & Dufresne, 2019), such as high aspect ratio, low density, high modulus of elasticity (Du *et al.*, 2019), high specific modulus, in addition to crystallinity, reactivity and low toxicity are in the interest of many research groups. These properties show promising possibilities for applications of nanocellulose, both in its original and modified form through a variety of surface reactions. Among the reported applications of cellulose nanoparticles, they are absorbent (Hubbe,

2019), membranes for water purification (Cervin, Aulin, Larsson & Wågberg, 2011; Chen *et al.*, 2014), reinforcement in nanocomposites with various polymers (Bras *et al.*, 2010), biomedical applications (Du *et al.*, 2019; Rojas, Bedoya & Ciro, 2015), preparation of Pickering emulsions (Hu, Ballinger, Pelton & Cranston, 2015; Tang *et al.*, 2014), drug delivery systems (Gao *et al.*, 2012), sensors (Ummartyotin & Manuspiya, 2015), other energies and electronic developments (Grishkewich, Mohammed, Tang & Tam, 2017).

In terms of emulsions stabilization or de-stabilization, nanocellulose is a potential material. Several works show that micro fibrillated and surface modified cellulose can be used as a surfactant that stabilizes diesel-water emulsions (Andresen & Stenius, 2007; Xhanari, Syverud & Stenius, 2011). The use of hydrophobic nanocellulose has also been reported for the stabilization of Pickering emulsions (Guo, Du, Gao, Cao & Yin, 2017; Nonappa *et al.*, 2018; Rein, Khalfin & Cohen, 2012). Feng *et al.*, (2010) studied the separation of W / O emulsions using modified cellulose, he found that modified cellulose can be adhered to the interface, displacing natural surfactants, also achieving a decrease in interfacial energy of the film, therefore producing water coalescence (Feng *et al.*, 2010).

In crude –oil extraction processes, the formation of W / O emulsions is very frequent due to the presence of natural surfactants such as asphaltenes, resins and naphthenic acids. The function of an emulsion breaker is to counteract the stabilization mechanisms of the interfacial films, allowing their drainage with the consequent coalescence of the water droplets. (Delgado, Pereira, Rondón, Bullón & Salager, 2016). The point of least stability of an emulsion is achieved when the interactions of the surfactants, present in the interfacial film, are equal for both water and oil. Designing a surfactant capable of breaking a W / O emulsion means creating a substance with an

opposite character to the natural surfactant of the mixture.

In this work, we obtained two types of cellulose nanocrystals. On one hand, we synthesized CNCOOH by oxidizing CNF and carrying out subsequent hydrolysis as described by Habibi *et al.*, (2006) to obtain smaller particles. By combining these two techniques, we were able to obtain particles of sizes from 300 to 500 nm with carboxylic groups on the surface. On the other hand, we synthesized CNC by acid hydrolysis with H₂SO₄ according to the method optimized by Bondeson, Mathew & Oksman (2006). These two types of nanocrystals can form stable water suspensions but poor organic counterparts. We derived several materials from these nanostructures by increasing their hydrophobicity.

The presence of carboxylic acids on the surface of the CNCOOH makes them susceptible to react with amines in order to form amides by using coupling agents, which are responsible for replacing the -OH groups with acid chlorides, anhydrides (mixed), carbon anhydrides or active esters, which this represents a good leaving group in the reaction with amines. Among the most used catalysts today, it is found the uronium salts, which show high efficiency. In this work, we carry out amidation reactions on nanocellulose with long side paraffinic amines using O-benzotriazole-1-yl-1,1, 3,3-tetramethyluronium tetrafluoroborate (TBTU) as a coupling agent and long chain amines as described in “Facile cellulose nanofibrils amidation using a 'one-pot' approach. Cellulose 24, 717-730 (2017) 9” (Gómez *et al.*, 2017), achieving efficient systems dispersed in xylene.

Nanocrystals obtained by acid hydrolysis were surface functionalized by an esterification process using palmitoyl phosphonate and NaH as a base, this allows the esterification of the OH groups in the nanocellulose.

We select our functionalization processes that did not require an initial drying of the nanocellulose, they could be carried out in suspensions and therefore, their final redispersion in xylene was simple for use as emulsion breakers.

4.3 Material and methods

4.3.1 CNCOOH preparation. Amidation of nanocellulose requires the presence of carboxylic acid groups on the surface of nanoparticles; we obtained the nanocrystals using oxidation processes with TEMPO radical as a catalyst, followed by acid hydrolysis with HCl according to the process described.

We prepared 100 mL of 1% suspension of microcrystalline cellulose, added 16 mg of TEMPO, 100 mg of NaBr, and 2 mmol of NaClO. We accomplished the reaction at room temperature, maintaining the pH at 10.5 by adding 0.1 M NaOH. From this process, we obtained NFC cellulose nanofibrils. Subsequently, we carried out a hydrolysis process to decrease the size of the nanocellulose and increase the crystallinity, obtaining oxidized cellulose nanocrystals (CNCOOH). We developed this process using 4N HCl for 4 hours at 80 ° C; we added water with ice to stop the reaction, centrifuged, washed, and subjected the sample to dialysis for five days.

To determine the number of carboxylic acid groups, present on the surface of the cellulose, we titrated the sample by conductometry, according to Habibi *et al.*, (2006).

4.3.2 CNC preparation. In the esterification process, the OH present in the surface of the nanocellulose is involved, due to this, we obtained nanocrystals (CNC) by acid hydrolysis, through the optimized method by Bondeson *et al.*, 2006.

We took 5 g of Whatman paper (5 g) and added 60 mL of concentrated sulfuric acid solution (60 mL, 62%), heated the mixture at 45 ° C for two hours in a Maria bath, the mixture is maintained with constant agitation. To stop the hydrolysis, we added 600 mL of ice-cold distilled water, after which we centrifuged the suspension at 4700 rpm and performed wash cycles and centrifuged with distilled water until reaching a pH of 1, as a final cleaning step, the suspension was subjected to dialysis with 12 kD membranes for ten days. To maintain the stable colloidal suspension, a sonication step was added for 20 minutes using an ultrasonic processor (Sonic vibracell VC750, 20 kHz, 750 watts) in an ice bath to prevent heating. The concentration of the CNC suspension was determined by gravimetric analysis.

4.3.3 Amidation. For amidation of nanocellulose, we prepared a 1% aqueous suspension of oxidized cellulose nanocrystals, 1 mL of Et₃N was added to 100 mL of this suspension. The TBTU salt is dispersed in 20 mL of DMF using a molar ratio of 2:1 to the acid groups present in the nanocellulose, once dissolved, it is added to the suspension and conditioned at room temperature with constant agitation for 30 minutes. The added amines must be dissolved in DMF. We used molar proportions of 4:1 for the carboxylic acids present in nanocellulose.

We carried out two amidations; one with dodecylamine and one with octadecylamine. Amidated nanocelluloses are labeled CNCONC12 when reacting with dodecylamine and CNCONC18 when reacting with octadecylamine. The reaction is carried out at room temperature for 4 hours with constant stirring. The product is washed with n-hexane, methanol, and 0.01N HCl

solution, employing washing and centrifugation cycles. It undergoes a final dialysis stage of 8 days. The degree of substitution was calculated based on Lasseguette method (Lasseguette, 2018).

4.3.4 CNC esterification. We took 100 mL of 1% nanocellulose suspension, added 100 mL of DMSO, removed the water by rotoevaporation, suspended the suspension in a nitrogen atmosphere, heated to 65 ° C, added 140 mg of NaH, increased the temperature to 85 ° C and we added 1250 mg of palmitoyl phosphonate, the reaction is maintained for 24 hours at 85 ° C with continuous agitation. Once the centrifugation time is complete, we performed two cycles of washing and centrifugation with DMSO followed by a cycle of washing and centrifugation with water. Finally, it was undergone for dialysis in deionized water with a 12 kD membrane for five days.

4.3.5 Characterization. FESEM images were carried on a FEI QUANTA FEG 650 (Oregon, USA) equipped with a Large Field Detector; samples were coated with a thin layer of gold before imaging, and the micrographs were taken at 10 kV. X-Ray diffraction analysis was performed on a Bruker D8 DISCOVER X-ray diffractometer (Billerica, MA) with a DaVinci geometry, using a $\text{CuK}\alpha 1$ radiation source (40 kV and 30 mA), an area detector VANTEC-500, and a poly (methyl methacrylate) sample holder. For attenuated total reflectance (ATR-IR) measurements we use a Bruker Tensor 27 (Billerica, MA) FTIR instrument equipped with a Platinum Diamond ATR unit A225/Q (Billerica, MA), using resolution of 2 cm^{-1} , and 32 scans were accumulated for each spectrum.

Crystallinity indices of the cellulose nanocrystals were determined using Segal's Method from the equation:

$$CI = ((I_{002} - I_{AM})/I_{002}) \times 100$$

Equation 5.

Where, I_{002} corresponds to the intensity at $2\theta = 24,2^\circ$ and I_{AM} the intensity at $2\theta = 24,2^\circ$ and I_{AM} the intensity in the amorphous region at $2\theta = 20^\circ$ (Park, Baker, Himmel, Parilla & Johnson, 2010)

NMR Measurements: We performed Solid-state ^{13}C -NMR experiments with a Bruker Advance DSX 450 MHz spectrometer, using proton decoupling and magic angle spinning (CP/MAS) methods. Experimental parameters for ^{13}C CP MAS NMR experiments include 7000 scans, spinning rate of 11.3 kHz, acquisition time of 0.02 s, and temperature of 278 K.

Thermal stability (TGA) to determine the thermal stability of samples, a thermogravimetric analysis was performed using a TA Instruments analyzer Discovery TGA (Newcastle, England) equipped with an infrared heating oven; a temperature controlled thermobalance, a gas supply module, and autosampler system. Nitrogen was used as inert gas nitrogen at a flow of 50 mL/min and a heating rate $10^\circ \text{C} / \text{min}$ starting from room temperature to 500°C

4.3.6 Bottle test. The functionalized nanocrystals were dispersed in xylene, 3 mL of an emulsion supplied by Ecopetrol, labeled "Chichimene" with BSW 50%, were poured into graded centrifuge tubes, 3 μl of the CNC's suspension were added in different concentrations: 500, 800, 1000, 1200, 1500 and 1500 ppm, subjected to stirring magnetically for 1 hour at room temperature and the amount of water released was measured.

The efficiency was determined by comparing this value with the BSW of the emulsion. Also, a

commercial emulsion breaker was used to compare the efficiency of our samples.

4.4 Hypotheses

It is possible to create a reliable surfactant from cellulose nanocrystals by acid hydrolysis, capable of destabilizing water-oil emulsions, W/O, produced during the extraction of heavy oils in Colombian wells. These surfactants are created by functionalization of nanocellulose by adding hydrophobic groups to their surface.

4.5 Results

4.5.1 Characterization

4.5.2 Morphology. Nanofibrils obtained by TEMPO presented elongated forms with widths of up to 300 nm and lengths of several microns. The hydrolysis process was efficient in reducing the size of particles, achieving lengths up to 500 nm and widths of 30 nm. Literature reports that the size of nanocrystals varies greatly according to the raw material and the method of obtaining it, even though our nanocrystals are within the expected range. (Brinchi, Cotana, Fortunati & Kenny, 2013).

Functionalization process does not affect morphology of the nanocrystals. SEM images show elongated shapes with sizes similar to non-functionalized nanocrystals (Figure 23). We determined the degree of oxidation by conductometric titration according to the method described by Follain et al. (Follain, Marais, Montanari & Vignon, 2010), while the degree of substitution is calculated by determining the amount of residual carboxylic groups after the amidation process. The results are shown in Table 2.

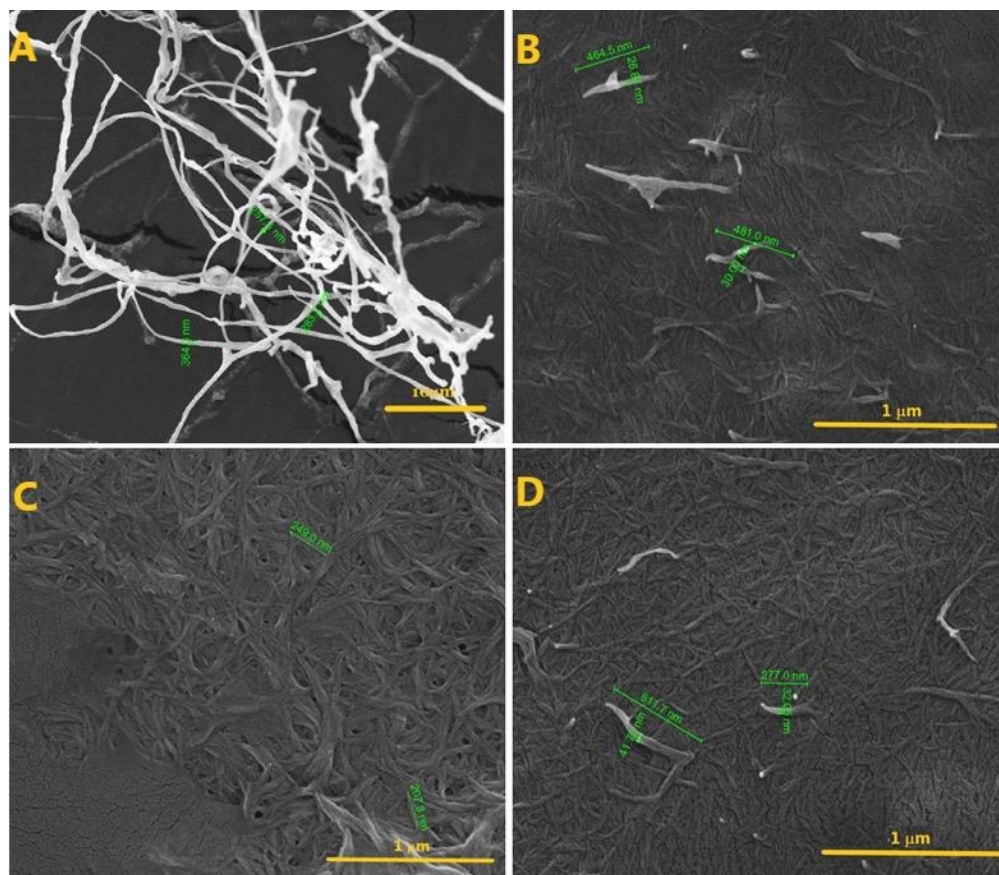


Figure 23. (A) CNF, (B) CNC, (C) CNCONC12, (D)CNCONC18

Table 2.

Oxidation degree (OD) and substitution degree (SD)

Sample	OD	SD
CNF	0,19	0
CNCOOH	0,14	0
CNCONC12	0,06	0,08
CNCONC18	0,075	0,065

Cellulose nanofibrils show a higher content of carboxylic groups than that of the nanocrystals. It indicates that there is loss of these groups in the hydrolysis process, or that there is a greater

presence of them in the amorphous region of the nanocellulose, which is removed during the hydrolysis as it has been reported to happen with sulfate groups (Roman & Winter, 2004).

$$DO = \frac{162\chi C\chi(V_2-V_1)}{w-36\chi C\chi(V_2-V_1)}$$

Equation 6

$$DO_2 = \frac{C\chi(V_2 - V_1)\chi [DO_1\chi(M_\alpha-4)+162]}{w_2 - C\chi(V_2 - V_1)\chi (40 - M_\alpha)}$$

Equation 7

When V_1 and V_2 are volumes of NaOH added. C is the concentration of NaOH; W is the weight of the initial sample of dried nanofibrils; M_α is the molar mass of primary amine and W_2 is the mass of the dry product.

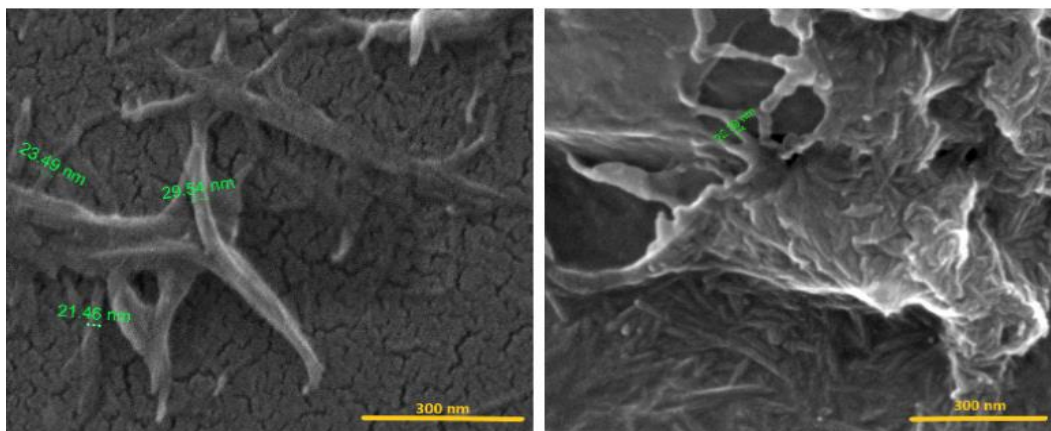


Figure 24. SEM CNC (left) y CNC-Palm (right)

In Figure 24. (left), we see the micrographs of the CNC and we find nanocrystals with elongated

forms, with lengths from 200 to 400 nm and widths between 20 and 30 nm. The superficial modification does not seem to affect the morphology of the nanocrystals significantly, as the CNC-Palm shows similar shapes and sizes (Figure 24. right).

One of the characteristics that makes the nanocellulose special is its aspect ratio, that is, its elongated forms. In the application of these molecules as surfactants, the size influences the mobility of the particles; because the smaller they are, the faster they can migrate to the interfacial region (Capron, Rojas & Bordes, 2017).

4.5.3 Spectral analysis

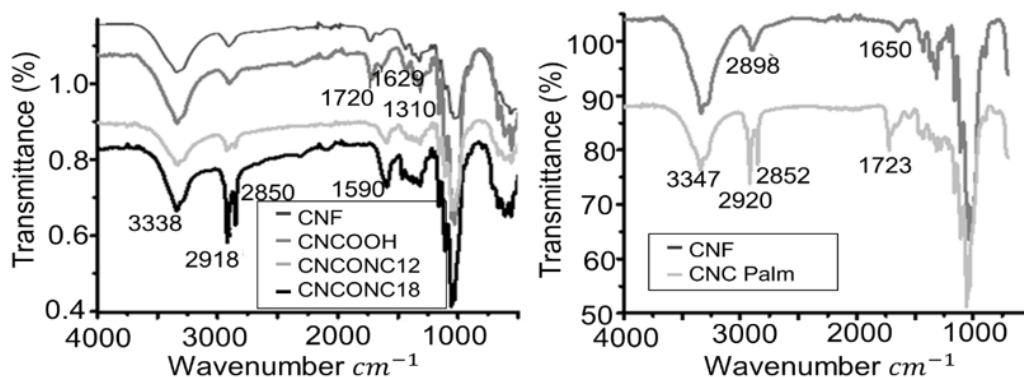


Figure 25. Infrared spectrum

The infrared spectrum of the nanofibrils and the nanocrystals (Figure 25.) shows the typical cellulose bands, with the presence of a wide band between 3600 and 3000 which is attributed to the presence of OH groups, specifically to vibrations by stretching this link (Khanjanzadeh *et al.*, 2018). The small peak towards 2900 corresponds to the stretching of the C-H bonds present in the rings of the cellulose. In addition, we find the band at 1155 cm^{-1} of the C-O-C bonds of the glycosidic bond, the flexion of the C6-H₂ bond between 1424 and 1315 cm^{-1} ; about 1050 cm^{-1} the

C-O bond and the vibration of the C-H group of the anomeric carbon is observed at 900 cm^{-1} (Abraham *et al.*, 2011). Furthermore, we observed at 1720 cm^{-1} the band corresponding to the stretching of the C=O bond of the COOH in the oxidized nanocellulose (Mabrouk, Vilar, Magnin, Belgacem & Boufi, 2011). We do not appreciate important changes between the CNF and CNCOOH spectra, which indicates that the hydrolysis process did not affect the functional groups present in the nanoparticles.

For the amidated nanocelluloses, we observed significant changes in the spectra, the band due to the carbonyl group (1720 cm^{-1}) of the acids present in the surface of the CNCOOH decreases since these are the sites where the reaction with the amines takes place to give the amide groups. The band due to stretching of the C-N bond of the amide group appears at 1590 cm^{-1} , which overlaps with the peak due to the flexion of the N-H bond and the stretching band of the C=O group of the amides. (Benkaddour, Journoux, Jradi, Robert & Daneault, 2014; Taubner, Čopíková, Havelka & Synytsya, 2013). We also observed an increase in the signals in the region between 2910 and 2850 cm^{-1} , corresponding to the CH stretches (Fujisawa, Saito & Isogai, 2012), which indicates the presence of the carbon chains of the amides, the bands present in the CNCONC18 sample are larger, possibly, due to a more significant substitution in addition to having longer chains than those present in CNCONC12. The stretching signal of the N-H bond of the amide group is overlapped with the band corresponding to the -OH groups in the region of 3300 cm^{-1} (Akhlaghi *et al.*, 2015)

The infrared spectrum of the CNC obtained by acid hydrolysis presents the characteristic bands of cellulose mentioned above, with the exception of the carboxyl peak that is not present in this sample. The functionalization process is evidenced by the appearance of a peak in 1723 cm^{-1} due

to the carbonyl groups of the formed esters, there is also an increase in the absorptions around 2900 cm^{-1} allocated to the CH_2 groups of palmitoyl. (Spinella *et al.*, 2016).

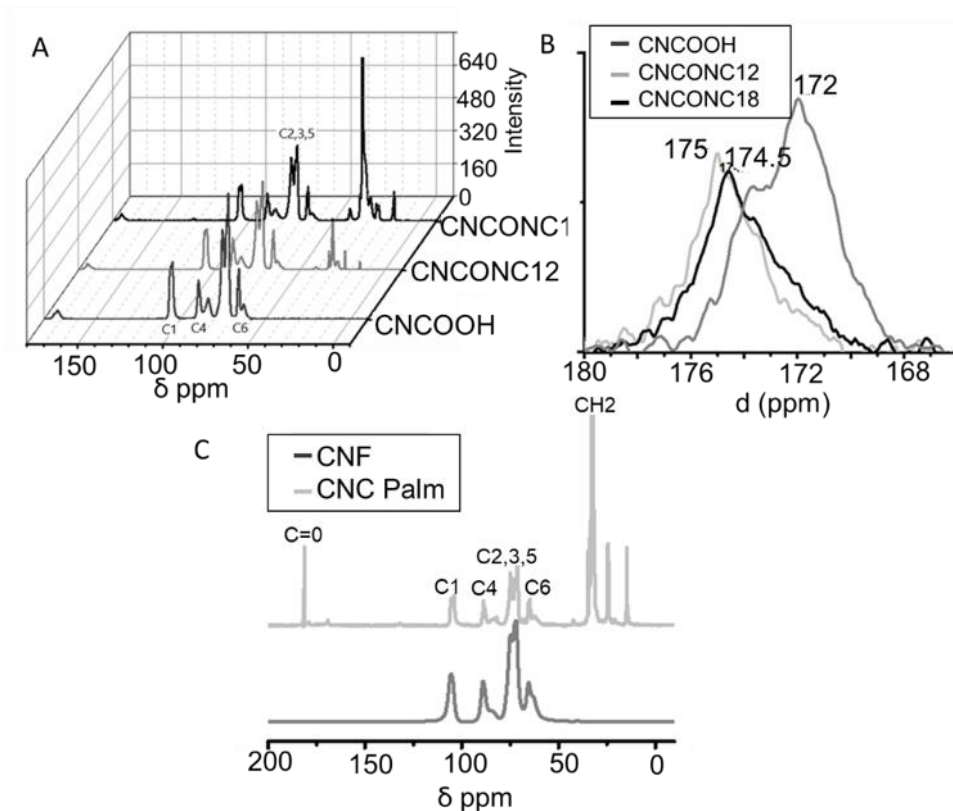


Figure 26 . (A) Full NMR ^{13}C -MAS spectrum for CNCOOH, CNCONC12 and CNCONC18 (B) Section NMR spectrum, (C) spectrum for CNC and CNC-Palm

The ^{13}C PMAS-NMR spectra of CNCOOH and its amidations are presented in Figure A, B, where the characteristic bands of cellulose appear, as the repeating unit is anhydroglucose, the assignment of peaks is made on this molecule as reported by Gårdebjer *et al.*, (2015). Thus, we find the resonances present in 104.5 ppm corresponding to C1, 89.15 ppm for C4, the bands between 75 and 71 corresponds to C2, C3 and C5, although C6 has bands between 65 and 63 ppm, the small peaks that appear at higher fields of C4 and C6 correspond to amorphous regions in the

nanocelluloses (Lasseguette, 2008). Also, we observe a peak at 172 ppm due to the presence of the carboxyl group of oxidized nanocellulose (Park *et al.*, 2010). The functionalized samples show the same peaks plus a high peak towards 30 ppm due to the presence of CH₂ of the aliphatic chains of the amides (Hu, Berry, Pelton & Cranston, 2017), and a displacement of the carboxylic group peak to 175 ppm caused for the amide bond. (Ramírez *et al.*, 2017; Ávila, Fortunati, Kenny, Torre & Foresti, 2014).

In Figure C, we present the NMR spectra of the CNC and CNC-palm. Initially, we can assign the peaks corresponding to the carbons of the anhydroglucose in a similar way, thus, 106 ppm for C1, 89 ppm for C4 of the crystalline region, of 75 at 71 ppm for C2, C3 and C5 and 65 ppm for C6. As expected, in the CNC sample no peak is observed in the region between 170 and 180 ppm, which indicates that it does not present oxidized groups. When the esterification reaction occurs, other peaks appear in NMR, in the region between 10 and 35 ppm due to the presence of carbon chains of the esters added to the nanocellulose. (Gårdebjer, *et al.*, 2015).

4.5.4 Crystallinity. The cellulose can be presented in several allotropic forms (I, II, III, and IV), from these; the cellulose I is the one that occurs in nature, the other crystalline forms are produced during the processes of obtaining and modifying the cellulose (Ramírez *et al.*, 2014).

The diffractogram shows five peaks at $2\theta = 16,3^\circ$, 18° , $21,8^\circ$, 24° and $35,8^\circ$ assigned to the planes (-101), (101), (021), (002), (040) respectively (Khanjanzadeh *et al.*, 2018; Peng *et al.*, 2013.), these peaks correspond to cellulose allotrope type I (Li *et al.*, 2018, Nieh *et al.*, 2018; Oudiani, Chaabouni, Msahli & Sakli, 2011). In the nanocrystals (CNCOOH and CNC), all the peaks are appreciated, whereas in the nanofibrils, the first two bands appear over-lapping.

The index of crystallinity of the nanofibrils was 78.7%, these values are due to the fact that the nanofibrils have both amorphous and crystalline regions (Li et al., 2018), the hydrolysis process presumably degrades the amorphous regions (Nonappa et al., 2018), which increases the crystallinity to 84%. The amidation processes cause a decrease in the crystallinity of the CNC due to the addition of the amorphous chains of the amines to the surface of the nanocrystals (Johnson, Zink-Sharp, Glasser, 2011; Lin et al., 2010), presenting values of 66.8% for amidation with C18 and 71.8% for amidation with C12. However, this process does not affect the type of cellulose allotrope presented, so the same peaks are appreciated but with different intensity. The crystallinity is determined by the Segal method as reported in previous reports.

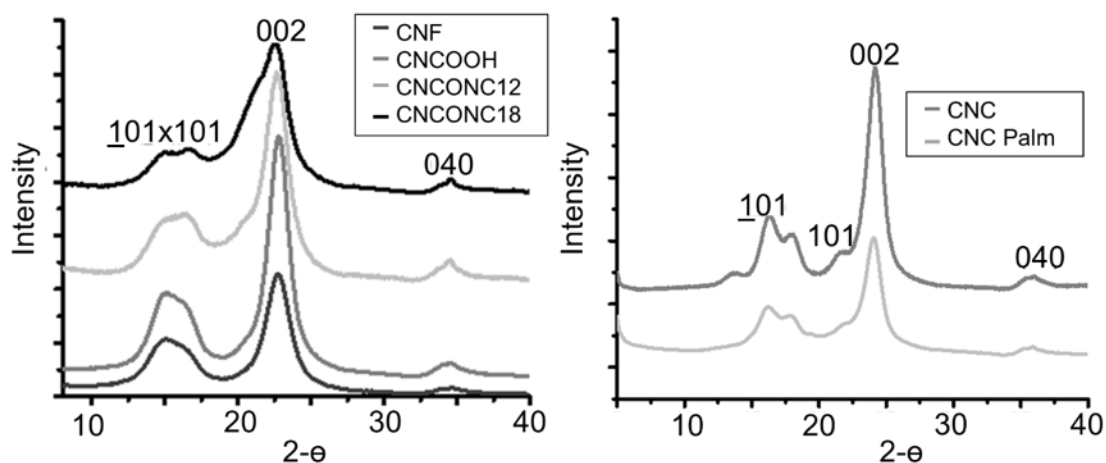


Figure 27. DRX for CNCOOH and amidated (left), CNC and CNC-Palm

The CNC showed a crystallinity of 87%, the functionalization process resulted in a decrease of the crystallinity index to 76%, both the spectrum of the raw nanocrystals and the modified ones show the typical peaks of cellulose I, so we deduce that the functionalization process did not change the crystalline structure of the cellulose, and the decrease in the crystallinity index is due to the fact that the carbon chains of the palmitoyl that were added to the cellulose are not ordered

in crystalline structures.

4.5.5 Thermal stability

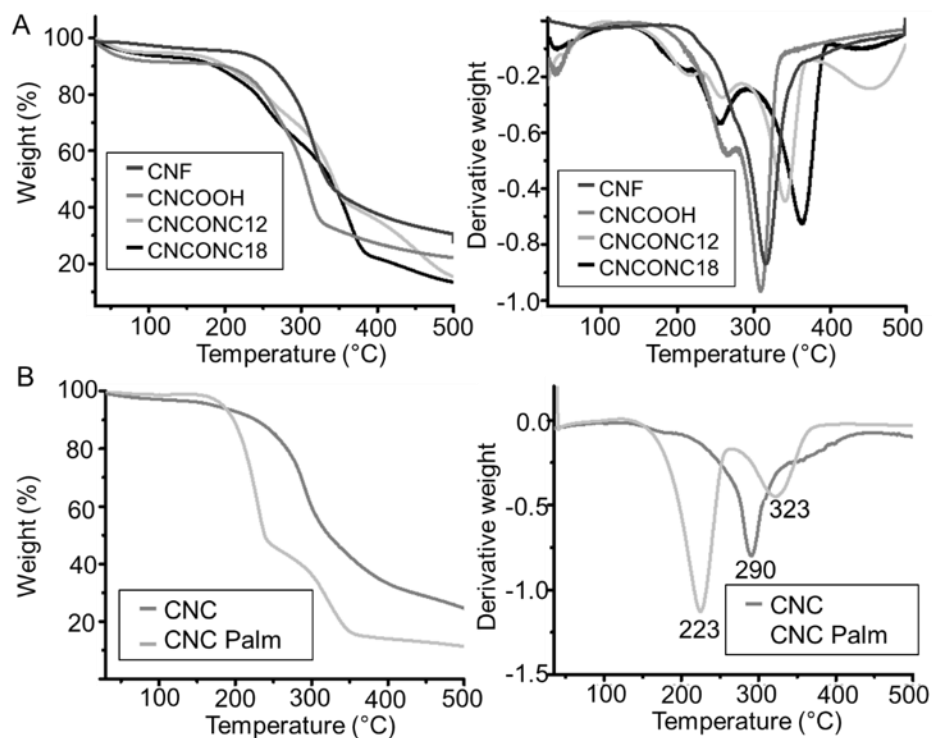


Figure 28. TGA and derivative

The thermal stabilities of the samples were studied by termogravimetric analysis. The results of the TGA for the CNCOOH samples and modifications are shown in Figure . We observe an initial loss of weight in the range from 30 to 500 ° C due to the presence of moisture in the samples. For the oxidized nanocrystals without functionalizing this loss is equivalent to 9%, for CNCN-C12 of 6% and for CNC-C18 of 5.2% which is consistent with the decrease in hydrophilicity expected for functionalized samples.

The following weight loss is attributed to the volatilization of the carbon chains, representing a

very low value for the nanocrystals without functionalizing (1.5%), whereas it is 6.2% for CNC-C12 and 7.2 % for C18, these peaks are presented at temperatures of 209 °C, 214 °C and 203 °C for CNC, CNC-C12 and CNC-C18 respectively. The loss of mass due to carboxylic units occurs at values of 263 °C for CNC, 254 °C for CNC-NC12 and 258 °c for CNC-NC18. In this case, the CNCs have a more extensive loss of 14%, while the CNC-NC12 is 8.7% and the CNC-NC18 is 13.6%.

The most significant loss of mass is attributed to depolymerization of the cellulose structure and its decomposition, these peaks are at 309°C for CNC with 40%, as expected functionalization increases the decomposition temperature reaching 340°C for CNC-NC12 with 36% and 363 °C for CNC-NC18 with 48% loss of mass. These results corroborate what it has been previously described by several authors (Ramírez *et al.*, 2014; Li, Wei, Xue, Wen & Li, 2016; Spinella *et al.*, 2016), which it is that surface functionalization affects the thermal stability of cellulose nanoparticles.

The samples of CNF and CNCOOH show a similar behavior, with an initial weight loss of 5%, first shoulder for CFN at 275 ° C and 264 for CNCOOH, the nanocrystals have a maximum of thermal decomposition at a temperature slightly lower than the one of nanofibrils, with 309 ° C for CNCOOH and 315 ° C for CNF.

In the analysis of thermal stability (Figure B), the unmodified CNCs show an initial mass loss of 4.5% in the region of 30-160 ° C, while for this same region the CNC-Palm only lose 2% mass, in this region, it is considered to eliminate the residual humidity of the samples, as expected, the percentage is lower for the modified nanocrystals, since the introduced hydrophobic groups had to decrease the hydrophilicity of the nanocellulose. (Lin *et al.*, 2010).

In the case of the modified nanocellulose, a second degradation occurs in the region between 200 and 250 ° C, which is attributed to the decomposition of the carbon chains of the palmitoyl groups present on the surface of the nanocellulose, reaching a loss of mass of 50%, this peak is not presented in the CNC without modification. The following process corresponds to the degradation of cellulose, by processes of dehydration, depolymerization and pyrolysis reactions. (Peng *et al.*, 2013) After this process, the amount of sample that persists is 33% for CNC and 15% for CNC-Palm. The peaks of this type of degradation are presented at 290 ° C for the raw nanocellulose and at 323 ° C for the functionalized nanocellulose. The lower temperature of thermal decomposition of the nanocrystals obtained by acid hydrolysis is due to the presence of the sulfate groups on its surface. These groups are released when heated, forming sulfuric acid that accelerates the degradation of cellulose. (Boujemaoui, Mongkhontreerat, Malmström & Carlmark, 2015).

4.5.6 Emulsion breaking test. Fan, Simon & Sjöblom (2009) conducted a study on nonionic surfactants as emulsion inhibitors. They found that the best demulsifier for the mixture they worked with had a HLB of 14.2. However, they agreed that the stability of an emulsion depends on many factors, not only on the surfactants present, therefore, it is necessary to perform a bottle test with each emulsion and surfactant to achieve maximum efficiency in separation.

We calculate the theoretical HLB for the amidated nanocrystal using the Davies equation (Davies, 1957) as shown in equations 8 and 9:

$$\begin{aligned} HLB &= 7 + 0.5(3 - D01) + (2.1D02) + 1.3 * 2 + 9.6(SD) - 0.475(6 + 12(SD) - D02) \\ &= 8.65 \end{aligned}$$

Equation 8. For CNCONC12

$$HLB = 7 + 0.5(3 - DO1) + (2.1DO2) + 1.3 * 2 + 9.6(SD) - 0.475(6 + 18(SD) - DO2)$$

$$= 8.63$$

Equation 9. For CNCONC18

The HLB values of the cellulose nanoparticles fall in the range in which they are considered as oil-in-water emulsion stabilizers and water-in-oil demulsifier (Davies, 1957).

To determine the capacity of breaking emulsions of the functionalized nanocellulose, we performed bottle tests, which are presented in Figure . The photographs were taken 24 hours after the application of the breakers, it should be noted that the control samples did not show any separation of phases; this is due to the great stability of the emulsion used.

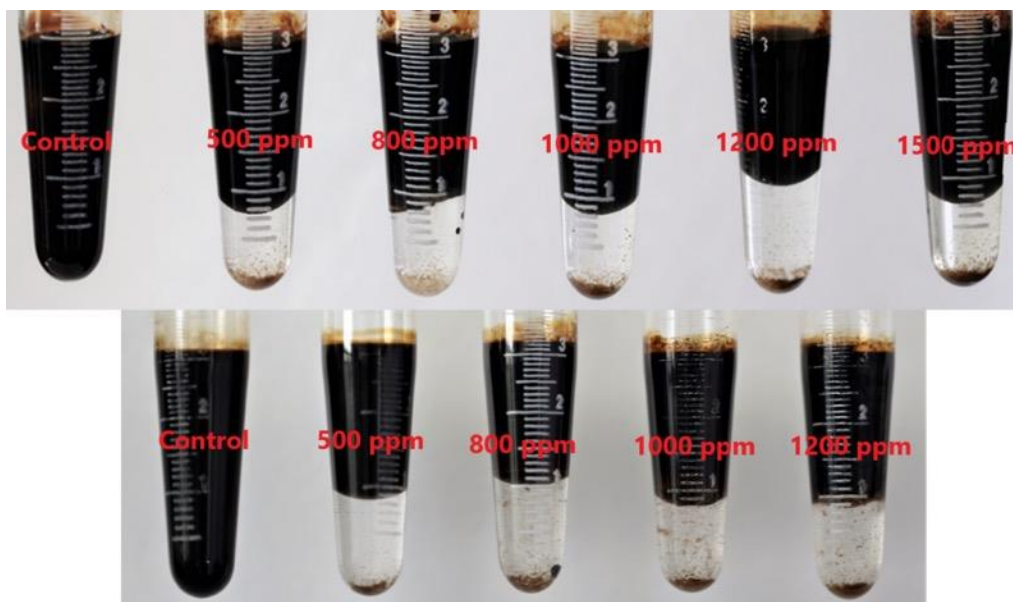


Figure 29. Bottle test using CNCONC18 (top) and CNCONC12 (bottom)

In Figure top, we observed the breaking results for CNCONC18. In this case, the efficiency was higher using a concentration of 1200 ppm, obtaining 1,1 mL of free water, corresponding to

an efficiency of 77%. Figure bottom shows the results of breaking using CNCONC12, where the greatest separation was obtained with 800 ppm of the surfactant, 1.2 mL of free water was obtained, which corresponds to an efficient separation of 76%. No cosurfactants were used for the assay.

The emulsion is stabilized by the natural surfactants present in it, in the case of the W / O emulsions of crude oil, the stability is related to the formation of a rigid interfacial film due, mainly, to the asphaltenes present in the crude (Fan *et al.*, 2009), the CNCOONC12 and CNCONC18 show that they can compete with the asphaltenes and reduce the stability of the interfacial film and so, achieving the coalescence of water droplets.

It has been reported that the stability of an emulsion decreases as the concentration of the demulsifiers increases, until reaching the point where the mixture of amphiphilic substances shows the same affinity between the aqueous phase and the oil phase (Fan *et al.*, 2009), if we increase the concentration of surfactant after that point, it will not improve the separation. Of the tested breaker testers, similar demulsifications were achieved 800 ppm of CNCONC12 (76%), 1200 ppm for CNCONC18 (77%), while the CNC-palm only recovered 38% of the water present at a concentration of 1000 ppm (see Figure 30.).

Using a commercial surfactant; 1,2 mL of free water could be obtained with 800 ppm of the breaker, which shows a higher efficiency than that of the surfactants prepared with nanocellulose; however, we consider that our results are impressive because they prove that it is possible to design surfactants capable of breaking emulsions of heavy crudes.



Figure 30. Bottle test with CNC-Palm.

In the Table 3 we show the percentage of water recovered using the different synthesized nanocellulose surfactants, we also present the results obtained by using a commercial surfactant.

Table 3.

The stability of an emulsion Vs demulsifiers

SAMPLE	500 ppm	800 ppm	1000 ppm	1200 ppm	1500 ppm
CNCONC18	43 %	46 %	50 %	77 %	55 %
CNCONC12	54 %	76 %	61 %	65 %	-
CNC-Palm	-	19 %	38%	32%	-
Commercial	-	78 %	-	-	78,5 %

4.6 Conclusions

IR-ATR and NMR spectra show that functionalization reactions were successful, in addition, RXD confirms that the process was carried out almost only on the surface since the crystalline structure of cellulose particles was not seriously affected. The modified nanocelluloses proved to be

thermally stable up to 200 ° C, which makes them suitable for breaking emulsions of real crudes.

The modified cellulose nanocrystals functioned as W / O emulsion breakers. The first step in the demulsification process is the drainage of the interfacial film, which was achieved by competing our surfactants with the natural emulsifiers present in the oil. We achieved a recovery up to 76% of the water present in the emulsion, achieving an effect similar to the commercial demulsifier with which the comparison was made.

However, it is known that to improve the performance of a demulsifier, it is convenient to make formulations with more of one surfactant, mixing different species and decreasing the dose required. (Delgado *et al.*, 2016)

4.7 References

- Abraham, E., Deepa, B., Pothan, L. a., Jacob, M., Thomas, S., Cvelbar, U., & Anandjiwala, R. (2011). Extraction of nanocellulose fibrils from lignocellulosic fibres: A novel approach. *Carbohydrate Polymers*, 86(4), 1468–1475. <http://doi.org/10.1016/j.carbpol.2011.06.034>
- Akhlaghi, S. P., Zaman, M., Mohammed, N., Brinatti, C., Batmaz, R., Berry, R., ... & Tam, K. C. (2015). Synthesis of amine functionalized cellulose nanocrystals: Optimization and characterization. *Carbohydrate Research*, 409, 48–55. <http://doi.org/10.1016/j.carres.2015.03.009>
- Andresen, M., & Stenius, P. (2007). Water-in-oil emulsions stabilized by hydrophobized microfibrillated cellulose. *Journal of Dispersion Science and Technology*, 28(6), 837–844. <https://doi.org/10.1080/01932690701341827>

- Ashori, A., Babae, M., Jonoobi, M., & Hamzeh, Y. (2014). Solvent-free acetylation of cellulose nanofibers for improving compatibility and dispersion. *Carbohydrate Polymers*, *102*(1), 369–375. <https://doi.org/10.1016/j.carbpol.2013.11.067>
- Batmaz, R., Berry, R., Loh, W., & Chiu, K. (2015). Synthesis of amine functionalized cellulose nanocrystals : optimization and characterization. *Carbohydrate Research*, *409*, 48–55. <http://doi.org/10.1016/j.carres.2015.03.009>
- Benkaddour, A., Journoux-Lapp, C., Jradi, K., Robert, S., & Daneault, C. (2014). Study of the hydrophobization of TEMPO-oxidized cellulose gel through two routes: Amidation and esterification process. *Journal of Materials Science*, *49*(7), 2832–2843. <http://doi.org/10.1007/s10853-013-7989-y>
- Blanco, A., Monte, M. C., Campano, C., Balea, A., Merayo, N., & Negro, C. (2018). Nanocellulose for industrial use: Cellulose nanofibers (CNF), cellulose nanocrystals (CNC), and bacterial cellulose (BC). In *Handbook of Nanomaterials for Industrial Applications*, 74-126. Elsevier.
- Bondeson, D., Mathew, A., & Oksman, K. (2006). Optimization of the isolation of nanocrystals from microcrystalline cellulose by acid hydrolysis. *Cellulose*, *13*(2), 171–180. <https://doi.org/10.1007/s10570-006-9061-4>
- Boujemaoui, A., Mongkhontreerat, S., Malmström, E., & Carlmark, A. (2015). Preparation and characterization of functionalized cellulose nanocrystals. *Carbohydrate Polymers*, *115*, 457–464. <https://doi.org/10.1016/j.carbpol.2014.08.110>

- Bras, J., Hassan, M. L., Bruzesse, C., Hassan, E. a., El-Wakil, N. a., & Dufresne, A. (2010). Mechanical, barrier, and biodegradability properties of bagasse cellulose whiskers reinforced natural rubber nanocomposites. *Industrial Crops and Products*, *32*(3), 627–633. <https://doi.org/10.1016/j.indcrop.2010.07.018>
- Brinchi, L., Cotana, F., Fortunati, E., & Kenny, J. M. (2013). Production of nanocrystalline cellulose from lignocellulosic biomass: technology and applications. *Carbohydrate Polymers*, *94*(1), 154–169. <https://doi.org/10.1016/j.carbpol.2013.01.033>
- Capron, I., Rojas, O. J., & Bordes, R. (2017). Behavior of nanocelluloses at interfaces. *Current Opinion in Colloid and Interface Science*, *29*, 83–95. <https://doi.org/10.1016/j.cocis.2017.04.001>
- Cervin, N. T., Aulin, C., Larsson, P. T., & Wågberg, L. (2011). Ultra porous nanocellulose aerogels as separation medium for mixtures of oil/water liquids. *Cellulose*, *19*(2), 401–410. <https://doi.org/10.1007/s10570-011-9629-5>
- Chen, W., Li, Q., Wang, Y., Yi, X., Zeng, J., Yu, H., ...& Li, J. (2014). Comparative study of aerogels obtained from differently prepared nanocellulose fibers. *ChemSusChem*, *7*(1), 154–161. <https://doi.org/10.1002/cssc.201300950>
- Davies, J. T. (1957). Emulsion Type . I . Physical Chemistry of the emulsifying agent. In *internatinal Congress Surface Activity* (pp. 426–438). London.
- Delgado-Linares, J. G., Pereira, J. C., Rondón, M., Bullón, J., & Salager, J. L. (2016). Breaking of Water-in-Crude Oil Emulsions. 6. Estimating the Demulsifier Performance at Optimum

- Formulation from Both the Required Dose and the Attained Instability. *Energy and Fuels*, 30(7), 5483–5491. <https://doi.org/10.1021/acs.energyfuels.6b00666>
- Du, H., Liu, W., Zhang, M., Si, C., Zhang, X., & Li, B. (2019). Cellulose nanocrystals and cellulose nanofibrils based hydrogels for biomedical applications. *Carbohydrate Polymers*, 209(November 2018), 130–144. <https://doi.org/10.1016/j.carbpol.2019.01.020>
- Eyley, S., & Thielemans, W. (2014). Surface modification of cellulose nanocrystals. *Nanoscale*, 6(14), 7764–7779. <http://doi.org/10.1039/C4NR01756K>
- Fan, Y., Simon, S., & Sjöblom, J. (2009). Chemical destabilization of crude oil emulsions: Effect of nonionic surfactants as emulsion inhibitors. *Energy and Fuels*, 23(9), 4575–4583. <https://doi.org/10.1021/ef900355d>
- Feng, X., Mussone, P., Gao, S., Wang, S., Wu, S. Y., Masliyah, J. H., & Xu, Z. (2010). Mechanistic study on demulsification of water-in-diluted bitumen emulsions by ethylcellulose. *Langmuir*, 26(5), 3050–3057. <https://doi.org/10.1021/la9029563>
- Filpponen, I., Kontturi, E., Nummelin, S., Rosilo, H., Kolehmainen, E., Ikkala, O., & Laine, J. (2012). Generic method for modular surface modification of cellulosic materials in aqueous medium by sequential “click” reaction and adsorption. *Biomacromolecules*, 13(3), 736–742. <https://doi.org/10.1021/bm201661k>
- Follain, N., Marais, M.-F., Montanari, S., & Vignon, M. R. (2010). Coupling onto surface carboxylated cellulose nanocrystals. *Polymer*, 51(23), 5332–5344. <https://doi.org/10.1016/j.polymer.2010.09.001>

- Fujisawa, S., Saito, T., & Isogai, A. (2012). Nano-dispersion of TEMPO-oxidized cellulose/aliphatic amine salts in isopropyl alcohol. *Cellulose*, 19(2), 459–466. <http://doi.org/10.1007/s10570-011-9648-2>
- Gao, L., Liu, G., Ma, J., Wang, X., Zhou, L., & Li, X. (2012). Drug nanocrystals: In vivo performances. *Journal of Controlled Release : Official Journal of the Controlled Release Society*, 160(3), 418–430. <https://doi.org/10.1016/j.jconrel.2012.03.013>
- Gårdebjer, S., Bergstrand, A., Idström, A., Börstell, C., Naana, S., Nordstierna, L., & Larsson, A. (2015). Solid-state NMR to quantify surface coverage and chain length of lactic acid modified cellulose nanocrystals, used as fillers in biodegradable composites. *Composites Science and Technology*, 107, 1–9. <https://doi.org/10.1016/j.compscitech.2014.11.014>
- Gómez, F. N., Combariza, M. Y., & Blanco-Tirado, C. (2017). Facile cellulose nanofibrils amidation using a ‘one-pot’ approach. *Cellulose*, 24(2), 717–730. <https://doi.org/10.1007/s10570-016-1174-9>
- Grishkewich, N., Mohammed, N., Tang, J., & Tam, K. C. (2017). Recent advances in the application of cellulose nanocrystals. *Current Opinion in Colloid and Interface Science*, 29, 32–45. <http://doi.org/10.1016/j.cocis.2017.01.005>
- Guo, J., Du, W., Gao, Y., Cao, Y., & Yin, Y. (2017). Cellulose nanocrystals as water-in-oil Pickering emulsifiers via intercalative modification. *Colloids and Surfaces A: Physicochemical and Engineering Aspects*, 529(April), 634–642. <https://doi.org/10.1016/j.colsurfa.2017.06.056>

Habibi, Y., Chanzy, H., & Vignon, M. R. (2006). TEMPO-mediated surface oxidation of cellulose whiskers. *Cellulose*, 13(6), 679–687. <http://doi.org/10.1007/s10570-006-9075-y>

Habibi, Y., Lucia, L. A., & Rojas, O. J. (2010). Cellulose nanocrystals: Chemistry, self-assembly, and applications. *Chemical Reviews*, 110(6), 3479–3500. <https://doi.org/10.1021/cr900339w>

Hu, Z., Ballinger, S., Pelton, R., & Cranston, E. D. (2015). Surfactant-enhanced cellulose nanocrystal Pickering emulsions. *Journal of Colloid and Interface Science*, 439, 139–148. <https://doi.org/10.1016/j.jcis.2014.10.034>

Hu, Z., Berry, R. M., Pelton, R., & Cranston, E. D. (2017). One-Pot Water-Based Hydrophobic Surface Modification of Cellulose Nanocrystals Using Plant Polyphenols. *ACS Sustainable Chemistry and Engineering*, 5(6), 5018–5026. <https://doi.org/10.1021/acssuschemeng.7b00415>

Hubbe, M. A. (2019). Review of the Mechanistic Roles of Nanocellulose, Cellulosic Fibers, and Hydrophilic Cellulose Derivatives in Cellulose-Based Absorbents. (Md. I. H. Mondal, Ed.). Raleigh: *Springer International Publishing* AG. https://doi.org/10.1007/978-3-319-77830-3_8

Johnson, R. K., Zink-Sharp, A., & Glasser, W. G. (2011). Preparation and characterization of hydrophobic derivatives of TEMPO-oxidized nanocelluloses. *Cellulose*, 18(6), 1599–1609. <http://doi.org/10.1007/s10570-011-9579-y>

Khalil, A. (2014). Production and modification of nanofibrillated cellulose using various

- mechanical process: a review. *Carbohydrate Polymers*, 99, 649–665.
- Khanjanzadeh, H., Behrooz, R., Bahramifar, N., Gindl-Altmutter, W., Bacher, M., Edler, M., & Griesser, T. (2018). Surface chemical functionalization of cellulose nanocrystals by 3-aminopropyltriethoxysilane. *International Journal of Biological Macromolecules*, 106, 1288–1296. <http://doi.org/10.1016/j.ijbiomac.2017.08.136>
- Lasseguette, E. (2008). Grafting onto microfibrils of native cellulose. *Cellulose*, 15(4), 571–580. <https://doi.org/10.1007/s10570-008-9200-1>
- Li, Q., Wei, B., Xue, Y., Wen, Y., & Li, J. (2016). Improving the physical properties of nano - cellulose through chemical grafting for potential use in enhancing oil recovery. *Journal of Bioresources and Bioproducts*, 1(4), 186–191.
- Li, X., Li, J., Gong, J., Kuang, Y., Mo, L., & Song, T. (2018). Cellulose nanocrystals (CNCs) with different crystalline allomorph for oil in water Pickering emulsions. *Carbohydrate Polymers*, 183(January), 303–310. <http://doi.org/10.1016/j.carbpol.2017.12.085>
- Li, Y., Wang, B., Ma, M., & Wang, B. (2018). Review of Recent Development on Preparation, Properties, and Applications of Cellulose-Based Functional Materials. *International Journal of Polymer Science*, 2018. <http://doi.org/10.1155/2018/8973643>
- Lin, N., Chang, P. R., Yu, J., Huang, J., & Feng, J. (2010). Surface acetylation of cellulose nanocrystal and its reinforcing function in poly(lactic acid). *Carbohydrate Polymers*, 83(4), 1834–1842. <http://doi.org/10.1016/j.carbpol.2010.10.047>
- Lu, P., & Hsieh, Y.-L. (2010). Preparation and properties of cellulose nanocrystals: Rods, spheres,

- and network. *Carbohydrate Polymers*, 82(2), 329–336.
<https://doi.org/10.1016/j.carbpol.2010.04.073>
- Ma, X., Wang, Y., Shen, Y., Huang, J., & Dufresne, A. (2019). Current Status of Nanocellulose-Based Nanocomposites. In L. N. Huang Jin, Dufresne Alain (Ed.), *Nanocellulose: From Fundamentals to Advanced Materials* (First Edit, pp. 155–200). Wiley-VCHVerlag GmbH& Co.
- Mabrouk, A. B., Vilar, M. R., Magnin, A., Belgacem, M. N., & Boufi, S. (2011). Synthesis and characterization of cellulose whiskers/polymer nanocomposite dispersion by mini-emulsion polymerization. *Journal of colloid and interface science*, 363(1), 129–36.
- Mariano, M., El Kissi, N., & Dufresne, A. (2014). Cellulose nanocrystals and related nanocomposites: Review of some properties and challenges. *Journal of Polymer Science, Part B: Polymer Physics*, 52(12), 791–806. <http://doi.org/10.1002/polb.23490>
- Nieh, W., Chan, K. J., Roberts, R., Eichhorn, S. J., Stinson-Bagby, K., Fox, D. M., ... Camarero-Espinosa, S. (2018). Current characterization methods for cellulose nanomaterials. *Chemical Society Reviews*, 47(8), 2609–2679. <http://doi.org/10.1039/c6cs00895j>
- Nonappa, Gröschel, A. H., Laaksonen, P., Kontturi, E., Ikkala, O., Rojas, O. J., & Linder, M. B. (2018). Advanced Materials through Assembly of Nanocelluloses. *Advanced Materials*, 30(24), 1703779. <http://doi.org/10.1002/adma.201703779>
- Oudiani, A. El, Chaabouni, Y., Msahli, S., & Sakli, F. (2011). Crystal transition from cellulose I to cellulose II in NaOH treated *Agave americana* L. fibre. *Carbohidrate Polymers*, 86,

1221–1229. <http://doi.org/10.1016/j.carbpol.2011.06.037>

Park, S., Baker, J. O., Himmel, M. E., Parilla, P. a, & Johnson, D. K. (2010). Cellulose crystallinity index: measurement techniques and their impact on interpreting cellulase performance. *Biotechnology for Biofuels*, 3, 10. <https://doi.org/10.1186/1754-6834-3-10>

Peng, Y., Gardner, D. J., Han, Y., Kiziltas, A., Cai, Z., & Tshabalala, M. A. (2013). Influence of drying method on the material properties of nanocellulose I: Thermostability and crystallinity. *Cellulose*, 20(5), 2379–2392. <http://doi.org/10.1007/s10570-013-0019-z>

Pereira, J. C., Delgado-Linares, J., Scorzza, C., Rondó, M., Rodríguez, S., & Salager, J. L. (2011). Breaking of water-in-Crude oil emulsions. 4. estimation of the demulsifier surfactant performance to destabilize the asphaltenes effect. *Energy and Fuels*, 25(3), 1045–1050. <https://doi.org/10.1021/ef100979y>

Phanthong, P., Reubroycharoen, P., Hao, X., Xu, G., Abudula, A., & Guan, G. (2018). Nanocellulose: Extraction and application. *Carbon Resources Conversion*, 1(1), 32–43. <https://doi.org/10.1016/j.crcon.2018.05.004>

Qiu, X., & Hu, S. (2013). “Smart” materials based on cellulose: A review of the preparations, properties, and applications. *Materials*. <http://doi.org/10.3390/ma6030738>

Ramírez, J. A., Fortunati, E., Kenny, J. M., Torre, L., & Foresti, M. L. (2017). Simple citric acid-catalyzed surface esterification of cellulose nanocrystals. *Carbohydrate Polymers*, 157, 1358–1364. <https://doi.org/10.1016/j.carbpol.2016.11.008>

Ramírez, J. A., Suriano, C. J., Cerrutti, P., & Foresti, M. L. (2014). Surface esterification of

- cellulose nanofibers by a simple organocatalytic methodology. *Carbohydrate Polymers*, 114, 416–423. <http://doi.org/10.1016/j.carbpol.2014.08.020>
- Rein, D. M., Khalfin, R., & Cohen, Y. (2012). Cellulose as a novel amphiphilic coating for oil-in-water and water-in-oil dispersions. *Journal of Colloid and Interface Science*, 386(1), 456–463. <https://doi.org/10.1016/j.jcis.2012.07.053>
- Rojas, J., Bedoya, M., & Ciro, Y. (2015). Current trends in the production of cellulose nanoparticles and nanocomposites for biomedical applications. In M. Poletto, & H. L. Ornaghi (Eds.). *Cellulose-Fundamental aspects and current trends* (pp. 193–228). Rijeka, Croatia: InTech. <http://doi.org/10.5772/61334>
- Roman, M., and Winter, W. T. (2004). Effect of sulfate groups from sulfuric acid hydrolysis on the thermal degradation behavior of bacterial cellulose. *Biomacromolecules*, 5(5), 1671–7. DOI: 10.1021/bm034519+
- Saito, T., Okita, Y., Nge, T., Sugiyama, J., & Isogai, A. (2006). TEMPO-Mediated Oxidation of Native Cellulose: Microscopic Analysis of Fibrous Fractions in the Oxidized Products. *Carbohydrate Polymers*, 65(4), 435–440. <https://doi.org/10.1016/j.carbpol.2006.01.034v>
- Spinella, S., Maiorana, A., Qian, Q., Dawson, N. J., Hepworth, V., Mccallum, S. A., ... Gross, R. A. (2016). Concurrent Cellulose Hydrolysis and Esterification to Prepare a Surface-Modified Cellulose Nanocrystal Decorated with Carboxylic Acid Moieties. *ACS Sustainable Chemistry and Engineering*, 4, 1538–1550. <https://doi.org/10.1021/acssuschemeng.5b01489>

- Tang, J., Lee, M. F. X., Zhang, W., Zhao, B., Berry, R. M., & Tam, K. C. (2014). Dual responsive pickering emulsion stabilized by poly[2-(dimethylamino) ethyl methacrylate] grafted cellulose nanocrystals. *Biomacromolecules*, 15(8), 3052–3060. <https://doi.org/10.1021/bm500663w>
- Tang, J., Sisler, J., Grishkewich, N., & Tam, K. C. (2017). Functionalization of cellulose nanocrystals for advanced applications. *Journal of Colloid and Interface Science*, 494, 397–409. <http://doi.org/10.1016/j.jcis.2017.01.077>
- Tardy, B. L., Yokota, S., Ago, M., Xiang, W., Kondo, T., Bordes, R., & Rojas, O. J. (2017). Nanocellulose–surfactant interactions. *Current Opinion in Colloid and Interface Science*, 29, 57–67. <https://doi.org/10.1016/j.cocis.2017.02.004>
- Taubner, T., Čopíková, J., Havelka, P., & Synytsya, A. (2013). Preparation of amidated derivatives of monocarboxy cellulose. *Cellulose*, 20(4), 2045–2055. <http://doi.org/10.1007/s10570-013-9938-y>
- Thomas, B., Raj, M. C., Athira, K. B., Rubiyah, M. H., Joy, J., Moores, A., & Drisko, G. L. (2018). Nanocellulose, a Versatile Green Platform: From Biosources to Materials and Their Applications. *Chemical Reviews*, 118, 11575–11625. <http://doi.org/10.1021/acs.chemrev.7b00627>
- Ummartyotin, S., & Manuspiya, H. (2015). A critical review on cellulose :cellulose: From fundamental to an approach on sensor technology. *Renewable and Sustainable Energy Reviews*, 41, 402–412. <https://doi.org/10.1016/j.rser.2014.08.050>

Wang, Y., Wang, X., Xie, Y., & Zhang, K. (2018). Functional nanomaterials through esterification of cellulose: a review of chemistry and application. *Cellulose*, 25(7), 3703–3731. <https://doi.org/10.1007/s10570-018-1830-3>

Xhanari, K., Syverud, K., & Stenius, P. (2011). Emulsions stabilized by microfibrillated cellulose: The effect of Hydrophobization, concentration and O/W ratio. *Journal of Dispersion Science and Technology*, 32(3), 447–452. <https://doi.org/10.1080/01932691003658942>

Zhen Zhangth. (2017). Surface Modification of Cellulose Nanocrystal for Advanced Applications. University of Waterloo. Thesis

Conclusions

We obtained cellulose particles at the nanoscopic scale and performed surface functionalization processes, the thermal stability of the raw and modified nanocellulose (higher than 200 ° C) makes them suitable for the purpose of this work, which is its use as a breaker / inhibitor of the formation of raw water emulsions.

The crystallographic characterization of the nanocellulose shows an increase in the crystallinity due to the hydrolysis process, in addition we verify that the functionalization processes do not affect the internal structure of the CNC, because the change in the crystallographic patterns is little.

The nanocrystals and cellulose nanofibrils, being hydrophilic, can be dispersed in water, which allowed their evaluation in emulsion inhibition processes. We verify that the CNC and the CNF compete effectively with the natural surfactants present in the oil (asphaltenes and resins) avoiding the formation of the rigid interfacial layer and allowing the separation of phases, achieving a recovery of 75% of the added water.

We tested the nanocellulose as a W / O emulsion breaker of real crudes, for this it was necessary to change its HLB, increasing its hydrophobicity, so that they could be dispersed in xylene. We achieved a separation efficiency of 77%, similar to those obtained with commercial surfactants

Studies with oil-in-water emulsions show that nanocellulose can form an effective layer around oil droplets, since they have different degrees of hydrophilicity on their faces (Salas et al, 2014, Capron et al 2017). Capron et al show us the ability to bend the CNCs on the oil surface, stabilizing the interface and inhibiting the coalescence of Pickering emulsions. We know that oil-in-water emulsifiers are suitable for carrying out the process of separating water-in-oil emulsions, this

allows us to infer that nanocellulose would be a good demulsifier for this type of mixture.

Several studies (Pereira et al, Liu et al 2015) show us that the effective demulsification of a W / O emulsion is achieved thanks to a synergistic effect between the natural emulsifier and the added demulsifier. We propose that nanocellulose has the ability to inhibit the formation of water-in-oil emulsions due to several factors, first its degree of hydrophobicity allows it to migrate to the water-oil interface coexisting with asphaltenes, which are the emulsifiers present in our samples Second, its hydrophilicity helps to vary the HLB of the nanocellulose-asphaltene mixture at the interface, reducing the stiffness of the film and favoring phase separation (Tardy et al, 2017).

The greater efficiency in the process of inhibition of the CNC is due to its smaller size, which allows a more efficient diffusion to the interface. (Pereira J. , Delgado-Linares J, Scorzza C, Rondó M, Rodríguez S, Salager J. 2011)

Some recommendations to continue research:

We suggest carrying out other tests using cosurfactants to decrease the amount of nanoparticles required.

Perform tests with hydrophilic materials (CNC and CNF) as demulsifiers.

Investigate the impact of the degree of oxidation of cellulose nanofibrils (CNF) on the efficiency in the processes of inhibition and breaking of emulsions.

Study contact angle measurement and surface energy calculations to establish the impacts of surface modifications of materials on their adhesion and cohesion properties.

References

- Abdurahman, N. H., & Mahmood, W. K. (2012). Stability of water-in-crude oil emulsions: Effect of cocamide diethanolamine (DEA) and Span83. *International Journal of Physical Sciences*, 7(41), 5585–5597. <https://doi.org/10.5897/IJPS12.405>
- Abitbol, T., Kloser, E., & Gray, D. G. (2013). Estimation of the surface sulfur content of cellulose nanocrystals prepared by sulfuric acid hydrolysis. *Cellulose*, 20(2), 785–794. <https://doi.org/10.1007/s10570-013-9871-0>
- Abraham, E., Deepa, B., Pothan, L. a., Jacob, M., Thomas, S., Cvelbar, U., & Anandjiwala, R. (2011). Extraction of nanocellulose fibrils from lignocellulosic fibres: A novel approach. *Carbohydrate Polymers*, 86(4), 1468–1475. <https://doi.org/10.1016/j.carbpol.2011.06.034>
- Akhlaghi, S. P., Zaman, M., Mohammed, N., Brinatti, C., Batmaz, R., Berry, R., ... & Tam, K. C. (2015). Synthesis of amine functionalized cellulose nanocrystals: Optimization and characterization. *Carbohydrate Research*, 409, 48–55. <http://doi.org/10.1016/j.carres.2015.03.009>
- Al-Sabagh, A. M., Nasser, N. M., & Abd El-Hamid, T. M. (2013). Investigation of Kinetic and Rheological Properties for the Demulsification Process. *Egyptian Journal of Petroleum*, 22(1), 117–127. <https://doi.org/10.1016/j.ejpe.2012.11.013>
- Al-Sabagh, A., Ahmed, N. S., Nassar, A. M., & Gabr, M. (2003). Synthesis and evaluation of some polymeric surfactants for treating crude oil emulsions. *Colloids and Surfaces A: Physicochemical and Engineering Aspects*, 216(1–3), 9–19. <https://doi.org/10.1016/s0927->

7757(02)00493-4

Andresen, M., & Stenius, P. (2007). Water-in-oil emulsions stabilized by hydrophobized microfibrillated cellulose. *Journal of Dispersion Science and Technology*, 28(6), 837–844. <https://doi.org/10.1080/01932690701341827>

Aoudia, M., Al-shibli, M. N., Al-kasimi, L. H., Al-maamari, R., & Al-bemani, A. (2006). Novel Surfactants for Ultralow Interfacial Tension in a Wide Range of Surfactant Concentration and Temperature, 9, 287–293.

Araki, J., & Mishima, S. (2015). Steric stabilization of “charge-free” cellulose nanowhiskers by grafting of poly(ethylene glycol). *Molecules*, 20(1), 169–184. <https://doi.org/10.3390/molecules20010169>

Araki, J., Wada, M., Kuga, S., & Okano, T. (1998). Flow properties of microcrystalline cellulose suspension prepared by acid treatment of native cellulose. *Colloids and Surfaces A: Physicochemical and Engineering Aspects*, 142(1), 75–82. [https://doi.org/10.1016/S0927-7757\(98\)00404-X](https://doi.org/10.1016/S0927-7757(98)00404-X)

Ashori, A., Babae, M., Jonoobi, M., & Hamzeh, Y. (2014). Solvent-free acetylation of cellulose nanofibers for improving compatibility and dispersion. *Carbohydrate Polymers*, 102(1), 369–375. <https://doi.org/10.1016/j.carbpol.2013.11.067>

Aveyard, R., Binks, B. P., & Clint, J. H. (2003). Emulsions stabilised solely by colloidal particles. *Advances in Colloid and Interface Science*, 100–102(SUPPL.), 503–546. [https://doi.org/10.1016/S0001-8686\(02\)00069-6](https://doi.org/10.1016/S0001-8686(02)00069-6)

- Bai, L., Huan, S., Xiang, W., & Rojas, O. J. (2018). Pickering emulsions by combining cellulose nanofibrils and nanocrystals: Phase behavior and depletion stabilization. *Green Chemistry*, 20(7), 1571–1582. <https://doi.org/10.1039/c8gc00134k>
- Batmaz, R., Berry, R., Loh, W., & Chiu, K. (2015). Synthesis of amine functionalized cellulose nanocrystals : optimization and characterization. *Carbohydrate Research*, 409, 48–55. <http://doi.org/10.1016/j.carres.2015.03.009>
- Becerril, J. Contaminantes emergentes en el agua. Revista Digital Universitaria Unam [en línea], (2009), (10) 8. Disponible en Internet: <<http://www.revista.unam.mx/vol.10/num8/art54/int54.htm>>
- Beck, S., Méthot, M., & Bouchard, J. (2015). General procedure for determining cellulose nanocrystal sulfate half-ester content by conductometric titration. *Cellulose*, 22(1), 101–116. <https://doi.org/10.1007/s10570-014-0513-y>
- Beck-Candanedo, S., Roman, M., & Gray, D. G. (2005). Effect of reaction conditions on the properties and behavior of wood cellulose nanocrystal suspensions. *Biomacromolecules*, 6(2), 1048–1054. <https://doi.org/10.1021/bm049300p>
- Benkaddour, A., Journoux-Lapp, C., Jradi, K., Robert, S., & Daneault, C. (2014). Study of the hydrophobization of TEMPO-oxidized cellulose gel through two routes: Amidation and esterification process. *Journal of Materials Science*, 49(7), 2832–2843. <https://doi.org/10.1007/s10853-013-7989-y>
- Berlioz, S., Molina-Boisseau, S., Nishiyama, Y., & Heux, L. (2009). Gas-phase surface

- esterification of cellulose microfibrils and whiskers. *Biomacromolecules*, *10*(8), 2144–2151. <https://doi.org/10.1021/bm900319k>
- Bhardwaj, A., & Hartland, S. (1993). Applications of Surfactants in Petroleum Industry. *Journal of Dispersion Science and Technology*, *14*(1), 87–116. <https://doi.org/10.1080/01932699308943389>
- Blanco, A., Monte, M. C., Campano, C., Balea, A., Merayo, N., & Negro, C. (2018). Nanocellulose for industrial use: Cellulose nanofibers (CNF), cellulose nanocrystals (CNC), and bacterial cellulose (BC). In *Handbook of Nanomaterials for Industrial Applications*, 74-126. Elsevier.
- Bondeson, D., Mathew, A., & Oksman, K. (2006). Optimization of the isolation of nanocrystals from microcrystalline cellulose by acid hydrolysis. *Cellulose*, *13*(2), 171–180. <https://doi.org/10.1007/s10570-006-9061-4>
- Bondeson, D., Mathew, A., & Oksman, K. (2006). Optimization of the isolation of nanocrystals from microcrystalline cellulose by acid hydrolysis. *Cellulose*, *13*(2), 171–180. <https://doi.org/10.1007/s10570-006-9061-4>
- Boujemaoui, A., Mongkhontreerat, S., Malmström, E., & Carlmark, A. (2015). Preparation and characterization of functionalized cellulose nanocrystals. *Carbohydrate Polymers*, *115*, 457–464. <https://doi.org/10.1016/j.carbpol.2014.08.110>
- Bras, J., Hassan, M. L., Bruzesse, C., Hassan, E. a., El-Wakil, N. a., & Dufresne, A. (2010). Mechanical, barrier, and biodegradability properties of bagasse cellulose whiskers

- reinforced natural rubber nanocomposites. *Industrial Crops and Products*, 32(3), 627–633.
<https://doi.org/10.1016/j.indcrop.2010.07.018>
- Braun, B., & Dorgan, J. R. (2009). Single-step method for the isolation and surface functionalization of cellulosic nanowhiskers. *Biomacromolecules*, 10(2), 334–341.
<https://doi.org/10.1021/bm8011117>
- Brinchi, L., Cotana, F., Fortunati, E., & Kenny, J. M. (2013). Production of nanocrystalline cellulose from lignocellulosic biomass: technology and applications. *Carbohydrate Polymers*, 94(1), 154–169. <https://doi.org/10.1016/j.carbpol.2013.01.033>
- Buffiere, J., Balogh-Michels, Z., Borrega, M., Geiger, T., Zimmermann, T., & Sixta, H. (2017). The chemical-free production of nanocelluloses from microcrystalline cellulose and their use as Pickering emulsion stabilizer. *Carbohydrate Polymers*, 178(September), 48–56.
<https://doi.org/10.1016/j.carbpol.2017.09.028>
- Capron, I., Guellec, F., Perrin, E., Cherhal, F., & Saidane, D. (2016). Some modification of cellulose nanocrystals for functional Pickering emulsions. *Philosophical Transactions of the Royal Society A: Mathematical, Physical and Engineering Sciences*, 374(2072), 20150139. <https://doi.org/10.1098/rsta.2015.0139>
- Capron, I., Rojas, O. J., & Bordes, R. (2017). Behavior of nanocelluloses at interfaces. *Current Opinion in Colloid and Interface Science*, 29, 83–95.
<https://doi.org/10.1016/j.cocis.2017.04.001>
- Cervin, N. T., Aulin, C., Larsson, P. T., & Wågberg, L. (2011). Ultra porous nanocellulose aerogels

- as separation medium for mixtures of oil/water liquids. *Cellulose*, 19(2), 401–410.
<https://doi.org/10.1007/s10570-011-9629-5>
- Chen, J., Liu, W., Liu, C. M., Li, T., Liang, R. H., & Luo, S. J. (2015). Pectin Modifications: A Review. *Critical Reviews in Food Science and Nutrition*, 55(12), 1684–1698.
<https://doi.org/10.1080/10408398.2012.718722>
- Chen, Q. H., Zheng, J., Xu, Y. T., Yin, S. W., Liu, F., & Tang, C. H. (2018). Surface modification improves fabrication of pickering high internal phase emulsions stabilized by cellulose nanocrystals. *Food Hydrocolloids*, 75, 125–130.
<https://doi.org/10.1016/j.foodhyd.2017.09.005>
- Chen, W., Li, Q., Wang, Y., Yi, X., Zeng, J., Yu, H., ...& Li, J. (2014). Comparative study of aerogels obtained from differently prepared nanocellulose fibers. *ChemSusChem*, 7(1), 154–161. <https://doi.org/10.1002/cssc.201300950>
- Cheng Q, Ye D, Chang C, Zhang L. (2017). Facile fabrication of superhydrophilic membranes consisted of fibrous tunicate cellulose nanocrystals for highly efficient oil/water separation. *J Memb Sci*, 525, 1–8. doi:10.1016/j.memsci.2016.11.084.
- Cunha, A. G., & Gandini, A. (2010). Turing polysaccharides into hydrophobization materiales a crítica, review. Part 1. Cellulose. *Cellulose*, 17, 875–889. <https://doi.org/10.1007/s10570-010-9434-6>
- Cunha, A. G., & Gandini, A. (2010). Turning polysaccharides into hydrophobic materials: A critical review. Part 2. Hemicelluloses, chitin/chitosan, starch, pectin and alginates.

Cellulose, 17(6), 1045–1065. <https://doi.org/10.1007/s10570-010-9435-5>

Cunha, A. G., Mougel, J. B., Cathala, B., Berglund, L. A., & Capron, I. (2014). Preparation of double pickering emulsions stabilized by chemically tailored nanocelluloses. *Langmuir*, 30(31). <https://doi.org/10.1021/la5017577>

Dalmazzone C, Bocard C, Ballerini D. (1995). IFP methodology for developing water-in-crude oil emulsion inhibitors. *Spill Sci Technol Bull*, 2, 143–50. doi:10.1016/S1353-2561(96)00013-8.

Dankovich, T. A., & Hsieh, Y. Lo. (2007). Surface modification of cellulose with plant triglycerides for hydrophobicity. *Cellulose*, 14(5), 469–480. <https://doi.org/10.1007/s10570-007-9132-1>

Davies, J. T. (1957). Emulsion Type . I . Physical Chemistry of the emulsifying agent. In *internatinal Congress Surface Activity* (pp. 426–438). London.

Delgado-Linares, J. G., Pereira, J. C., Rondón, M., Bullón, J., & Salager, J. L. (2016). Breaking of Water-in-Crude Oil Emulsions. 6. Estimating the Demulsifier Performance at Optimum Formulation from Both the Required Dose and the Attained Instability. *Energy and Fuels*, 30(7), 5483–5491. <https://doi.org/10.1021/acs.energyfuels.6b00666>

Djuve, J., Yang, X., Fjellanger, I. J., Sjöblom, J., & Pelizzetti, E. (2001). Chemical destabilization of crude oil based emulsions and asphaltene stabilized emulsions. *Colloid and Polymer Science*, 279(3), 232–239. <https://doi.org/10.1007/s003960000413>

Du, H., Liu, W., Zhang, M., Si, C., Zhang, X., & Li, B. (2019). Cellulose nanocrystals and cellulose

- nanofibrils based hydrogels for biomedical applications. *Carbohydrate Polymers*, (209), 130–144. <https://doi.org/10.1016/j.carbpol.2019.01.020>
- Durán, N., Lemes, A. P., & Seabra, A. B. (2012). Review of cellulose nanocrystals patents: preparation, composites and general applications. *Recent Patents on Nanotechnology*, 6(1), 16–28. Retrieved from <http://www.ncbi.nlm.nih.gov/pubmed/21875405>
- Eyley, S., & Thielemans, W. (2014). Surface modification of cellulose nanocrystals. *Nanoscale*, 6(14), 7764–7779. <https://doi.org/10.1039/c4nr01756k>
- Fan, Y., Simon, S., & Sjöblom, J. (2009). Chemical destabilization of crude oil emulsions: Effect of nonionic surfactants as emulsion inhibitors. *Energy and Fuels*, 23(9), 4575–4583. <https://doi.org/10.1021/ef900355d>
- Feng, X., Mussone, P., Gao, S., Wang, S., Wu, S. Y., Masliyah, J. H., & Xu, Z. (2010). Mechanistic study on demulsification of water-in-diluted bitumen emulsions by ethylcellulose. *Langmuir*, 26(5), 3050–3057. <https://doi.org/10.1021/la9029563>
- Fernandez, A., Salager, J., & Scorzza, C. S. (2004). IV Surfactantes no Iónicos. *Universidad de los Andes, Mérida (Venezuela)*.
- Filpponen, I., Kontturi, E., Nummelin, S., Rosilo, H., Kolehmainen, E., Ikkala, O., & Laine, J. (2012). Generic method for modular surface modification of cellulosic materials in aqueous medium by sequential “click” reaction and adsorption. *Biomacromolecules*, 13(3), 736–742. <https://doi.org/10.1021/bm201661k>
- Filson, P. B., & Dawson-andoh, B. E. (2009). Sono-chemical preparation of cellulose nanocrystals

- from lignocellulose derived materials. *Bioresource Technology*, 100(7), 2259–2264.
<https://doi.org/10.1016/j.biortech.2008.09.062>
- Follain, N., Marais, M.-F., Montanari, S., & Vignon, M. R. (2010). Coupling onto surface carboxylated cellulose nanocrystals. *Polymer*, 51(23), 5332–5344.
<https://doi.org/10.1016/j.polymer.2010.09.001>
- French, A. D. (2014). Idealized powder diffraction patterns for cellulose polymorphs. *Cellulose*, 21(2), 885–896. <https://doi.org/10.1007/s10570-013-0030-4>
- French, A. D., & Santiago Cintrón, M. (2013). Cellulose polymorphy, crystallite size, and the Segal Crystallinity Index. *Cellulose*, 20(1), 583–588. <https://doi.org/10.1007/s10570-012-9833-y>
- Fujisawa, S., Okita, Y., Fukuzumi, H., Saito, T., & Isogai, A. (2011). Preparation and characterization of TEMPO-oxidized cellulose nanofibril films with free carboxyl groups. *Carbohydrate Polymers*, 84(1), 579–583. <https://doi.org/10.1016/j.carbpol.2010.12.029>
- Fujisawa, S., Saito, T., & Isogai, A. (2012). Nano-dispersion of TEMPO-oxidized cellulose/aliphatic amine salts in isopropyl alcohol. *Cellulose*, 19(2), 459–466.
<http://doi.org/10.1007/s10570-011-9648-2>
- Fujisawa, S., Togawa, E., & Kuroda, K. (2017). Nanocellulose-stabilized Pickering emulsions and their applications. *Science and Technology of Advanced Materials*, 18(1), 959–971.
<https://doi.org/10.1080/14686996.2017.1401423>
- Fukuzumi, H., Saito, T., & Isogai, A. (2013). Influence of TEMPO-oxidized cellulose nanofibril

- length on film properties. *Carbohydrate Polymers*, 93(1), 172–177.
<https://doi.org/10.1016/j.carbpol.2012.04.069>
- Gao, L., Liu, G., Ma, J., Wang, X., Zhou, L., & Li, X. (2012). Drug nanocrystals: In vivo performances. *Journal of Controlled Release : Official Journal of the Controlled Release Society*, 160(3), 418–430. <https://doi.org/10.1016/j.jconrel.2012.03.013>
- Gårdebjer, S., Bergstrand, A., Idström, A., Börstell, C., Naana, S., Nordstierna, L., & Larsson, A. (2015). Solid-state NMR to quantify surface coverage and chain length of lactic acid modified cellulose nanocrystals, used as fillers in biodegradable composites. *Composites Science and Technology*, 107, 1–9. <https://doi.org/10.1016/j.compscitech.2014.11.014>
- George, J. (2012). High performance edible nanocomposite films containing bacterial cellulose nanocrystals. *Carbohydrate Polymers*, 87(3), 2031–2037.
<https://doi.org/10.1016/j.carbpol.2011.10.019>
- George, J., & Sabapathi, S. N. (2015). Cellulose nanocrystals: Synthesis, functional properties, and applications. *Nanotechnology, Science and Applications*, 8, 45–54.
<https://doi.org/10.2147/NSA.S64386>
- Gestranus, M., Stenius, P., Kontturi, E., Sjöblom, J., & Tammelin, T. (2017). Phase behavior and droplet size of oil-in-water Pickering emulsions stabilised with plant-derived nanocellulosic materials. *Colloids and Surfaces A: Physicochemical and Engineering Aspects*, 519, 60–70. <https://doi.org/10.1016/j.colsurfa.2016.04.025>
- Giraldo-Dávila, D., Chacón-Patiño, M. L., McKenna, A. M., Blanco-Tirado, C., & Combariza, M.

- Y. (2018). Correlations between Molecular Composition and Adsorption, Aggregation, and Emulsifying Behaviors of PetroPhase 2017 Asphaltenes and Their Thin-Layer Chromatography Fractions. *Energy & Fuels*, *acs.energyfuels.7b02859*. <https://doi.org/10.1021/acs.energyfuels.7b02859>
- Gómez, F. N., Combariza, M. Y., & Blanco-Tirado, C. (2017). Facile cellulose nanofibrils amidation using a ‘one-pot’ approach. *Cellulose*, *24*(2), 717–730. <https://doi.org/10.1007/s10570-016-1174-9>
- Goussé, C., Chanzy, H., Excoffier, G., Soubeyrand, L., & Fleury, E. (2002). Stable suspensions of partially silylated cellulose whiskers dispersed in organic solvents. *Polymer*, *43*(9), 2645–2651. [https://doi.org/10.1016/S0032-3861\(02\)00051-4](https://doi.org/10.1016/S0032-3861(02)00051-4)
- Grishkewich, N., Mohammed, N., Tang, J., & Tam, K. C. (2017). Recent advances in the application of cellulose nanocrystals. *Current Opinion in Colloid and Interface Science*, *29*, 32–45. <http://doi.org/10.1016/j.cocis.2017.01.005>
- Guo, J., Du, W., Gao, Y., Cao, Y., & Yin, Y. (2017). Cellulose nanocrystals as water-in-oil Pickering emulsifiers via intercalative modification. *Colloids and Surfaces A: Physicochemical and Engineering Aspects*, *529*(April), 634–642. <https://doi.org/10.1016/j.colsurfa.2017.06.056>
- Guo, X., Rong, Z., & Ying, X. (2006). Calculation of hydrophile-lipophile balance for polyethoxylated surfactants by group contribution method. *Journal of Colloid and Interface Science*, *298*(1), 441–450. <https://doi.org/10.1016/j.jcis.2005.12.009>

- Habibi, Y., Chanzy, H., & Vignon, M. R. (2006). TEMPO-mediated surface oxidation of cellulose whiskers. *Cellulose*, *13*(6), 679–687. <https://doi.org/10.1007/s10570-006-9075-y>
- Habibi, Y., Foulon, L., Aguié-Béghin, V., Molinari, M., & Douillard, R. (2007). Langmuir-Blodgett films of cellulose nanocrystals: preparation and characterization. *Journal of Colloid and Interface Science*, *316*(2), 388–397. <https://doi.org/10.1016/j.jcis.2007.08.041>
- Habibi, Y., Lucia, L. A., & Rojas, O. J. (2010). Cellulose nanocrystals: Chemistry, self-assembly, and applications. *Chemical Reviews*, *110*(6), 3479–3500. <https://doi.org/10.1021/cr900339w>
- Hjartnes TN, Sørland GH, Simon S, Sjöblom J. (2019). Demulsification of Crude Oil Emulsions Tracked by Pulsed Field Gradient (PFG) Nuclear Magnetic Resonance (NMR). Part I: Chemical Demulsification. *Ind Eng Chem Res*, *58*, 2310–23. doi:10.1021/acs.iecr.8b05165
- Hou, J., Feng, X., Masliyah, J., & Xu, Z. (2012). Understanding interfacial behavior of ethylcellulose at the water-diluted bitumen interface. *Energy and Fuels*, *26*(3), 1740–1745. <https://doi.org/10.1021/ef201722y>
- Hou, J., Feng, X., Masliyah, J., & Xu, Z. (2012). Understanding Interfacial Behavior of Ethylcellulose at the Water – Diluted Bitumen Interface.
- Hu, Z., Ballinger, S., Pelton, R., & Cranston, E. D. (2015). Surfactant-enhanced cellulose nanocrystal Pickering emulsions. *Journal of Colloid and Interface Science*, *439*, 139–148. <https://doi.org/10.1016/j.jcis.2014.10.034>
- Hu, Z., Berry, R. M., Pelton, R., & Cranston, E. D. (2017). One-Pot Water-Based Hydrophobic

- Surface Modification of Cellulose Nanocrystals Using Plant Polyphenols. *ACS Sustainable Chemistry and Engineering*, 5(6), 5018–5026. <https://doi.org/10.1021/acssuschemeng.7b00415>
- Hubbe, M. A. (2019). Review of the Mechanistic Roles of Nanocellulose, Cellulosic Fibers, and Hydrophilic Cellulose Derivatives in Cellulose-Based Absorbents. (Md. I. H. Mondal, Ed.). Raleigh: *Springer International Publishing* AG. https://doi.org/10.1007/978-3-319-77830-3_8
- Hubbe, M. a., Rojas, O. J., Lucia, L. a., & Sain, M. (2008). Cellulosic Nanocomposites: a Review. *BioResources*, 3(3), 929–980. <https://doi.org/10.15376/biores.3.3.929-980>
- Islam, M. T., Alam, M. M., & Zoccola, M. (2013). Review on modification of nanocelulose for application in composites. *International Journal of Innovative Research in Science, Engineering and Technology*, 2(10), 5444–5451.
- Isogai, A., Saito, T., & Fukuzumi, H. (2011). TEMPO-oxidized cellulose nanofibers. *Nanoscale*, 3(1), 71–85. <https://doi.org/10.1039/c0nr00583e>
- Jiang, F., & Hsieh, Y. Lo. (2013). Chemically and mechanically isolated nanocellulose and their self-assembled structures. *Carbohydrate Polymers*, 95(1), 32–40. <https://doi.org/10.1016/j.carbpol.2013.02.022>
- Johnson, R. K., Zink-Sharp, A., & Glasser, W. G. (2011). Preparation and characterization of hydrophobic derivatives of TEMPO-oxidized nanocelluloses. *Cellulose*, 18(6), 1599–1609. <https://doi.org/10.1007/s10570-011-9579-y>

- Jonoobi, M., Oladi, R., Davoudpour, Y., Oksman, K., Dufresne, A., Hamzeh, Y., & Davoodi, R. (2015). Different preparation methods and properties of nanostructured cellulose from various natural resources and residues: a review. *Cellulose*. <https://doi.org/10.1007/s10570-015-0551-0>
- Kalashnikova, I., Bizot, H., Cathala, B., & Capron, I. (2012). Modulation of cellulose nanocrystals amphiphilic properties to stabilize oil/water interface. *Biomacromolecules*, *13*(1), 267–275. <https://doi.org/10.1021/bm201599j>
- Kang, W., Xu, B., Wang, Y., Li, Y., Shan, X., An, F., & Liu, J. (2011). Stability mechanism of W/O crude oil emulsion stabilized by polymer and surfactant. *Colloids and Surfaces A: Physicochemical and Engineering Aspects*, *384*(1–3), 555–560. <https://doi.org/10.1016/j.colsurfa.2011.05.017>
- Khalil, A. (2014). Production and modification of nanofibrillated cellulose using various mechanical process: a review. *Carbohydrate Polymers*, *99*, 649–665. <http://doi.org/10.1016/j.carbpol.2013.08.069>
- Khalil, H. A., Davoudpour, Y., Islam, M. N., Mustapha, A., Sudesh, K., Dungani, R., & Jawaid, M. (2014). Production and modification of nanofibrillated cellulose using various mechanical processes: a review. *Carbohydrate polymers*, *99*, 649–665.
- Khanjanzadeh, H., Behrooz, R., Bahramifar, N., Gindl-Altmutter, W., Bacher, M., Edler, M., & Griesser, T. (2018). Surface chemical functionalization of cellulose nanocrystals by 3-aminopropyltriethoxysilane. *International Journal of Biological Macromolecules*, *106*, 1288–1296. <http://doi.org/10.1016/j.ijbiomac.2017.08.136>

- Kim, H., & Wasan, T. (1995). A study of dynamic interfacial mechanisms for demulsification of water-in-oil emulsions. *Colloids and Surface*, *95*, 235–247.
- Kokal, S. L. (2005). Crude Oil Emulsions: A State-Of-The-Art Review. *SPE Production & Facilities*, *20* (01), 5–13. <https://doi.org/10.2118/77497-PA>
- Kokal, S. L. (2006). Crude Oil Emulsions: A State-Of-The-Art Review. *SPE Production & Facilities*, *20*(01), 5–13. <https://doi.org/10.2118/77497-pa>
- Korhonen, J. T., Kettunen, M., Ras, R. H. a, & Ikkala, O. (2011). Hydrophobic nanocellulose aerogels as floating, sustainable, reusable, and recyclable oil absorbents. *ACS Applied Materials & Interfaces*, *3*(6), 1813–1816. <https://doi.org/10.1021/am200475b>
- Krishnamachari, P., Hashaikeh, R., & Tiner, M. (2011). Modified cellulose morphologies and its composites; SEM and TEM analysis. *Micron*, *42*(8), 751–761. <https://doi.org/10.1016/j.micron.2011.05.001>
- Krishnamachari, P., Hashaikeh, M., Chiesa, M., Gad, K. R. (2012). Effects of acid hydrolysis time on cellulose nanocrystals properties: Nanoindentation and thermogravimetric studies. *Cellulose Chemistry and Technology*, *46*(1–2), 13–18. Retrieved from [http://www.cellulosechemtechnol.ro/pdf/CCT1-2\(2012\)/p.13-18.pdf](http://www.cellulosechemtechnol.ro/pdf/CCT1-2(2012)/p.13-18.pdf)
- Laitinen, O., Ojala, J., Sirviö, J. A., & Liimatainen, H. (2017). Sustainable stabilization of oil in water emulsions by cellulose nanocrystals synthesized from deep eutectic solvents. *Cellulose*, *24*(4), 1679–1689. <https://doi.org/10.1007/s10570-017-1226-9>
- Lam, E., Male, K. B., Chong, J. H., Leung, A. C. W., & Luong, J. H. T. (2012). Applications of

- functionalized and nanoparticle-modified nanocrystalline cellulose. *Trends in Biotechnology*, 30(5), 283–290. <https://doi.org/10.1016/j.tibtech.2012.02.001>
- Lasseguette, E. (2008). Grafting onto microfibrils of native cellulose. *Cellulose*, 15(4), 571–580. <https://doi.org/10.1007/s10570-008-9200-1>
- Leal-Calderon, F., & Schmitt, V. (2008). Solid-stabilized emulsions. *Current Opinion in Colloid and Interface Science*, 13(4), 217–227. <https://doi.org/10.1016/j.cocis.2007.09.005>
- Lee, K. Y., & Bismarck, A. (2012). Susceptibility of never-dried and freeze-dried bacterial cellulose towards esterification with organic acid. *Cellulose*, 19(3), 891–900. <https://doi.org/10.1007/s10570-012-9680-x>
- Lee, K. Y., Quero, F., Blaker, J. J., Hill, C. A. S., Eichhorn, S. J., & Bismarck, A. (2011). Surface only modification of bacterial cellulose nanofibres with organic acids. *Cellulose*, 18(3), 595–605. <https://doi.org/10.1007/s10570-011-9525-z>
- Lemarchand, C., Couvreur, P., Vauthier, C., Costantini, D., & Gref, R. (2003). Study of emulsion stabilization by graft copolymers using the optical analyzer Turbiscan. *International Journal of Pharmaceutics*, 254(1), 77–82. [https://doi.org/10.1016/S0378-5173\(02\)00687-7](https://doi.org/10.1016/S0378-5173(02)00687-7)
- Li, Q., Wei, B., Lu, L., Li, Y., Wen, Y., Pu, W., ... Wang, C. (2017). Investigation of physical properties and displacement mechanisms of surface-grafted nano-cellulose fluids for enhanced oil recovery. *Fuel*, 207, 352–364. <https://doi.org/10.1016/j.fuel.2017.06.103>
- Li, Q., Wei, B., Xue, Y., Wen, Y., & Li, J. (2016). Improving the physical properties of nano -

- cellulose through chemical grafting for potential use in enhancing oil recovery. *Journal of Bioresources and Bioproducts*, 1(4), 186–191.
- Li, S., Li, C., Li, C., Yan, M., Wu, Y., Cao, J., & He, S. (2013). Fabrication of nano-crystalline cellulose with phosphoric acid and its full application in a modified polyurethane foam. *Polymer Degradation and Stability*, 98(9), 1940–1944. <https://doi.org/10.1016/j.polyimdegradstab.2013.06.017>
- Li, X., Li, J., Gong, J., Kuang, Y., Mo, L., & Song, T. (2018). Cellulose nanocrystals (CNCs) with different crystalline allomorph for oil in water Pickering emulsions. *Carbohydrate Polymers*, 183(1), 303–310. <https://doi.org/10.1016/j.carbpol.2017.12.085>
- Li, Y., Wang, B., Ma, M., & Wang, B. (2018). Review of Recent Development on Preparation, Properties, and Applications of Cellulose-Based Functional Materials. *International Journal of Polymer Science*, 2018. <https://doi.org/10.1155/2018/8973643>
- Lif, A., Stenstad, P., Syverud, K., Nydén, M., & Holmberg, K. (2010). Fischer–Tropsch diesel emulsions stabilised by microfibrillated cellulose and nonionic surfactants. *Journal of colloid and interface science*, 352(2), 585–592. <https://doi.org/10.1016/j.jcis.2010.08.052>
- Lin, J. H., Chang, Y. H., & Hsu, Y. H. (2009). Degradation of cotton cellulose treated with hydrochloric acid either in water or in ethanol. *Food Hydrocolloids*, 23(6), 1548–1553. <https://doi.org/10.1016/j.foodhyd.2008.10.005>
- Lin, N., Chang, P. R., Yu, J., Huang, J., & Feng, J. (2010). Surface acetylation of cellulose nanocrystal and its reinforcing function in poly(lactic acid). *Carbohydrate Polymers*,

83(4), 1834–1842. <https://doi.org/10.1016/j.carbpol.2010.10.047>

Liu, D., Chen, X., Yue, Y., Chen, M., & Wu, Q. (2011). Structure and rheology of nanocrystalline cellulose. *Carbohydrate Polymers*, 84(1), 316–322. <https://doi.org/10.1016/j.carbpol.2010.11.039>

Liu, D., Zhong, T., Chang, P. R., Li, K., & Wu, Q. (2010). Starch composites reinforced by bamboo cellulosic crystals. *Bioresource Technology*, 101(7), 2529–2536. <https://doi.org/10.1016/j.biortech.2009.11.058>

Liu, H., Liu, D., Yao, F., & Wu, Q. (2010). Fabrication and properties of transparent polymethylmethacrylate/cellulose nanocrystals composites. *Bioresource Technology*, 101(14), 5685–5692. <https://doi.org/10.1016/j.biortech.2010.02.045>

Liu, Y., Wang, H., Yu, G., Yu, Q., Li, B., & Mu, X. (2014). A novel approach for the preparation of nanocrystalline cellulose by using phosphotungstic acid. *Carbohydrate Polymers*, 110, 415–422. <https://doi.org/10.1016/j.carbpol.2014.04.040>

Lu, P., & Hsieh, Y.-L. (2010). Preparation and properties of cellulose nanocrystals: Rods, spheres, and network. *Carbohydrate Polymers*, 82(2), 329–336. <https://doi.org/10.1016/j.carbpol.2010.04.073>

Lu, P., & Hsieh, Y.-L. (2012). Preparation and characterization of cellulose nanocrystals from rice straw. *Carbohydrate Polymers*, 87(1), 564–573. <https://doi.org/10.1016/j.carbpol.2011.08.022>

Ma, X., Wang, Y., Shen, Y., Huang, J., & Dufresne, A. (2019). Current Status of Nanocellulose-

- Based Nanocomposites. In L. N. Huang Jin, Dufresne Alain (Ed.), *Nanocellulose: From Fundamentals to Advanced Materials* (First Edit, pp. 155–200). Wiley-VCHVerlag GmbH& Co.
- Maaref, S., & Ayatollahi, S. (2018). The effect of brine salinity on water-in-oil emulsion stability through droplet size distribution analysis: A case study. *Journal of Dispersion Science and Technology*, 39(5), 721–733. <https://doi.org/10.1080/01932691.2017.1386569>
- Mabrouk, A. B., Vilar, M. R., Magnin, A., Belgacem, M. N., & Boufi, S. (2011). Synthesis and characterization of cellulose whiskers/polymer nanocomposite dispersion by mini-emulsion polymerization. *Journal of colloid and interface science*, 363(1), 129–36.
- Mandal, A., & Chakrabarty, D. (2011). Isolation of nanocellulose from waste sugarcane bagasse (SCB) and its characterization. *Carbohydrate Polymers*, 86(3), 1291–1299. <https://doi.org/10.1016/j.carbpol.2011.06.030>
- Marfisi, S (2005). “Estabilidad de emulsiones relacionada con el proceso de deshidratación de crudos.” Universidad de los Andes.
- Mariano, M., El Kissi, N., & Dufresne, A. (2014). Cellulose nanocrystals and related nanocomposites: Review of some properties and challenges. *Journal of Polymer Science, Part B: Polymer Physics*, 52(12), 791–806. <https://doi.org/10.1002/polb.23490>
- Martínez-Sanz, M., Lopez-Rubio, A., & Lagaron, J. M. (2011). Optimization of the nanofabrication by acid hydrolysis of bacterial cellulose nanowhiskers. *Carbohydrate Polymers*, 85(1), 228–236. <https://doi.org/10.1016/j.carbpol.2011.02.021>

- McClements, D. J. (2004). Protein-stabilized emulsions. *Current Opinion in Colloid & Interface Science*, 9(5), 305–313. <https://doi.org/10.1016/j.cocis.2004.09.003>
- Mikulcová, V., Bordes, R., & Kašpárková, V. (2016). On the preparation and antibacterial activity of emulsions stabilized with nanocellulose particles. *Food Hydrocolloids*, 61, 780–792. <https://doi.org/10.1016/j.foodhyd.2016.06.031>
- Mikulcová, V., Bordes, R., Minařík, A., & Kašpárková, V. (2018). Pickering oil-in-water emulsions stabilized by carboxylated cellulose nanocrystals – Effect of the pH. *Food Hydrocolloids*, 80, 60–67. <https://doi.org/10.1016/j.foodhyd.2018.01.034>
- Molnes, S. N., Mamonov, A., Paso, K. G., Strand, S., & Syverud, K. (2018). Investigation of a new application for cellulose nanocrystals: a study of the enhanced oil recovery potential by use of a green additive. *Cellulose*, 25(4), 2289–2301. <https://doi.org/10.1007/s10570-018-1715-5>
- Molnes, S. N., Paso, K. G., Strand, S., & Syverud, K. (2017). The effects of pH, time and temperature on the stability and viscosity of cellulose nanocrystal (CNC) dispersions: implications for use in enhanced oil recovery. *Cellulose*, 24(10), 4479–4491. <https://doi.org/10.1007/s10570-017-1437-0>
- Molnes, S. N., Torrijos, I. P., Strand, S., Paso, K. G., & Syverud, K. (2016). Sandstone injectivity and salt stability of cellulose nanocrystals (CNC) dispersions—Premises for use of CNC in enhanced oil recovery. *Industrial Crops and Products*, 93, 152–160. <https://doi.org/10.1016/j.indcrop.2016.03.019>

- Nieh, W., Chan, K. J., Roberts, R., Eichhorn, S. J., Stinson-Bagby, K., Fox, D. M., ... Camarero-Espinosa, S. (2018). Current characterization methods for cellulose nanomaterials. *Chemical Society Reviews*, 47(8), 2609–2679. <http://doi.org/10.1039/c6cs00895j>
- Niu, F., Han, B., Fan, J., Kou, M., Zhang, B., Feng, Z.-J., ... Zhou, W. (2018). Characterization of structure and stability of emulsions stabilized with cellulose macro/nano particles. *Carbohydrate Polymers*, 199(April), 314–319. <https://doi.org/10.1016/j.carbpol.2018.07.025>
- Nonappa, Gröschel, A. H., Laaksonen, P., Kontturi, E., Ikkala, O., Rojas, O. J., & Linder, M. B. (2018). Advanced Materials through Assembly of Nanocelluloses. *Advanced Materials*, 30(24), 1703779. <http://doi.org/10.1002/adma.201703779>
- Ojala, J., Sirviö, J. A., & Liimatainen, H. (2016). Nanoparticle emulsifiers based on bifunctionalized cellulose nanocrystals as marine diesel oil-water emulsion stabilizers. *Chemical Engineering Journal*, 288, 312–320. <https://doi.org/10.1016/j.cej.2015.10.113>
- Oksman, K., Aitomäki, Y., Mathew, A. P., Siqueira, G., Zhou, Q., Butylina, S., ... & Hooshmand, S. (2016). Review of the recent developments in cellulose nanocomposite processing. *Composites Part A: Applied Science and Manufacturing*, 83, 2–18. <https://doi.org/10.1016/j.compositesa.2015.10.041>
- Oliveira, P. F., Santos, I. C. V. M., Vieira, H. V. P., Fraga, A. K., & Mansur, C. R. E. (2017). Interfacial rheology of asphaltene emulsions in the presence of nanoemulsions based on a polyoxide surfactant and asphaltene dispersant. *Fuel*, 193, 220–229. <https://doi.org/10.1016/j.fuel.2016.12.051>

- Ortiz, D. P., Baydak, E. N., & Yarranton, H. W. (2010). Effect of surfactants on interfacial films and stability of water-in-oil emulsions stabilized by asphaltenes. *Journal of Colloid and Interface Science*, *351*(2), 542–555. <https://doi.org/10.1016/j.jcis.2010.08.032>
- Oudiani, A. El, Chaabouni, Y., Msahli, S., & Sakli, F. (2011). Crystal transition from cellulose I to cellulose II in NaOH treated *Agave americana* L. fibre. *Carbohydrate Polymers*, *86*, 1221–1229. <http://doi.org/10.1016/j.carbpol.2011.06.037>
- Park, S., Baker, J. O., Himmel, M. E., Parilla, P. a, & Johnson, D. K. (2010). Cellulose crystallinity index: measurement techniques and their impact on interpreting cellulase performance. *Biotechnology for Biofuels*, *3*, 10. <https://doi.org/10.1186/1754-6834-3-10>
- Peng, B. L., Dhar, N., Liu, H. L., & Tam, K. C. (2011). Chemistry and applications of nanocrystalline cellulose and its derivatives: A nanotechnology perspective. *Canadian Journal of Chemical Engineering*. <https://doi.org/10.1002/cjce.20554>
- Peng, Y., Gardner, D. J., Han, Y., Kiziltas, A., Cai, Z., & Tshabalala, M. A. (2013). Influence of drying method on the material properties of nanocellulose I: Thermostability and crystallinity. *Cellulose*, *20*(5), 2379–2392. <https://doi.org/10.1007/s10570-013-0019-z>
- Pereira, J. C., Delgado-Linares, J., Scorzza, C., Rondó, M., Rodríguez, S., & Salager, J. L. (2011). Breaking of water-in-Crude oil emulsions. 4. estimation of the demulsifier surfactant performance to destabilize the asphaltenes effect. *Energy and Fuels*, *25*(3), 1045–1050. <https://doi.org/10.1021/ef100979y>
- Phanthong, P., Reubroycharoen, P., Hao, X., Xu, G., Abudula, A., & Guan, G. (2018).

- Nanocellulose: Extraction and application. *Carbon Resources Conversion*, 1(1), 32–43.
<https://doi.org/10.1016/j.crcon.2018.05.004>
- Qiao, C., Chen, G., Zhang, J., & Yao, J. (2016). Structure and rheological properties of cellulose nanocrystals suspension. *Food Hydrocolloids*, 55, 19–25.
<https://doi.org/10.1016/j.foodhyd.2015.11.005>
- Qiu, X., & Hu, S. (2013). “Smart” materials based on cellulose: A review of the preparations, properties, and applications. *Materials*. <https://doi.org/10.3390/ma6030738>
- Ramírez, J. A., Fortunati, E., Kenny, J. M., Torre, L., & Foresti, M. L. (2017). Simple citric acid-catalyzed surface esterification of cellulose nanocrystals. *Carbohydrate Polymers*, 157, 1358–1364. <https://doi.org/10.1016/j.carbpol.2016.11.008>
- Ramírez, J. A., Suriano, C. J., Cerrutti, P., & Foresti, M. L. (2014). Surface esterification of cellulose nanofibers by a simple organocatalytic methodology. *Carbohydrate Polymers*, 114, 416–423. <https://doi.org/10.1016/j.carbpol.2014.08.020>
- Rein, D. M., Khalfin, R., & Cohen, Y. (2012). Cellulose as a novel amphiphilic coating for oil-in-water and water-in-oil dispersions. *Journal of Colloid and Interface Science*, 386(1), 456–463. <https://doi.org/10.1016/j.jcis.2012.07.053>
- Revol, J. F., Bradford, H., Giasson, J., Marchessault, R. H., & Gray, D. G. (1992). Helicoidal self-ordering of cellulose microfibrils in aqueous suspension. *International Journal of Biological Macromolecules*, 14(3), 170–172. [https://doi.org/10.1016/S0141-8130\(05\)80008-X](https://doi.org/10.1016/S0141-8130(05)80008-X)

- Rincón, M., & Martínez, D. (2009). Análisis de las propiedades del aceite de palma en el desarrollo de su industria. *Revista Palmas*, 30(2), 11–24. Retrieved from <http://publicaciones.fedepalma.org/index.php/palmas/article/view/1432>
- Rojas, J., Bedoya, M., & Ciro, Y. (2015). Current trends in the production of cellulose nanoparticles and nanocomposites for biomedical applications. In M. Poletto, & H. L. Ornaghi (Eds.). *Cellulose-Fundamental aspects and current trends* (pp. 193–228). Rijeka, Croatia: InTech. <http://doi.org/10.5772/61334>
- Rojas, O. J., Bullon, J., Ysambertt, F., Forgiarini, A., Salager, J.-L., & Argyropoulos, D. S. (2007). Lignins as emulsion stabilizers. In *ACS symposium series* (Vol. 954, pp. 182–199). Oxford University Press. Retrieved from <http://cat.inist.fr/?aModele=afficheN&cpsidt=18707830>
- Rol, F., Belgacem, M. N., Gandini, A., & Bras, J. (2019). Recent advances in surface-modified cellulose nanofibrils. *Progress in Polymer Science*, 88, 241–264. <https://doi.org/10.1016/j.progpolymsci.2018.09.002>
- Roman, M., & Winter, W. T. (2004). Effect of sulfate groups from sulfuric acid hydrolysis on the thermal degradation behavior of bacterial cellulose. *Biomacromolecules*, 5(5), 1671–1677. <https://doi.org/10.1021/bm034519+>
- Rondón, M., Bouriat, P., Lachaise, J., & Salager, J. L. (2006). Breaking of water-in-crude oil emulsions. 1. Physicochemical phenomenology of demulsifier action. *Energy and Fuels*, 20(4), 1600–1604. <https://doi.org/10.1021/ef060017o>

- Rondón, M., Pereira, J. C., Bouriat, P., Graciaa, A., Lachaise, J., & Salager, J. L. (2008). Breaking of water-in-crude-oil emulsions. 2. Influence of asphaltene concentration and diluent nature on demulsifier action. *Energy and Fuels*, 22(2), 702–707. <https://doi.org/10.1021/ef7003877>
- Roodbari NH, Badiei A, Soleimani E, Khaniani Y. (2016). Tweens demulsification effects on heavy crude oil/water emulsion. *Arab J Chem*, 9, S806–11. doi:10.1016/j.arabjc.2011.08.009.
- Rosa, M. F., Medeiros, E. S., Malmonge, J. a., Gregorski, K. S., Wood, D. F., Mattoso, L. H. C., ... & Imam, S. H. (2010). Cellulose nanowhiskers from coconut husk fibers: Effect of preparation conditions on their thermal and morphological behavior. *Carbohydrate Polymers*, 81(1), 83–92. <https://doi.org/10.1016/j.carbpol.2010.01.059>
- Sadeghifar, H., Filpponen, I., Clarke, S. P., Brougham, D. F., & Argyropoulos, D. S. (2011). Production of cellulose nanocrystals using hydrobromic acid and click reactions on their surface. *Journal of Materials Science*, 46(22), 7344–7355. <https://doi.org/10.1007/s10853-011-5696-0>
- Saito, T., Kimura, S., Nishiyama, Y., & Isogai, A. (2007). Cellulose nanofibers prepared by TEMPO-mediated oxidation of native cellulose. *Biomacromolecules*, 8(8), 2485–2491. <https://doi.org/10.1021/bm0703970>
- Saito, T., Okita, Y., Nge, T., Sugiyama, J., & Isogai, A. (2006). TEMPO-Mediated Oxidation of Native Cellulose: Microscopic Analysis of Fibrous Fractions in the Oxidized Products. *Carbohydrate Polymers*, 65(4), 435–440. <https://doi.org/10.1016/j.carbpol.2006.01.034v>

- Salager, J. (1992). *El mundo de los surfactantes* (first, Vol. 01). Mérida-Venezuela: Universidad de los Andes.
- Salajkova, M., Berglund, L. a., Zhou, Q., Salajková, M., Berglund, L. a., & Zhou, Q. (2012). Hydrophobic cellulose nanocrystals modified with quaternary ammonium salts. *Journal of Materials Chemistry*, 22(37), 19798. <https://doi.org/10.1039/c2jm34355j>
- Salam, K. K., Alade, a. O., Arinkoola, a. O., & Opawale, a. (2013). Improving the Demulsification Process of Heavy Crude Oil Emulsion through Blending with Diluent. *Journal of Petroleum Engineering*, 2013, 1–6. <https://doi.org/10.1155/2013/793101>
- Salas, C., Nypelö, T., Rodriguez-Abreu, C., Carrillo, C., & Rojas, O. J. (2014). Nanocellulose properties and applications in colloids and interfaces. *Current Opinion in Colloid & Interface Science*, 19(5), 383–396. <https://doi.org/10.1016/j.cocis.2014.10.003>
- Schramm, L. L. (2001). *Surfactants: Fundamentals and Applications in the Petroleum Industry*. Cambridge University Press (First, Vol. 16). Cambridge: press syndicate of the University of Cambridge. <https://doi.org/10.2307/3515635>
- Sèbe, G., Ham-Pichavant, F., & Pecastaings, G. (2013). Dispersibility and emulsion-stabilizing effect of cellulose nanowhiskers esterified by vinyl acetate and vinyl cinnamate. *Biomacromolecules*, 14(8), 2937-2944.
- Sèbe, G., Ham-Pichavant, F., Ibarboure, E., Koffi, A. L. C., & Tingaut, P. (2012). Supramolecular structure characterization of cellulose II nanowhiskers produced by acid hydrolysis of cellulose I substrates. *Biomacromolecules*, 13(2), 570-578. <https://doi.org/bm201777j>

- Segal, L., Creely, J. J., Martin, A. E., & Conrad, C. M. (1959). An Empirical Method for Estimating the Degree of Crystallinity of Native Cellulose Using the X-Ray Diffractometer. *Textile Research Journal*, 29(10), 786–794. <https://doi.org/10.1177/004051755902901003>
- Sheltami, R. M., Abdullah, I., Ahmad, I., Dufresne, A., & Kargarzadeh, H. (2012). Extraction of cellulose nanocrystals from mengkuang leaves (*Pandanus tectorius*). *Carbohydrate Polymers*, 88(2), 772–779. <https://doi.org/10.1016/j.carbpol.2012.01.062>
- Song, Q., Winter, W., Bujanovic, B., & Amidon, T. (2014). Nanofibrillated Cellulose (NFC): A High-Value Co-Product that Improves the Economics of Cellulosic Ethanol Production. *Energies*, 7(2), 607–618. <https://doi.org/10.3390/en7020607>
- Spinella, S., Maiorana, A., Qian, Q., Dawson, N. J., Hepworth, V., Mccallum, S. A., ... Gross, R. A. (2016). Concurrent Cellulose Hydrolysis and Esterification to Prepare a Surface-Modified Cellulose Nanocrystal Decorated with Carboxylic Acid Moieties. *ACS Sustainable Chemistry and Engineering*, 4, 1538–1550. <https://doi.org/10.1021/acssuschemeng.5b01489>
- Tanaka, R., Saito, T., & Isogai, A. (2012). Cellulose nanofibrils prepared from softwood cellulose by TEMPO/NaClO/NaClO₂ systems in water at pH 4.8 or 6.8. *International Journal of Biological Macromolecules*, 51(3), 228–234. <https://doi.org/10.1016/j.ijbiomac.2012.05.016>
- Tang, J., Lee, M. F. X., Zhang, W., Zhao, B., Berry, R. M., & Tam, K. C. (2014). Dual responsive pickering emulsion stabilized by poly[2-(dimethylamino) ethyl methacrylate] grafted cellulose nanocrystals. *Biomacromolecules*, 15(8), 3052–3060.

<https://doi.org/10.1021/bm500663w>

- Tang, J., Sisler, J., Grishkewich, N., & Tam, K. C. (2017). Functionalization of cellulose nanocrystals for advanced applications. *Journal of Colloid and Interface Science*, 494, 397–409. <https://doi.org/10.1016/j.jcis.2017.01.077>
- Tardy, B. L., Yokota, S., Ago, M., Xiang, W., Kondo, T., Bordes, R., & Rojas, O. J. (2017). Nanocellulose–surfactant interactions. *Current Opinion in Colloid and Interface Science*, 29, 57–67. <https://doi.org/10.1016/j.cocis.2017.02.004>
- Taubner, T., Čopíková, J., Havelka, P., & Synytsya, A. (2013). Preparation of amidated derivatives of monocarboxy cellulose. *Cellulose*, 20(4), 2045–2055. <http://doi.org/10.1007/s10570-013-9938-y>
- Thomas, B., Raj, M. C., Athira, K. B., Rubiyah, M. H., Joy, J., Moores, A., & Drisko, G. L. (2018). Nanocellulose, a Versatile Green Platform: From Biosources to Materials and Their Applications. *Chemical Reviews*, 118, 11575–11625. <https://doi.org/10.1021/acs.chemrev.7b00627>
- Ummartyotin, S., & Manuspiya, H. (2015). A critical review on cellulose :cellulose: From fundamental to an approach on sensor technology. *Renewable and Sustainable Energy Reviews*, 41, 402–412. <https://doi.org/10.1016/j.rser.2014.08.050>
- Vuoti, S., Talja, R., Johansson, L. S., Heikkinen, H., & Tammelin, T. (2013). Solvent impact on esterification and film formation ability of nanofibrillated cellulose. *Cellulose*, 20(5), 2359–2370. <https://doi.org/10.1007/s10570-013-9983-6>

- Wang, J., Hu, F-L., Li, C-Q., Li, J., Yang, Y., (2010) Synthesis of dendritic polyether surfactants for demulsification, *Separation and Purification Technology*, 73(3), pp.349-354.
- Wang, N., Ding, E., & Cheng, R. (2007). Thermal degradation behaviors of spherical cellulose nanocrystals with sulfate groups. *Polymer*, 48(48), 3486–3493.
<https://doi.org/10.1016/j.polymer.2007.03.062>
- Wang, Y., Wang, W., Jia, H., Gao, G., Wang, X., Zhang, X., & Wang, Y. (2018). Using Cellulose Nanofibers and Its Palm Oil Pickering Emulsion as Fat Substitutes in Emulsified Sausage. *Journal of Food Science*, 0. <https://doi.org/10.1111/1750-3841.14164>
- Wang, Y., Wang, X., Xie, Y., & Zhang, K. (2018). Functional nanomaterials through esterification of cellulose: a review of chemistry and application. *Cellulose*, 25(7), 3703–3731.
<https://doi.org/10.1007/s10570-018-1830-3>
- Wei, B., Li, H., Li, Q., Wen, Y., Sun, L., Wei, P., ... Li, Y. (2017). Stabilization of Foam Lamella Using Novel Surface-Grafted Nanocellulose-Based Nanofluids. *Langmuir*, 33(21), 5127–5139. <https://doi.org/10.1021/acs.langmuir.7b00387>
- Wei, B., Li, Q., Jin, F., Li, H., & Wang, C. (2016). The Potential of a Novel Nanofluid in Enhancing Oil Recovery. *Energy and Fuels*, 30(4), 2882–2891.
<https://doi.org/10.1021/acs.energyfuels.6b00244>
- Wei, B., Wang, Y., Wen, Y., Xu, X., Wood, C., & Sun, L. (2018). Bubble breakup dynamics and flow behaviors of a surface-functionalized nanocellulose based nanofluid stabilized foam in constricted microfluidic devices. *Journal of Industrial and Engineering Chemistry*, 68,

24–32. <https://doi.org/10.1016/j.jiec.2018.07.025>

Wei, S., Kumar, V., & Banker, G. S. (1996). Phosphoric acid mediated depolymerization and decrystallization of cellulose: Preparation of low crystallinity cellulose - A new pharmaceutical excipient. *International Journal of Pharmaceutics*, *142*(2), 175–181. [https://doi.org/10.1016/0378-5173\(96\)04673-X](https://doi.org/10.1016/0378-5173(96)04673-X)

Wen, Y., Cheng, H., Lu, L. J., Liu, J., Feng, Y., Guan, W., ... Huang, X. F. (2010). Analysis of biological demulsification process of water-in-oil emulsion by *Alcaligenes* sp. S-XJ-1. *Bioresource Technology*, *101*(21), 8315–8322. <https://doi.org/10.1016/j.biortech.2010.05.088>

Winuprasith, T., & Suphantharika, M. (2013). Microfibrillated cellulose from mangosteen (*Garcinia mangostana* L.) rind: Preparation, characterization, and evaluation as an emulsion stabilizer. *Food Hydrocolloids*, *32*(2), 383–394. <https://doi.org/10.1016/j.foodhyd.2013.01.023>

Xhanari, K., Syverud, K., & Stenius, P. (2011). Emulsions stabilized by microfibrillated cellulose: The effect of Hydrophobization, concentration and O/W ratio. *Journal of Dispersion Science and Technology*, *32*(3), 447–452. <https://doi.org/10.1080/01932691003658942>

Xia, L., Lu, S., & Cao, G. (2004). Stability and demulsification of emulsions stabilized by asphaltenes or resins. *Journal of Colloid and Interface Science*, *271*(2), 504–506. <https://doi.org/10.1016/j.jcis.2003.11.027>

Ye, Z., Feng, M., Gou, S., Liu, M., Huang, Z., & Liu, T. (2013). Hydrophobically associating

- acrylamide-based copolymer for chemically enhanced oil recovery. *Journal of Applied Polymer Science*, 130(4), 2901–2911. <https://doi.org/10.1002/app.39424>
- Yu, H., Qin, Z., & Zhou, Z. (2011). Cellulose nanocrystals as green fillers to improve crystallization and hydrophilic property of poly(3-hydroxybutyrate-co-3-hydroxyvalerate). *Progress in Natural Science: Materials International*, 21(6), 478–484. [https://doi.org/10.1016/S1002-0071\(12\)60086-0](https://doi.org/10.1016/S1002-0071(12)60086-0)
- Yuan, H., Nishiyama, Y., & Kuga, S. (2005). Surface Esterification of Cellulose by Vapor-Phase Treatment With Trifluoroacetic Anhydride. *Cellulose*, 12(5), 543–549. <https://doi.org/10.1007/s10570-005-7136-2>
- Yuan, H., Nishiyama, Y., Wada, M., & Kuga, S. (2006). Surface acylation of cellulose whiskers by drying aqueous emulsion. *Biomacromolecules*, 7(3), 696–700. <https://doi.org/10.1021/bm050828j>
- Zaman, M., Xiao, H., Chibante, F., & Ni, Y. (2012). Synthesis and characterization of cationically modified nanocrystalline cellulose. *Carbohydrate Polymers*, 89(1), 163–170. <https://doi.org/10.1016/j.carbpol.2012.02.066>
- Zhen Zhangth. (2017). Surface Modification of Cellulose Nanocrystal for Advanced Applications. University of Waterloo. Thesis
- Zhu, H., Luo, W., Ciesielski, P. N., Fang, Z., Zhu, J. Y., Henriksson, G., ... Hu, L. (2016). Wood-Derived Materials for Green Electronics, Biological Devices, and Energy Applications. *Chemical Reviews*, 116(16), 9305–9374. <https://doi.org/10.1021/acs.chemrev.6b00225>

Zoppe, J. O., Venditti, R. A., & Rojas, O. J. (2012). Pickering emulsions stabilized by cellulose nanocrystals grafted with thermo-responsive polymer brushes. *Journal of Colloid and Interface Science*, *369*(1), 202–209. <https://doi.org/10.1016/j.jcis.2011.12.011>

Zouambia, Y., Moulai-Mostefa, N., & Krea, M. (2009). Structural characterization and surface activity of hydrophobically functionalized extracted pectins. *Carbohydrate Polymers*, *78*(4), 841–846. <https://doi.org/10.1016/j.carbpol.2009.07.007>

